2005

Infrared and x-ray spectroscopic studies of the copper(II) oxide mediated reactions of chlorinated aromatic precursors to PCDD/F

Steven L. Alderman
Louisiana State University and Agricultural and Mechanical College, salder1@lsu.edu

INFRARED AND X-RAY SPECTROSCOPIC STUDIES OF THE COPPER(II) OXIDE MEDIATED REACTIONS OF CHLORINATED AROMATIC PRECURSORS TO PCDD/F

A Dissertation

Submitted to the Graduate Faculty of the
Louisiana State University and
Agricultural and Mechanical College
in partial fulfillment of the
requirements for the degree of
Doctor of Philosophy

in

The Department of Chemistry

by
Steven L. Alderman
B.S., Mississippi State University, 1998
May, 2005

TABLE OF CONTENTS

LIST OF TABLES

LIST OF FIGURES

ABSTRACT

Polychlorinated dibenzo-*p*-dioxins and dibenzofurans (PCDD/F) are toxic compounds produced in combustion systems such as incinerators, and their emissions are an important environmental issue. Chlorinated phenols and benzenes form PCDD/F through heterogeneous reactions following adsorption onto fly-ash surfaces. Current research implicates transition metals in promoting formation of phenoxyl radicals that react to form PCDD/F, although this has not been studied extensively. This objective of this work is to better understand PCDD/F formation from chlorinated aromatic precursors.

Using 2-chlorophenol as a model PCDD/F precursor and silica as a fly-ash surrogate, time-dependent chemisorption of 2-chlorophenol onto silica was studied *in situ* from 200-500 °C with Fourier transform infrared spectroscopy. Chlorophenolate adsorption products and partial oxidation products were detected and characterized. Rates of chemisorption were also determined. Since copper species accelerate the formation of PCDD/F, further infrared spectroscopic studies were conducted to investigate the reactions of 2-chlorophenol, 1,2-dichlorobenzene and chlorobenzene with a copper oxide containing silica surface. Chemisorption mechanisms were determined and kinetics of the adsorption were measured. It was discovered that chlorinated benzenes react to produce the same phenolate species as phenols and this may place much greater emphasis on chlorinated benzenes as PCDD/F precursors.

An X-ray adsorption near-edge structure (XANES) spectroscopic study was conducted to examine the role of copper oxide in the formation of phenoxyl radicals. The time-dependent reduction of Cu(II) in a CuO/silica mixture was characterized in the presence of the three above mentioned PCDD/F precursors from 275-375 °C. The rate of reduction and Arrhenius parameters are given for each system, as well as copper speciation throughout the reaction. The

results obtained support the contention the redox reactions of copper species promote the formation of phenoxyl radicals.

Additionally, a predictive model was developed to correlate PCDD/F emissions with gas-phase chlorophenol concentrations. The primary motivation for this is the desire to continuously monitor PCDD/F emission by measuring chlorophenol levels, since the gas-phase concentration of chlorinated phenols in combustion systems is much higher that those of PCDD/F. The results of the model give new insight into the formation of PCDD/F from aromatic precursors.

CHAPTER 1: INTRODUCTION

1.1 Introduction to PCDD/F: Occurrence, Toxicity and Sources

Polychlorinated dibenzo-*p*-dioxins and polychlorinated dibenzofurans (PCDD/F or "dioxins", collectively) are a class of extremely toxic, tricyclic aromatic compounds and are members of the family of halogenated aromatic compounds that include polychlorinated biphenyls (PCBs), naphthalenes, terphenyls, azo and azoxybenzenes and quaterphenyls. The dibenzo-*p*-dioxin and dibenzofuran structures and substituent numbering schemes are shown in Figure 1.1, as well as the most toxic dioxin isomer, 2,3,7,8-tetrachlorodibenzo-*p*-dioxin.

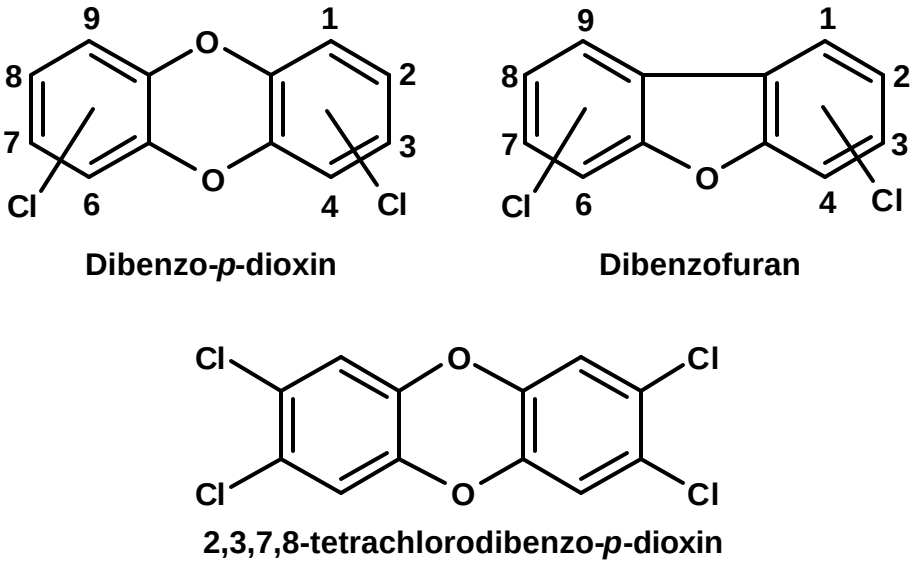

Figure 1.1 The structure and substituent position numbering of dibenzo-*p*-dioxin and dibenzofuran and the most toxic PCDD/F isomer, 2,3,7,8-dibenzo-*p*-dioxin.

There are 75 possible PCDD isomers and 135 possible PCDF isomers. Only PCDD/F isomers with chlorine at each lateral (2,3,7,8) position are assigned a toxic equivalency factor (TEQ), which is a benchmark value used for regulatory and risk assessment purposes to characterize and report cumulative PCDD/F emissions. Collectively, there are 17 toxic PCDD/F isomers. The toxicity of these compounds is diminished as the degree of chlorination increases and chlorinated dioxins are more toxic than chlorinated furans. The ratio of TEQ, on a mass

basis, to that of total PCDD/F output varies with the congener distribution, but typically is about 1:60.

Dioxins are ubiquitous environmental contaminants and are found in sediment, soil, vegetation, fish, mammalian tissue, and bovine and human milk.[1.1,1.2] They are highly lipophilic molecules and are very resistant to environmental degradation and as a result, they readily ascend the food chain.[1.1] The dietary route is the primary source of human exposure to dioxins, with the general population having a body burden of 13 ng TEQ/kg body weight and a daily dietary intake of 1-3 pg of TEQ/kg body weight per day.[1.3]

Dioxins are known to be carcinogenic, mutagenic, teratogenic and to possess endocrine disrupting properties.[1.1-1.4] Other toxic effects are either known or suspected, such as immune, digestive and metabolic disorders.[1.3] These toxic effects can be brought about from very low nanogram to microgram per kilogram mammalian body weight exposures, further emphasizing dioxin toxicity.[1.2] Studies on the mechanisms of dioxin toxicity have shown that many of the toxic effects are brought about when PCDD/F species bind with high affinity to the aromatic hydrocarbon receptor, which is associated with the microsomal cytochrome P4501A1 enzyme.[1.3,1.4]

Dioxins are introduced to the environment from a variety of combustion sources and are formed from practically any combination of C, H, O, and Cl under suitable conditions of time and temperature.[1.5] A leading source of dioxins to the environment, a source that has generated considerable public and regulatory scrutiny, is waste incineration, where dioxins are formed as products of incomplete combustion. It is estimated that in the U.S., municipal waste incinerator emissions are from 1000-9,000 g TEQ PCDD/F per year.[1.6,1.7] Medical waste incinerators are thought to emit between 100-1000 g TEQ PCDD/F per year,[1.7,1.8] while hazardous waste

incinerators contribute 15-75 g TEQ per year.[1.6,1,7,1.9] These numbers can be compared with U.S. coal combustion, which generates an estimated 10 g TEQ PCDD/F per year.[1.6]

Industrial sources such as the production of chlorinated phenols and chlorinated benzenes and products derived from them generate PCDD/F and the use of such chemicals also contributes to dioxin emissions, as in the treatment of wood products with formulations containing pentachlorphenol.[1.10,1.11] Domestic combustion processes, such as open barrel burning of household waste are also thought to significantly contribute to dioxin emissions; so much so that measurements by the Environmental Protection Agency indicate that backyard burning of domestic waste emits more PCDD/F on a mass of refuse burned basis than various types of municipal waste combustors.[1.12] There is good evidence to suggest that hydroxyl radicals initiate atmospheric photochemical synthesis of octachlorodibenzo-*p*-dioxin (OCDD) from pentachlorophenol and may make a significant contribution to measured OCDD levels.[1.13] Also, it is estimated that 800-1000 g TEQ/year is emitted through industrial, domestic and forest wood burning.[1.6]

Because of the trace chemical processes that occur during combustion, it is thought that PCDD/F formation may proceed through common mechanisms for a variety of sources.[1.14] However, the following discussions of PCDD/F formation that follow are derived from studies most applicable to incineration conditions.

Dioxins were first reported as a component of a municipal solid waste incinerator effluent in 1977.[1.15] Since then, a considerable amount of research has been directed at characterizing their emissions, identifying the conditions that facilitate dioxin formation and the reagents involved in formation and identifying dioxin formation mechanisms.[1.5,1.16,1.17] Still, many mechanistic details involved in PCDD/F formation are poorly understood, partly because

PCDD/Fs are side reaction products and their yields, in real-world and most laboratory conditions, are miniscule compared to major combustion products. Gas-phase and heterogeneous reactions form PCCD/F and essentially three major formation pathways have been proposed: 1) homogeneous, gas-phase synthesis from molecular precursors, i.e., chlorophenols and chlorinated biphenyls or phenyl ethers, 2) direct surface-mediated formation from chemically similar precursors, most notably chlorinated phenols and benzenes and 3) *de novo* oxidation and chlorination of native carbon in fly-ash via gas-solid and solid-solid reactions that release PCDD/F directly from the carbon matrix.[1.17-1.21]

1.2 Gas-Phase Formation of PCDD/F

The most studied and seemingly dominant gas-phase precursors of PCDD/F are the chlorinated phenols.[1.22-1.25] In addition to being the most direct precursors to PCDD/F, chlorinated phenols and are among the most abundant aromatic compounds found in incinerator effluent.[1.26] In actual incinerators, gas-phase synthesis occurs in the region between the primary combustion chamber exit and the air pollution control device inlet. The temperature in this region varies from approximately 1000-500 °C and is characterized by residence times of 2-10 s. Above 600 °C, PCDD/F destruction becomes favored over formation and at 900 °C practically all PCDD/F are destroyed.[1.27,1.28] Although a kinetic modeling study questioning the relative importance of PCDD/F derived from gas-phase synthesis from chlorinated phenols concluded that such reactions were too slow to account for yields in full-scale combustors,[1.29] it is now believed that gas-phase formation from chlorinated phenols makes a significant contribution to observed emissions.[1.21,1.27,1.30]

Much of what is known concerning gas-phase PCDD/F formation has come about by studying the thermal decomposition of chlorinated phenols under pyrolytic and oxidative

conditions. Through this work, plausible, well-scrutinized elementary reaction mechanisms have been developed through the identification of reaction intermediates and the specific dioxin and furan isomers formed from individual chlorinated phenols.[1.19,1.31,1.32] In practice, the specific PCDD/F isomers formed from reactions of a given chlorinated phenol can be predicted with good accuracy.[1.19.,1.21,1.25] The validity of the reaction mechanisms has been corroborated and further refined though theoretical calculations.[1.30,1.33]

Of central importance in the gas-phase formation of PCDD/F from chlorinated phenols is the neutral, resonance stabilized (chloro)phenoxy radical, which is formed from (chloro)phenol via hydroxyl hydrogen abstraction by unimolecular, bimolecular, or possibly other pathways.[1.24] As this is a delocalized system, radical character is present at the phenolic oxygen, as well as at *ortho-* and *para-* carbon sites,[1.34] as illustrated in Figure 1.2.

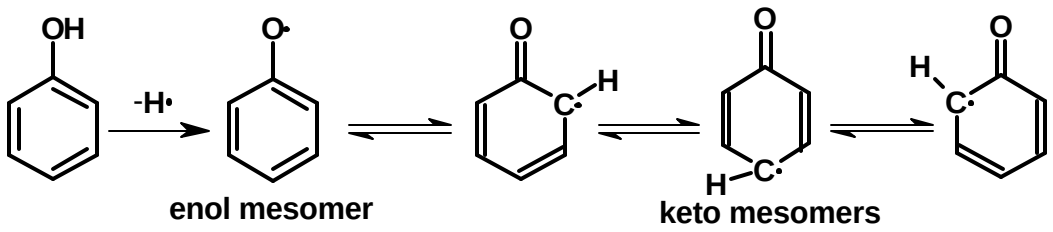

Figure 1.2 The resonance stabilized phenoxy radical.

Formation of PCDD/F occurs though coupling of the phenoxy radicals with chlorophenol molecules (radical-molecule) and through radical dimerization reactions (radical-radical) at temperatures greater than 500 °C.[1.19,1.21,1.24,1.25,1.35] The oxygen-centered enol mesomer and the *ortho-* carbon-centered keto mesomer are primarily responsible for PCDD/F formation. Each class of reaction will be briefly discussed using 2-chlorophenol as the illustrative example.

In the radical-molecule pathway shown in Figure1.3, the oxygen-centered mesomer of the 2-chlorophenoxy radical reacts with a 2-chlorophenol molecule though chlorine displacement to form a chlorohydroxy diphenyl ether intermediate. H· is extracted from the ring hydroxyl

group, presumably by H·, followed by formation of dibenzo-*p*-dioxin by intra-annular Cl· displacement.[1.24,1.36] Although not illustrated in Figure 1.3, ring closure to form PCDD proceeds though a five-member ring intermediate, the well documented Smiles rearrangement,[1.37] to produce isomer pairs. This behavior cannot be empirically observed for 2-chlorophenol since its self-reactions to PCDD/F form the non- and mono- chlorinated isomers. However, it is well established that 2,4,6-trichlorophenol oxidation yields both 1,3,7,9- and 1,3,6,8-tertrachlorodibenzo-*p*-dioxin.[1.21] These authors also observed analogous brominated dioxin isomers from reaction of 2,4,6-tribromophenol. Further supporting the Smiles intermediate was the observation by Mulholland *et al.* that 2,6-dichlorophenol condenses to yield the expected, 1,6- and 1,9-dichlordibenzo-*p*-dioxin. [1.25] Furthermore, at high temperature, the ratio of the two isomers agreed closely with calculated thermodynamic distributions, while at low temperature, preferential formation of the 1,6- isomer demonstrated kinetic control.

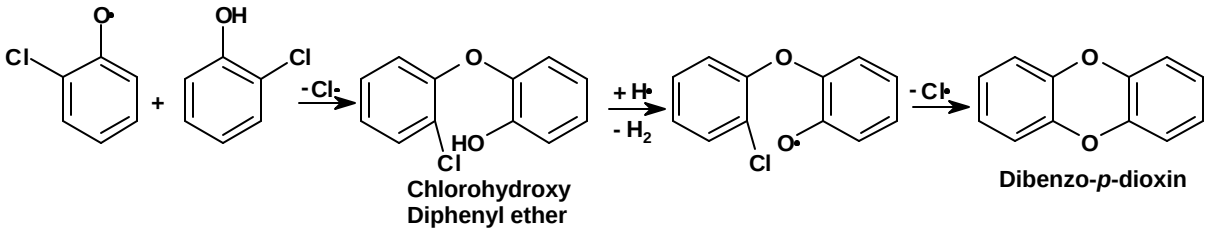

Figure 1.3 Radical-molecule pathway to dibenzo-*p*-dioxin.

It has been suggested that the radical-molecule pathway to dioxin from chlorophenol may be too slow to fully account for PCDD formation.[1.30,1.35] Alternatively, a radical-radical pathway has been developed[1.24,1.35] and is illustrated in Figure 1.4. In this pathway, the phenolic oxygen-centered radical dimerizes with a chlorine substituted carbon-centered phenoxy radical to form keto ether, which can tautomerize to an enol form. Ring closure to form dibenzodioxin proceeds as described in the radical-molecule pathway.

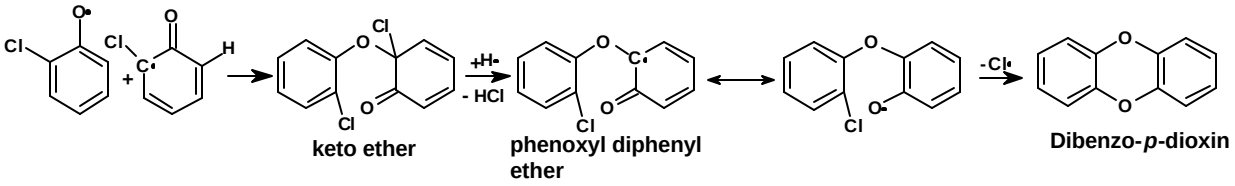

Figure 1.4 Radical-radical pathway to dibenzo-*p*-dioxin.

A radical-radical mechanism to 1-monochlorodibenzo-*p*-dioxin has been developed[1.24,1.30] and can be seen in Figure 1.5. In this pathway, the phenolic oxygen-centered radical dimerizes with a hydrogen substituted, carbon-centered phenoxy radical to form keto ether. Phenoxy diphenyl ether is formed following hydrogen extraction, followed again by inter-annular chlorine displacement to form 1-monochlorodibenzo-*p*-dioxin.

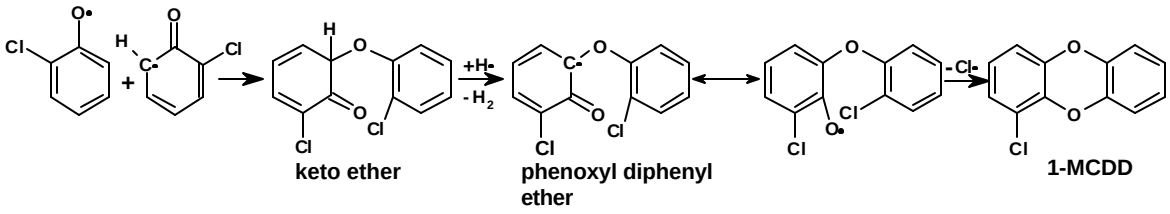

Figure 1.5 Radical-radical pathway to 1-monochlorodibenzo-*p*-dioxin.

The gas-phase formation of 4,6-dichlorodibenzofuran from chlorinated phenols occurs though the dimerization of two carbon-centered phenoxy radicals, which forms a diketo dimer, as shown in Figure 1.6. Ring hydrogen is abstracted to form the carbon-centered diketo radical, which tautomerizes to the oxygen-centered radical. Ring closure to form dichlorodibenzofuran is accomplished by displacement of the hydroxyl on the neighboring ring.

In Figure 1.6, the diketo dimer radical is formed following hydrogen abstraction from a ring carbon and enolization back to the oxygen centered radical. In the view of Wiater and Louw, the diketo radical is formed via hydrogen abstraction from one phenolic group of the diketo dimer[1.31], which is to say, hydrogen abstraction follows enolisation, rather than from the ring

carbon in the enol form. However, both of these pathways result in the same diketo dimer and consequently, the same PCDF isomer.

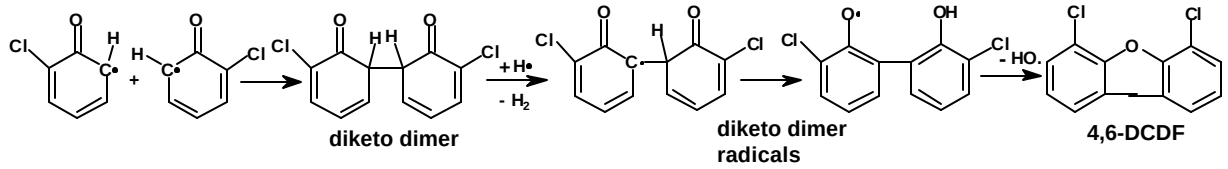

Figure 1.6 Radical-radical pathway to 4,6-dichlorodibenzofuran.

Yang, Mulholland, and Akki have demonstrated that the yield of DCDF from 4-chlorophenol>3-chlorophenol>2-chlorophenol, with the differences being quite substantial.[1.32] This indicates the strong influence of the position of Cl on phenoxy radical coupling.

The presence or absence of *ortho*- chlorine dictates whether PCDD, PCDF, or both, will form from chlorophenol. Molecules with one *ortho*- chlorine combine to form PCDD and PCDF, demonstrated in the 2-chlorophenol examples. When both *ortho*- sites are chlorinated, only PCDD is formed.[1.21,1.25,1.38] No PCDF is formed since "tautomerisation to the biphenyl skeleton is impossible".[1.31] When no *ortho*- chlorine is present only PCDF isomers are formed,[1.32] since the chlorine substituent of a keto ether formed from reactions analogous to those shown in Figures 1.4 and 1.5 will not be in a position to facilitate ring closure to PCDD.

1.3 Surface-Mediated PCDD/F Formation

Heterogeneous formation of PCDD/F occurs in the low temperature, post-combustion region of incinerators where temperatures span 600-200 °C. The time scale for reactions here can be quite long since reactive surfaces and reactants can become immobilized. Air pollution control devices (APCD) such as electrostatic precipitators and fabric filters are housed in this region and a number of reports in the literature have demonstrated that PCDD/F levels are substantially higher at the exit of the APCD than at the entrance.[1.5,1.39] These observations strongly suggest that heterogeneous reactions are responsible for the majority of emissions, since

gas-phase synthesis is not favorable at these temperatures. Furthermore, within the dioxin research community, there is virtual unanimous agreement that most PCDD/F are formed via surface-mediated processes.[1.16,1.17]

However, a subject of considerable uncertainty is the relative contribution of *de novo* PCDD/F formation from carbon in incinerator fly-ash vs. that of fly-ash mediated reactions of chemically similar precursors. Experimental evidence has demonstrated that both pathways produce dioxins and more recent evidence suggests that the two pathways may be more closely related than once thought. Although the initial reactants differ in each pathway, the conditions critical to PCDD/F formation are very similar.

A reactive surface facilitates formation in both cases and this mediator is combustion generated fly-ash. Fly-ash is essentially the non-combustible material in incinerator waste feed. SiO_2 (20-40 wt. %) and Al_2O_3 (10-20 wt. %) typically make up the bulk of the fly-ash.[1.41,1.42] Mineralized Ca, Na, and K are also abundant and macromolecular carbon is present as soot and char. Various metallic species are present from ppm levels to a few percent by weight and both *de novo* and precursor work has revealed that a transition metal catalyst is essential for PCDD/F formation.[1.43] Countless *de novo* and precursors experiments using actual and synthetic fly-ash substrates find the temperature window for PCDD/F formation to be 250-450 °C, with maximum formation occurring around 350 °C.[1.17, 1.40, 1.44] Copper oxides and chlorides, which are relatively abundant in fly-ash, have been shown to have the strongest effect on PCDD/F formation under *de novo* and precursor conditions. Limited studies have shown that iron oxides also promote PCDD/F formation.[1.45]

De novo experiments yield PCDD to PCDF ratios <<1, which is the case in actual incinerators; however, the formation rates observed do not seem fast enough to account for

full-scale emissions. Surface-mediated formation from chlorinated phenol precursors occurs at sufficient rates to account for full scale emissions; however, a criticism of the precursor theory has been that more PCDD is formed than PCDF.[1.20,1.45] This is partly because many of the chlorophenol isomers investigated were doubly *ortho*- chlorinated, and as with gas-phase formation, the surface catalyzed coupling reactions do not lead to PCDF as a major product.

1.3.1 *De Novo* Formation of PCDD/F

De novo formation is defined as a two-step process involving: 1) catalytic addition of chlorine to the surface of carbon found in fly-ash and 2) the subsequent release of the newly formed chlorinated carbon structure through further carbon degradation, resulting in the release of PCDD/F.[1.46] Most *de novo* experiments are performed by heating real or synthetic fly-ash under varying temperature and atmosphere, in the absence of a specific gas-phase precursor, and analyzing the volatile reaction products formed. Trace amounts of PCDD/F are formed *de novo* under pyrolytic conditions but rates are substantially accelerated in the presence of oxygen.[1.43,1.44]

Possible roles of a transition metal catalyst when native carbon is the initial reagent are chlorination of carbon prior to breakdown of the macromolecules, followed by oxidation and gasification of the carbon and chlorination of intermediates or PCDD/F.[1.47] Experiments by Weber have demonstrated that $CuCl_2$ participates in carbon chlorination reactions and it was demonstrated that Cu(II) is reduced in the process.[1.48] Stieglitz has reported the formation of C-Cl bonds at a carbon surface in a fly-ash matrix containing $CuCl_2$ and also reported the Cu(II) is reduced, as evidenced by X-ray spectroscopy.[1.46] However, gaseous reactants such as Cl_2 and HCl are also effective chlorinators,[1.49] so the role of metallic species like $CuCl_2$ in *de novo* PCDD/F formation is probably not limited to chlorinating aromatic rings.

The temperature required for oxidation and gasification of carbon, measured by analyzing evolved CO_2, is usually between 500-600 °C; however, the addition of inorganic compounds reduced this by 200 °C. This indicates that metal ions take part in carbon degradation, as well as chlorination reactions.[1.46] It was proposed that oxygen may transfer to the metal, increasing the valency state, followed by oxygen transfer to the carbon and reduction of the metal. It was also suggested that a transition of π electrons from the carbon to the d orbitals of the metal occurs and that this reduces the activation energy for the formation and release of carbon-oxygen complexes at the surface. Taken together, it seems that metals participate in carbon chlorination and degradation to produce PCDD/F.

A variety of other chlorocompounds are produced from *de novo* reactions and chlorinated benzenes make the greatest contribution. In an experiment performed by Stieglitz, polychlorinated benzenes accounted for 84.3 % of the mass balance of volatile compounds. PCDD and PCDF contributed 1.44 and 6.55 %, respectively, while polychlorophenols levels were at a low 0.01 %.[1.46] A *de novo* experiment conducted by Pekarek *et al.* showed chlorobenzene to exceed 30 times the formation of chlorinated phenol.[1.44] It's been suggested that chlorinated phenols are lost on fly-ash by irreversible chemisorption and undergo polymerization reactions.[1.45]

Since chlorinated benzene and some chlorinated phenols are formed during *de novo* reactions, it may be that "precursors" are formed "*de novo*", which then react to form PCDD/F. This is partially supported by the observation that a surrogate fly-ash used in a *de novo* experiment, containing equal amounts of ^{13}C and ^{12}C, formed only a few percent of mixed-ring PCDF, while 50% of the PCDD formed had one aromatic ring with either carbon isotope.[1.20] This was also observed by others in a related, previous experiment.[1.50] This implies that furan

structures can be chlorinated and directly released from the carbon matrix, but PCDD most likely forms from intermediates synthesized "*de novo*".

1.3.2 Formation from Chlorinated Aromatic Precursors

It was first demonstrated in 1987 that the fly-ash mediated reactions of chlorinated phenol precursors form PCDD.[1.22] These reactions have since been investigated in countless flow-reactor studies and the referenced publications are representative.[1.40,1.51,1.52] In most experiments, gas-phase chlorophenol precursors were passed over actual or model fly-ash beds while the temperature-dependent reactions products were collected and analyzed. These studies have been invaluable for identifying the temperature range of dioxin formation, identifying reactive components of fly-ash and other related parameters such as the effect of oxygen and other gas-phase species. These type studies have also confirmed that, as in gas-phase synthesis, the observed PCDD/F isomer pattern is dependent on the chlorophenol used.[1.53] However, many of these studies have utilized complex surfaces and highly chlorinated phenol congeners which have limited the elucidation of mechanistic details. Of particular interest is the nature of absorption of known PCDD/F precursors to active surfaces, the role of transition metals, and if and how surface-mediated reactions of chlorinated phenols relate to gas-phase synthesis of PCDD/F.

It is postulated that chlorophenols adsorb onto catalytic sites in fly-ash to form chlorophenolate, followed by reaction to PCDD/F, desorption of PCDD/F, and re-adsorption of chlorinated phenols.[1.54] Milligan and Altwicker have suggested on the basis of model fitting to experimental data that PCDD are formed via a Langmuir-Hinshelwood (LH) mechanism in which two adsorbed chlorophenols react to form PCDD.[1.52,1.54] However, the authors provided little mechanistic interpretation. Their findings were partially confirmed in one of the few

infrared spectroscopic studies conducted in the field. Huang *et al.* examined the adsorption of pentachlorophenol on incinerator fly-ash and concluded that pentachlorophenol adsorbed to fly-ash though the phenolic O-H bond and formed octachlorodibenzo-*p*-dioxin via a (LH) pathway.[1.55]

A detailed investigation was conducted by Lomnicki and Dellinger who used 2-chlorophenol as a model PCDD/F precursor and CuO supported on silica as a model fly-ash. They concluded that PCDD are formed through an Eley-Rideal (ER) mechanism in which a surface bound molecule reacts with a gas-phase molecule.[1.40] Their results strongly suggested that PCDF are form from two adsorbed chlorinated phenols, via the (LH) pathway. Interestingly, the main PCDD/F products formed from their experiments were the same products expected based on gas-phase radical-molecule and radical-radical reactions.[1.19,1.21] From this observation, it was suspected that surface associated phenoxyl radicals form PCDD/F in a manner similar to that of gas-phase formation. Using EPR spectroscopy, they found solid evidence supporting the existence of such a radical when 2-chlorophenol is adsorbed onto CuO/silica.[1.40] They went on to suggest that chlorophenol adsorbs to a Cu(II) site as chlorophenolate and a surface associated radical is formed following electron transfer from chlorophenolate to the metal cation site, thus reducing Cu(II) to Cu(I), all illustrated in Figure 1.7. The one e^- reduction of Cu(II) is supported by an X-ray adsorption experiment conducted by Farquar *et al.* demonstrating the CuO is reduced to primarily Cu_2O in the presence of 2-chlorophenol vapor at 375 °C.[1.56]

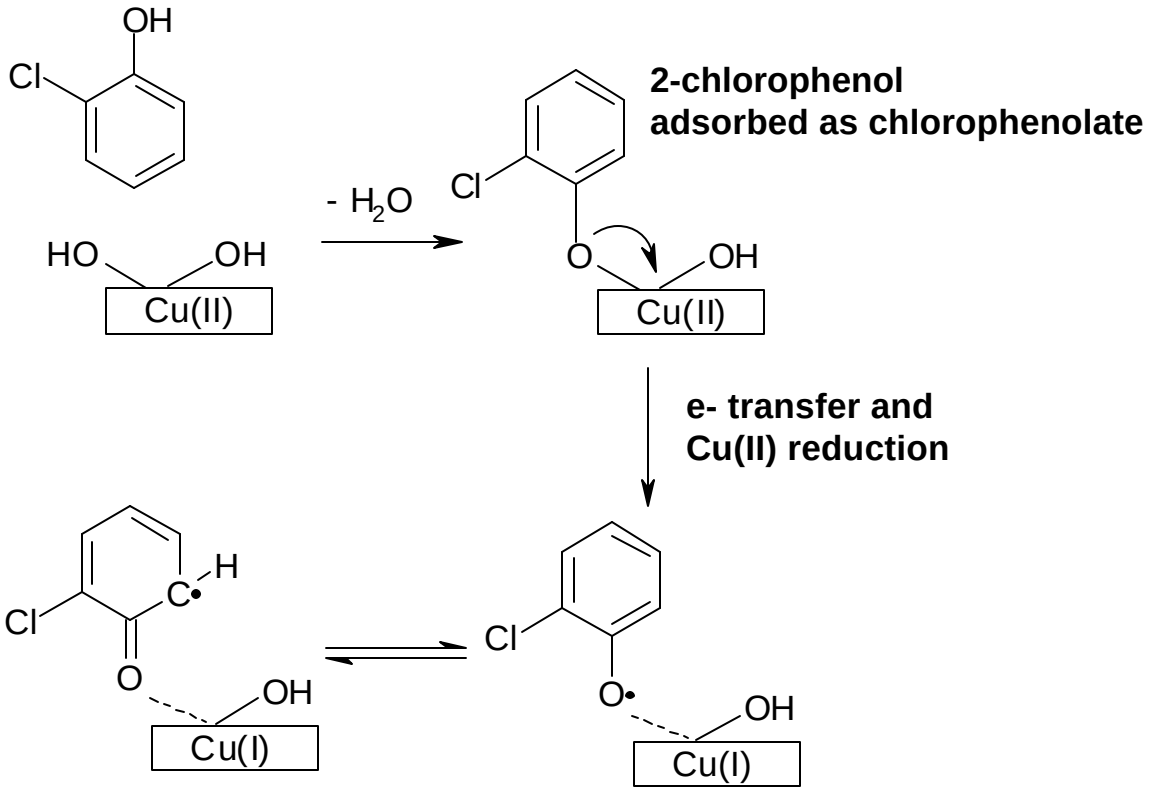

Figure 1.7 Adsorption of 2-chlorophenol at a cupric hydroxyl group and formation of a resonance stabilized chlorophenoxyl radical.

Others have supported that copper redox reactions and phenoxyl radicals are important for dioxin formation. Tuppurainen and Ruuskanen, using semi-empirical and *ab initio* calculations, theorized that reactive phenoxonium cations (which couple to form dioxins) are formed by double one e^- transfer within an antiferromagnetically coupled, phenoxy-bridged dinuclear Cu(II) complex from the bridging phenolate to both Cu(II) ions to produce Cu(I).[1.34] Voncina and Solmajer chemisorbed 2,4,6-trichlorophenol onto $Al(OH)_3$ and proposed 2,4,6-trichlorophenoxy radical formation by thermally induced homolytic cleavage of the Al-O bond of the adsorbed chlorophenol.[1.57] Although not directly related to dioxin formation, Boyd and Mortland demonstrated with EPR spectroscopy the formation of a radical cation when 4-chlorophenol was adsorbed to a smectite clay impregnated with Cu(II) and also showed that Cu(II) is reduced to Cu(I).[1.58]

Although chlorinated benzenes are often implicated as PCDD/F precursors, studies have primarily focused on chlorinated phenols. Very few studies have shown the formation of PCDD/F from chlorinated benzenes as initial reactants. Ghorishi and Altwicker observed the formation of PCDD/F in a spouted bed combustor for 10% 1,2-dichlorobenzene in n-heptane from 130 to 430 C.[1.59] PCDD to PCDF ratios ranged from 0.6 to 0.9. Chlorinated phenols and higher chlorinated benzenes were also formed. This is an interesting and possibly important result, as higher chlorinated benzene to phenol ratios resulted in the lower PCDD to PCDF ratios, which suggests that chlorinated benzenes promoted PCDF formation, while chlorinated phenols promoted PCDD formation.

If chlorinated benzenes chemisorb as chlorophenolate to potentially active surface sites, as illustrated in Figure 1.7 for 2-chlorophenol, it is possible that dioxin formation will take place, especially though reaction of two surface bound molecules though the (LH) pathway, which probably forms PCDF. Infrared spectroscopy has shown 1,2-dichlorobenzene to adsorb in this manner on a titania based SCR-DeNO$_X$ catalyst.[1.60] Another consideration is that chlorinated benzenes concentrations in incinerator effluent are up to 100x greater than those of chlorinated phenols[1.61] and chlorinated benzenes are formed *de novo* from macromolecular carbon at much higher concentrations than phenols.[1.44,1.46]

1.4 Approach

Figure 1.8 presents an extended precursor pathway to PCDD/F that is a unified view of dioxin formation in combustion processes that incorporates both *de novo* and precursor concepts by including carbonaceous materials as a source of reactants and transition metals as catalysts or mediators for specific steps in the formation of PCDD/F.

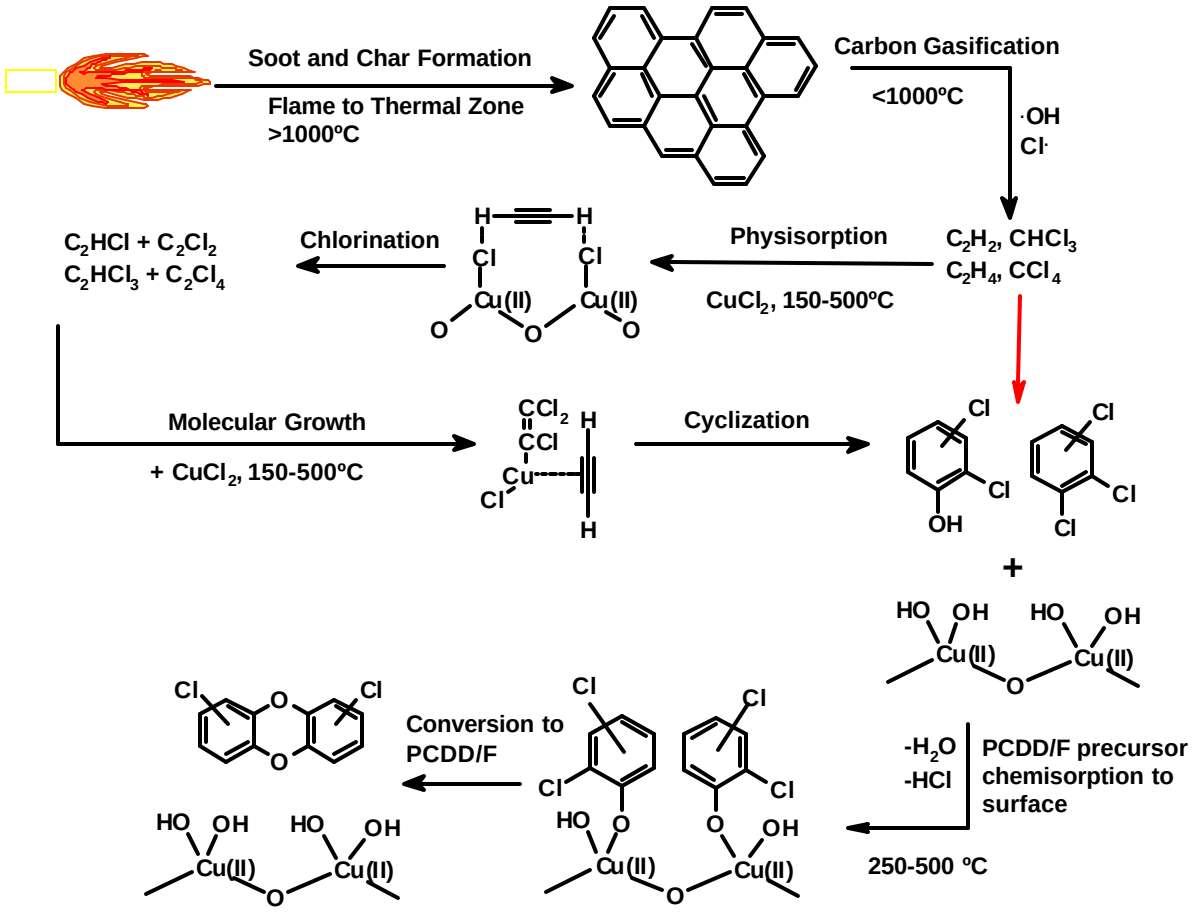

Figure 1.8 A unified pathway for the formation of PCDD/F in combustion systems.

In this pathway, combustion generated carbon particulate matter reacts with combustion generated radicals, such as ·OH or ·Cl, or reactive molecular species (e.g., NO, NO_2, H_2O_2) to form simple olefinic hydrocarbons or chlorocarbons. Khachatryan and Dellinger gave evidence supporting this occurrence using an excimer laser to photolytically generate either ·OH or ·Cl in the presence of graphitic carbon. They demonstrated that unchlorinated olefins are liberated by ·OH and chlorinated methanes are formed by reaction of ·Cl with the carbon network.[1.62,1.63] They developed reasonable mechanisms based on ·OH and ·Cl addition to the carbon lattice.

The hydrocarbons and chlorocarbons may then undergo metal catalyzed chlorination, molecular growth, and cyclization reactions to form chlorinated phenols and chlorinated benzenes. It has been demonstrated experimentally that acetylene and ethylene undergo chlorination and molecular growth to form chlorinated aromatics, such as hexachlorobenzene, when passed over a cupric chloride bed at typical post combustion temperatures.[1.64] Froese and Huntzinger showed that polychlorinated benzene, phenol and PCDD/F are formed when acetylene is reacted with HCl/air under heterogeneous combustion conditions between 300 °C and 600 °C over a model and real fly-ashes.[1.65] Additionally, chlorinated phenols and benzenes may be directly liberated from the carbon network, thus circumventing the molecular growth steps, indicated by the red arrow in Figure 1.8. Regardless, once formed, these aromatic species further react with fly-ash surfaces to produce dioxins.

Relatively few spectroscopic studies have been employed to investigate the elementary reaction steps involved in the surface-mediated conversion of chlorinated aromatics to PCDD/F, which is depicted in the lower line of Figure 1.8. As a result, many of the mechanistic details involved in PCDD/F formation are either speculative or completely unknown. Specifically, the kinetics and nature of PCDD/F precursor adsorption to potentially active surface sites and the effect catalytic metal species have in promoting dioxin formation are not well understood. *The primary objective of the work presented in this dissertation is to improve our understanding of these key steps in surface-mediated PCDD/F formation.*

Two complimentary spectroscopic techniques, Fourier transform infrared spectroscopy (FTIR) and X-ray absorption near-edge structure (XANES) spectroscopy, were used to study reactions of model PCDD/F precursors on surrogate fly-ash surfaces. A temperature controlled dosing cell was assembled to allow for *in situ* spectroscopic studies and kinetic studies and

experiments were carried out in the temperature range characteristic of post-combustion surface-mediated PCDD/F formation.

Additionally, a predictive model was developed to examine the correlation between gas-phase chlorophenol concentrations and PCDD/F emissions. The primary motivation for this is the desire to continuously monitor PCDD/F emissions by measuring chlorophenol levels, since the gas-phase concentration of chlorinated phenols in combustion systems is much higher that those of PCDD/F. Thus, a continuous emission monitor could presumably more readily detect chlorinated phenols than PCDD/F. However, the modeling results also gave new insight into the role of chlorinated phenols as PCDD/F precursors.

An improved understanding of the origin and mechanisms of formation of PCDD/F could lead to adjustments in operating parameters to minimize emissions. Such a method of pollutant formation prevention would be better than add-on control techniques, which only transfers the PCDD/F burden from the stack gas to another residue which must then be subjected to additional treatment and disposal. For example, the temperature history and flue-gas composition may be modified to produce fly-ash surfaces which resist chemisorption and thus prevent surface catalysis.

1.5 Literature Review

Table 1.1 presents a review of the literature from 1998-2004. Key findings concerning the conditions that facilitate dioxin formation and the mechanisms of dioxin formation are summarized.

1.6 References

1.1 Safe, S.; Huntzinger, O. In *Environmental Toxic Series 3: Polychlorinated Dibenzo- p-dioxins and –furans (PCDDs/PCDFs)*; Safe, S.Huntzinger, O., Hill, T.A. Eds.; Springer-Verlag: Berlin Heidelberg, 1990.

Table 1.1 Summary of the key findings in the dioxin formation literature from 1998-2004

Authors (Year)	Title	Key Findings	Ref.
R. Addink, E. Altwicker (2004)	Formation of Polychlorinated Dibenzo-*p*-Dioxins and Dibenzofurans on Secondary Combustor/Boiler Ash from a Rotary Kiln Burning Hazardous Waste	The title ash was treated under *de novo* conditions in the lab. PCDD/F were formed for up to 90 minutes in 10% O_2 and gave yields proportional to the amount of ash. Copper and iron in the ash were identified as the catalytic species.	1.66
R. Addink, E. Altwicker (2004)	Formation of Polychlorinated Dibenzo-*p*-dioxins/Dibenzofurans from Soot of Benzene and *o*-Dichlorobenzene Combustion	Both benzene and dichlorobenzene soot produced appreciable PCDD/F after the addition of $CuCl_2$, but not copper and CuO. Dichlorobenzene soot produced more PCDD/F than chlorobenzene, indicting the pre-existing C-Cl bonds did factor into PCDD/F formation.	1.67
S. Ryan, E. Altwicker (2004)	Understanding the Role of Iron Chlorides in the De Novo Synthesis of Polychlorinated Dibenzo-*p*-dioxins/ Dibenzofurans.	Iron (II) and iron(III) cmps. both play a role in chlorination rxns. Iron(III)oxychloride is converted to iron(III)chloride and is a key step. OCDF was the dominant product observed. The oxide matrix support is also an important parameter.	1.68
R. Addink, E. Altwicker (2001)	Formation of Polychlorinated Dibenzo-p-dioxin/ Dibenzofurans from Residual Carbon on Municipal Solid Waste Incinerator Fly Ash using $Na^{37}Cl$.	The labeling study showed NaCl to be a poor chlorinator. Native Cl in the ash was 17 times more reactive.	1.69
K. Hell, L. Stieglitz, E. Altwicker, R. Addink, R. Will (2001)	Reactions of 2,4,6-trichlorophenol on Model Fly Ash: Oxidation to CO and CO_2, Condensation to PCDD/F and Conversion into Related	Conversion to CO and CO_2 increases from 3% to 75% from 250-450 °C. Other products formed are polychlorinated benzenes, PCDD/F, and phenols. Chlorobenzene isomer patterns suggest ipso-position chlorination of the trichlorophenol.	1.51

(table con'd)

Authors (Year)	Title	Key Findings	Ref.
S. Ryan, E. Altwicker (2000)	The Formation of Polychlorinated Dibenzo-*p*-dioxins/Dibenzofurans from Carbon Model Mixtures Containing Ferrous Chloride	Carbon morphology is important parameter in PCDD/F formation. Ferrous chloride pre-chlorinates carbon fully before expulsion of PCDD/F from carbon matrix. Lower chlorinated congeners result from dechlorination rxns.	1.70
K. Hell, E. Altwicker, L. Stieglitz, R. Addink (2000)	Comparison of 2,4,6-trichlorophenol Conversion to PCDD/PCDF on a MSWI-fly ash and Model Fly Ash.	Observed 3x higher formation on MSWI ash than model ash. Both substrates resulted in PCDD:PCDF >>1.	1.71
R. Addink, E. Altwicker (1998)	Role of Copper Compounds in the De Novo Synthesis of Polychlorinated Dibenzo-*p*-dioxins/Dibenzofurans	Addition of CuCl or $CuCl_2$ to extracted fly-ash drastically enhances PCDD/F formation rate. With CuCl Rxn. is first-order in $[Cu^+]$ and first order in $[Cu^{2+}]$ when $CuCl_2$ is < 160 micromole/g. Rates of PCDD/F formation are comparable and the metal chlorides are more important as Cl source than as a true catalyst.	1.47
A. Buekens, P. Brown, K. Jay (2003)	Chlorination of dibenzofuran, dibenzo-p-dioxin, and Activated Carbon During Digestion of Samples in Boiling 10% HCl	The chlorination levels of dibenzofuran increased with $Fe_2O_3<MnO_2<PbO_2$.	1.72
H. Huang, A. Buekens (2001)	Chemical Kinetic Modelling of De Novo Synthesis of PCDD/F in Municipal Waste Incinerators	When the model that was developed was applied to industrial applications, PCDD/F formation levels of 0.1-0.5 µg/N m^3 in the gas phase and 0.1-1.2 µg/N m^3 in the solid phase are calculated.	1.73
H. Huang, A. Buekens (2000)	Chemical Kinetic Modelling of PCDD Formation from Chlorophenol Catalysed by Incinerator Fly Ash	Key step in surface-mediated PCDD formation is a Langmuir-Hinshelwood type elementary rxn. step. When the model developed was applied to industrial incineration conditions, at the most, a PCDD yield of 10^{-3} µg/N m^3 is calculated.	1.74

(table con'd)

Authors (Year)	Title	Key Findings	Ref.
H. Huang, A. Buekens, P. Jacobs (1999)	PCDD Formation from Chlorophenol on Fly Ash Surface Studied by Fourier Transform Infrared Spectroscopy	Used FTIR to show OCDD is formed from pentachlorophenol via a Langmuir-Hinshelwood pathway.	1.55
L. Khachatryan, R. Asatryan, B. Dellinger (2004)	An Elementary Reaction Kinetic Model of the Gas-Phase Formation of Polychlorinated Dibenzofurans from Chlorinated Phenols	Formation of PCDF is due to the conversion of 2,4,6-TCP to 2,4-DCP, which forms a resonance stabilized chlorophenoxy radical.	1.75
S. Alderman, G. Farquar, E. Poliakoff, B. Dellinger (2004)	Reaction of 2-chlorophenol with CuO: XANES and SEM Analysis.	CuO is reduced to primarily Cu_2O for 275-375 °C reaction. Redox cycling affects the CuO surface morphology and rxn. rate. E_a for reduction is 109 kJ mol^{-1}.	1.76
C. Evans, B. Dellinger (2003)	Mechanisms of Dioxin Formation from the High-Temperature Pyrolysis of 2-bromophenol	Dioxin and non-dioxin products are the same as those observed from 2-chlorophenol pyrolysis, but in contrast DD is the major products rather than naphthalene. The expect 4,6-DBDF was not observed due to the pyrolytic conditions.	1.77
L. Khachatryan, R. Asatryan, B. Dellinger (2003)	Development of Expanded and Core Kinetic Models for the Gas Phase Formation of Dioxins from Chlorinated Phenols	The displacement of Cl on trichlorophenol by trichlorophenoxy radical is the rate determining step in TeCDD formation. Rxn. is 1^{st} order in PCDD at low temp., 2^{nd} order at high temp. Removal of phenoxy radicals by O_2 is insignificant. Gas-phase routes to DD are significant.	1.30
L. Khachatryan, A. Burcat, B. Dellinger (2003)	An Elementary Reaction-Kinetic Model for the Gas-Phase Formation of 1,3,6,8- and 1,3,7,8-tetrachlorinated dibenzo-*p*-dioxins from 2,4,6-trichlorophenol	The high temperature, gas-phase reactions of chlorinated phenols that contain ortho-chlorine will form PCDD in yields approximately four to five orders of magnitude than that predicted by previous modeling results.	1.33

(table con'd)

Authors (Year)	Title	Key Findings	Ref.
C. Evans, B. Dellinger (2003)	Mechanisms of Dioxin Formation from the High-Temperature Pyrolysis of 2-chlorophenol	Developed detailed rxn. mechanisms for the gas-phase formation of PCDD/F. Show that CO elimination from chlorophenoxy radical to form chlorocyclopentadienyl radical yields naphthalene and chloronapthalene via radical recombination and rearrangement.	1.24
S. Lomnicki, B. Dellinger (2003)	A Detailed Mechanism of the Surface-Mediated Formation of PCDD/F from the Oxidation of 2-Chlorophenol on a CuO/Silica Surface	PCDD/F products same as those in gas-phase formation from 2-MCP. EPR evidence showed existence of carbon centered chlorophenoxy radical. Showed PCDD form via Eley-Rideal pathway and PCDF form via Langmuir-Hinshelwood pathway. Saw evidence of a chloroquinone and chlorocatechol intermediates.	1.40
G. Farquar, S. Alderman, E. Poliakoff, B. Dellinger (2003)	X-ray Spectroscopic Study of the High Temperature Reduction of Cu(II)O by 2-chlorophenol on a Simulated Fly-Ash Surface	First application of XANES spectroscopy to PCDD/F formation. Showed that CuO is reduced to primarily Cu_2O and some Cu(0) in the presence of 2-MCP at 375 °C. The observed reduction indicates the mechanism by which a surface associated phenoxy radical is formed.	1.56
R. Asatryan, A. Davtyan, L. Khachatryan, B. Dellinger (2002)	Theoretical Study of Open Shell Ipso-Addition and Bis-Keto Dimer Interconversion Reactions Related to Gas-phase Formation of PCDD/Fs from Chlorinated Phenols	The trichlorophenol molecule is more stable and less reactive than the phenoxy radical. Results suggest that radical-radical pathways to PCDD dominate over radical-molecule.	1.78
S. Lomnicki, B. Dellinger (2002)	Formation of PCDD/F from the Pyrolysis of 2-chlorophenol on the Surface of Dispersed Copper Oxide Particles	Despite pyrolytic conditions, the majority of chlorophenol is oxidized to CO and CO_2. Approximately 0.5% of the chlorophenol was converted to PCDD/F. PCDD forms via an Eley-Rideal mechanism, while PCDF forms via a Langmuir Hinshelwood mechanism. Only, 4,6-DCDF was observed, but much higher chlorinated PCDD was formed, indicating the formation of surface bond PCDD that is further chlorinated on the surface before being desorbed.	1.79

(table con'd)

Authors (Year)	Title	Key Findings	Ref.
P. Taylor, S. Sidhu, W. Rubey, B. Dellinger, A. Wehrmeier, D. Lenoir, K. Schramm (1998)	Evidence for a Unified Pathway of Dioxin Formation from Aliphatic Hydrocarbons	In the presence of HCl, acetylene is converted to perchlorinated gas-phase intermediates, including hexachlorobenzene via molecular growth and cyclization reactions on a borosilicate foam impregnated with CuO.	1.80
H. Fiedler (1998)	Thermal Formation of PCDD/PCDF: A Survey	Review article covering the basic aspects of *de novo* and precursor PCDD/F formation.	1.81
E. Wikstrom, S. Ryan, A. Touati, D. Tabor, B. Gullett (2004)	Origin of Carbon in Polychlorinated Dioxins and Furans Formed During Sooting Combustion	The presence of soot and ash were the two major factors controlling PCDD/F yields. Low Cl homologues were formed in or near the combustion chamber, higher Cl homologues were formed further in the post-combustion region. PCDDs, in part, were formed from C_6 fragments.	1.82
E. Wikstrom, S. Ryan, A. Touati, B. Gullett (2004)	In Situ Formed Soot Deposit as a Carbon Source for Polychlorinated Dibenzo-*p*-dioxins and Dibenzofurans	The presence of soot alone is not sufficient to initiate *de novo* formation. Fly-ash must be present. PCDF are formed by direct release from the carbon network. PCDD are formed via this manner and from condensation of C_6 fragments.	1.83
E. Wikstrom, S. Ryan, A. Touati, M. Telfer, D. Tabor, B. Gullett (2003)	Importance of Chlorine Speciation on the de Novo Formation of Polychlorinated Dibenzo-*p*-dioxins and Polychlorinated Dibenzofurans	Ash bound Cl alone was found to be sufficient for PCDD/F formation. HCl did not influence yields or degree of chlorination. Cl_2 (only at temps high enough to produce Cl radicals) increased yields, especially of hepta- and octa-congeners, but ash bound seems to be the dominant chlorinating agent.	1.84
E. Wikstrom, S. Ryan, A. Touati, B. Gullett (2003)	Key Parameters for de Novo Formation of Polychlorinated Dibenzo-*p*-dioxins and Dibenzofurans	Fast *de novo* formation occurs within the first mins. on the order of 100s of pmol/min. Gas phase Cl_2 is an important PCDF rate controlling parameter. Rxn. temp. found to be most important parameter.	1.85
S. Ryan, A. Touati, E. Wikstrom, B. Gullett (2003)	Gas- and Solid-phase Partitioning of PCDDs/Fs on MSWI Fly Ash and the Effects of Sampling	Developed a novel sampling technique to determine the actual partitioning between PCDD/F in the gas and solid phase.	1.86

(table con'd)

Authors (Year)	Title	Key Findings	Ref.
M. Telfer, B. Gullett (2002)	Experimental Investigations of Homogeneous Gas-phase SO_2 and Cl_2 Reactions for PCDD/F Supression	Gas-phase interactions of title compounds may affect PCDD/F formation from molecular precursors.	1.87
F. Iino, D. Tabor, T. Imagawa, B. Gullett (2001)	Experimental dechlorination isomer patterns of PCDFs, PCDDs, PCNs, and PCBs from their fully chlorinated species	Thermal dechlorination (by CuO) experiments resulted in isomer patterns similar to those from MWIs.	1.88
E. Wikstrom, A. Touati, M. Telfer, B. Gullett (2001)	The Importance of Chlorine Sources During 1 Second *De Novo* Formation of PCDD and PCDF in an Entrained-Flow Reactor	Cl_2 is the major chlorination agent that controls chlorination during fast *de novo* formation.	1.89
B. Gullett, J. Dunn, K. Raghunathan (2000)	Effect of Cofiring Coal on Formation of Polychlorinated Dibenzo-*p*-Dioxins and Dibenzofurans during Waste Combustion	Higher S content in coal lowers PCDD/F formation. Proposed that higher SO_2 conc. from co-firing coal displaces sulfate/chlorine equilibrium in surface wall deposits, thereby decreasing Cl contact with active sites to produce PCDD/F.	1.90
B. Gullett, A. Touati, C. Lee (2000)	Formation of Chlorinated Dioxins and Furans in a Hazardous-Waste-Firing Industrial Boiler	Boiler tube deposits are sinks for PCDD/F reactants (C, Cu, Cl) and PCDD/F, which results in PCDD/F formation long after waste co-firing is ceased.	1.91
F. Iino, T. Imagawa, B. Gullett (2000)	Dechlorination-Controlled Polychlorinated Dibenzofuran Isomer Patterns from Municipal Waste Incinerators	Tetra- though hepta- PCDF are formed by dechlorination of an octa- chlorinated furan parent. This did not hold true for PCDD formation, indicating separate formation mechanisms.	1.92
B. Gullett, E. Wikstrom (1998)	Use of Mono- to Tri-chlorinated Dibenzodioxin (CDD) and Dibenzofuran (CDF) Congeners/Homologues as Indicator of Tetra- or Octa-CDD/CDF Emissions from Municipal Waste/Coal Combustion	1,2,3-TrCDF and 2,4,6-TrCDF can serve as indicators for flue gas PCDD/F concentrations.	1.93

(table con'd)

Authors (Year)	Title	Key Findings	Ref.
H. Hunsinger, H. Seifert, K. Jay (2003)	Formation of PCDD/F During Start-up of MSWI	PCDD/F are formed in large amounts during start up due to ineffective combustion conditions. Increased SO_2 concentrations can reduce PCDD/F emissions.	1.94
H. Hunsinger, K. Jay, J. Vehlow (2002)	Formation and Destruction of PCDD/F Inside a Grate Furnace	High PCDF formation was observed during fuel burnout. Formation was greatly influenced by fuel composition and the burnout characteristics of the fuel bed. Fuel with low Cl and Cu content resulted in negligible PCDD/F formation.	1.28
P. Lemieux, C. Lutes, J. Abbott, K. Aldous (2000)	Emissions of Polychlorinated Dibenzo-*p*-dioxins and Polychlorinated Dibenzofurans from Open Burning of Household Waste in Barrels	Backyard burning emits more PCDD/F on a mass burned basis than various types of incinerators. 2-40 household burning their trash daily can produce average PCDD/F emission comparable to a 182,000 kg/day MWC facility.	1.12
V. De Jong, M. Cieplik, R. Louw (2004)	Formation of Dioxins in the Catalytic Combustion of Chlorobenzenes and a Micropollutant-Like Mixture on Pt/γ-Al_2O_3	With ClBz, at intermediate T, mostly polychlorinated benzenes are formed, along with PCDD/F. With the micropollutant mixture, where Cl level were 20 fold lower, PCDD/F levels were 30x higher, which is attributed to small amount of Clphenols in the mix.	1.95
R. Louw, S. Ahonkhai (2002)	Radical/Radical vs. Radical/Molecule Reactions in the Formation of PCDD/Fs from (chloro)phenols in Incinerators	O-H bond of 2,4,6-TCP and PCP is 5 and 4 kcal mol^{-1}, respectively, than for phenol. Finds radical-molecule route to PCDD to be negligible.	1.35
I. Wiater-Protas, R. Louw (2001)	Gas-Phase Chemistry of Chlorinated Phenols – Formation of Dibenzofurans and Dibenzodioxins in Slow Combustion	Phenol, *o*-chlorophenol, 2,4,6-trichlorophenol and pentachlorophenol differ little in overall rates of conversion to CO and CO_2. Show evidence to support radical-molecule route to PCDD to be insignificant since in real systems, most chlorinated phenol reactants will have on *ortho*- H available, which will result in mostly PCDF formation via radical-radical pathways.	1.96

(table con'd)

Authors (Year)	Title	Key Findings	Ref.
I. Wiater, J. Born, R. Louw (2000)	Products, Rates, and Mechanism of Gas-Phase Condensation of Phenoxy Radical between 500-840 K	Phenoxy radical dimerization (C-C) occurs close to 10^{10} M^{-1} s^{-1}. Extended rxn. mechanism regarding the fate of phenoxy radical upon various coupling geometries.	1.31
M. Cieplik, M. Oviedo, R. Louw (2000)	On the Possible Roles of Acetylene in Gas-Phase Dioxin Formation	Slow combustion of benzene/phenol yields dibenzofuran as a major product of combustion. Addition of acetylene did not alter yields, thus questioning the role of molecular growth in PCDD/F formation.	1.97
I. Wiater, R. Louw (1999)	Reactions of Diphenyl Ether with Chlorine and Bromine Atoms Around 750 K – Relevance for Gas Phase "Dioxin" Formation	With Cl and Br, splitting of diphenyl ether to halobenzene and phenoxy radical was found to be in competition with H atom abstraction. Based on this, displacement of Cl and Br must have $E_a > 20$ kcal mol^{-1}, indicating that the radical-molecule route to PCDD is insignificant.	1.98
G. Soederstroem, S. Marklund (2004)	Formation of PBCDD and PBCDF During Flue Gas Cooling	PBCDD/F show increased halogenation as the flue gas is sampled as port of decreasing T. The Cl/Br ratio also increased with reduction in T.	1.99
S. Marklund, G. Soederstroem (2003)	Different Formation Mechanisms of Dioxins in Combustion Systems When Chlorine or Bromine is Present	Brominated aromatics form more readily than their chlorinated counterparts do. The HBr level is a greater factor in bromination rxns. and not the number of catalytic sites as is the case for chlorination. A Br-Cl exchange on the molecule or enhanced Cl radical formation from BrCl explains higher chlorination when Br is present.	1.100
G. Soederstroem, S. Marklund (2002)	PBCDD and PBCDF from Incineration of Waste-Containing Brominated Flame Retardants	PBDD/F are formed more readily than PCDD/F, however, the addition of Br increases the PCDD/F levels.	1.101
V. Pekarek, R. Grabic, S. Marklund, M. Puncochar, J, Ullrich (2001)	Effects of Oxygen on Formation of PCB and PCDD/F on Extracted Fly Ash in the Presence of Carbon and Cupric Salt	*De novo* PCDD/F and PCB formation is greatly enhanced by presence of oxygen. Oxygen regenerated Cu(II), which is reduced to Cu(I) during rxn. Observed chlorinated benzenes 30x higher than chlorinated phenols.	1.44

(table con'd)

Authors (Year)	Title	Key Findings	Ref.
J. Ryu, J. Mulholland, J. Dunn, F, Iino, B. Gullett (2004)	Potential Role of Chlorination Pathways in PCDD/F Formation in a Municipal Waste Incinerator	A conditional probability model was developed to correlate predicted and observed PCDD/F isomer patterns. Observed PCDF isomers patters agreed well with the predicted, PCDD did not, suggesting that DD chlorination is not an important factor.	1.102
J. Oh, A. Touati, B. Gullett, J. Mulholland (2004)	PCDD/F TEQ Indicators and Their Mechanistic Implications	Chlorination/dechlorination rxns. control PCDF isomers, whereas condensation of phenol precursors determines the ultimate PCDD isomer yields.	1.103
J. Ryu, J. Mulholland, J. Oh, D. Nakahata, D. Kim (2004)	Prediction of Polychlorinated Dibenzofuran Congener Distribution from Gas-Phase Phenol Condensation Pathways	The distribution of dibenzofuran and the 135 PCDF congeners can be predicted from gas-phase chlorophenol concentrations.	1.104
J. Ryu, J. Mulholland, B. Chu (2003)	Chlorination of Dibenzofuran and Dibenzo-*p*-dioxin Vapor by Copper (II) Chloride	Total yields of CDF/CDD products suggested nearly 100% of available $CuCl_2$ was utilized. With a contact time of 5s, OCDF was the dominant furan product. DF/DD chlorination was strongly favored at lateral sites.	1.105
J. Ryu, J. Mulholland (2002)	Dioxin and Furan Formation on $CuCl_2$ from Chlorinated Phenols with One Ortho Chlorine	PCDD formation was favored of PCDF. 2,3,4-TCP formed PCDD in the greatest yield. 2,3-DCP and 2,3,4,5-TeCP formed PCDF in the greatest yield. Cl substitution in the phenol coupling step was analogous to gas-phase formation.	1.106
J. Mulholland, U. Akki, Y. Yang, J. Ryu (2001)	Temperature Dependence of DCDD/F Isomer Distributions from Chlorophenol Precursors	At high T, product distributions are consistent with calculated thermodynamic distributions. This was not the case at low T, indicating kinetic control.	1.25
J. Mulholland, J. Ryu (2001)	Formation of Polychlorinated Dibenzo-*p*-dioxins by $CuCl_2$-Catalyzed Condensation of 2,6 Chlorinated Phenols	PCDD yields were greatest between 350-450 °C, with 60% conversion of phenols (2,6-, 2,3,4,6- and penta) at a gas velocity of 2.7 cm/s. 1,2,3,4,6,8-HCDD was the dominant isomer form from 2,4,6-TrCP and penta, and is also a major constituent of actual incinerators.	1.107

(table con'd)

Authors (Year)	Title	Key Findings	Ref.
D. Nakahata, J. Mulholland (2000)	Effect of Dichlorophenol Substitution Pattern on Furan and Dioxin Formation	2,3-, 2,4-, and 2,5-DCP was investigated (gas-phase). TeCDF yields were greatest from 2,3- and 2,5-DCP. DCDD yields were greatest 2,3- and 2,4-DCP.	1.108
Y. Yang, J. Mulholland, U. Akki (1998)	Formation of Furans by Gas-phase Reactions of Chlorophenols	Maximum yields observed between 600-650 °C. O_2 lowers maximum. Statistical and steric factors control product distribution.	1.32
A. Fullana, H. Nakka, A. Sidhu (2003)	Carbon Chlorination in De Novo Formation Mechanisms	Presented new results which contradict the *de novo* theory, which states than chlorination and oxidation of solid carbon produces PCDD/F. Instead, the yield of PCDD/F appears to be directly related to the soluble organic fraction of carbon.	1.109
S. Sidhu, A. Fullana (2003)	Impact of Soot Concentration on PCDD/F Emissions	Soot oxidation without fly-ash didn't produce semi-volatiles. Only when fly-ash (catalyst) was present were chlorinated benzenes formed, although most (90%) were formed from material adsorbed to the fly-ash rather than carbonaceous materials.	1.110
S. Sidhu, P. Edwards (2002)	Role of Phenoxy Radicals in PCDD/F Formation	The suspected PCDD/F products were formed from 2-chlorophenol, along with some PCDD/F due to dechlorination and condensation of 2-chlorophenol. The radical-radical mechanism is dominant.	1.111
P. Weber, E. Dinjus, L. Stieglitz (2001)	The Role of Copper(II) Chloride in the Formation of Organic Chlorine in Fly-Ash	Under and inert atmosphere, chlorination rxns. stop after all Cu(II) has been reduced. Copper reduction is essential for the formation of organic Cl.	1.48
K. Hell, L. Stieglitz, E. Dinjus (2001)	Mechanistic Aspects of the De-Novo Formation of PCDD/PCDF on Model Mixtures and MSWI Fly Ashes Using Amorphous ^{12}C- and ^{13}C-Labeled Carbon	Approximately half of PCDD is derived from smaller, C_6 chlorophenol or chlorobenzene precursors. The condensation rxns. of these C_6 species don't play a role in the formation of PCDF.	1.20

(table con'd)

Authors (Year)	Title	Key Findings	Ref.
L. Stieglitz (1998)	Selected Topics on the De Novo Synthesis of PCDD/PCDF on Fly Ash	Cu(II)Cl is essential for chlorinating macromolecular carbon and oxidation degradation of the carbon matrix to liberate PCDD/F.	1.46
K. Tuppurainen, A. Asikainen, P. Ruokojarvi, J. Ruuskanen (2003)	Perspectives on the Formation of Polychlorinated Dibenzo-p-dioxins and Dibenzofurans during Municipal Solid Waste (MSW) Incineration and Other Combustion Processes	A review focusing on metal catalyzed PCDD/F formation from chlorinated phenols. A final conclusion is that chlorophenols are among the most important species for PCDD/F formation.	1.112
K. Tuppurainen, P. Ruokojarvi, A. Asikainen, M. Aatamila, J. Ruuskanen (2000)	Chlorophenols as Precursors of PCDD/Fs in Incineration Processes: Correlations, PLS Modeling, and Reaction Mechanisms	Almost all chlorophenol isomers correlate with PCDD/F in the gas-phase, but primarily 2,3,4,6,- and 2,3,4,5,6- correlate in the particle phase, indicating that their coupling/dechlorination/chlorination rxns. may be most important for PCDD/F formation.	1.113
K. Tuppurainen, J. Ruuskanen (1999)	A Plausible Mechanism for Copper-Catalyzed Oxidative Chlorophenol Coupling Reactions. Semi-empirical AM1 and *Ab Initio* 3-21 G Molecular Orbital Studies	The only aromatic carbon bearing a substantial positive charge is the para carbon of the chlorophenoxonium cation, indicating PCDD/F formation mechanism for copper-catalyzed oxidative phenol coupling in which dinuclear phenolate-bridged Cu(II) species act as intermediates affording chlorophenoxonium cations after a double-bond one-electron transfer.	1.34
R. Weber, K. Nagai, J. Nishino, H. Shiraishi, M. Ishida, T. Takasuga, K. Konndo, M. Hiraoka (2002)	Effects of Selected Metal Oxides on the Dechlorination and Destruction of PCDD and PCDF	Copper compounds showed the highest activity for dechlorination and destruction. After 30 minutes at 340 °C, less than 1% of initial OCDD and OCDF was recovered as TeCDD/F-OCDD/F. Model fly-ash $Ca(OH)_2$ exhibited highest destruction, but lowest dechlorination potential.	1.114

(table con'd)

Authors (Year)	Title	Key Findings	Ref.
R. Weber, H. Hagenmaier (1999)	Mechanism of the Formation of Polychlorinated Dibenzo-*p*-dioxins and Dibenzofurans from Chlorophenols in Gas-Phase Reactions	Developed detailed PCDD/F gas-phase formation mechanisms based on phenoxy radical coupling rxns. Identified a dihydrobiphenyl PCDF intermediate and *ortho*-phenoxyphenols intermediate in PCDD formation. Extended a very through discussion on Cl position on the aromatic ring in determining which and if PCDD and PCDF isomers form.	1.19
R. Weber, T. Takasuga, H. Hagenmaier (1999)	Role of Basic Oxides on the De Novo Synthesis of PCDD/PCDF and the Influence of the Gas Phase Composition	Basic oxides decrease *de novo* PCDD/F formation. HCl can decrease the inhibitory effect without neutralizing the ash itself.	1.115
R. Weber, H. Hagenmaier (1998)	PCDD/PCDF Formation in Fluidized Bed Incineration	PCDD/F isomer distributions patters in fluidized bed incinerators are distinctly different from grate fired combustors. Chlorophenols in the fly-ash correlate better with PCDD/F than those in the gas-phase.	1.116
R. Grabic, V. Pekarek, E. Fiserova, J. Ullrich, J. Karban, S. Crhova, T. Tomsej (2002)	Study of the Effect of Matrix on Formation of PCDD, PCDF, PCB, and PCBz by De Dovo Synthesis Reactions under Model Laboratory Conditions	PCDD/F formed from a fly-ash matrix has a different composition vs. silica gel matrix. CaO increase the matrix pH and decreases *de novo* synthesis.	1.117
J. Conesa, A. Fullana, R. Font (2002)	De Novo Synthesis of PCDD/F by Thermogravimetry	$CuCl_2$ greatly accelerates carbon degradation. The presence of Cl generating species is also critical for carbon degradation. $CuCl_2$ produces almost 100 times more PCDD/F than CuO+HCl.	1.118
E. Voncina, T. Solmajer (2002)	Thermolysis of 2,4,6-trichlorophenol Chemisorbed on Aluminum Oxides as Example of Fly Ash Mediated Surface Catalysis Reaction in PCDD/PCDF Formation	2,4,6-TCP chemisorbs to alumina as chlorophenoxy. Thermolysis results in homolytic cleavage of the Al-O bond, which results in the formation of trichlorophenoxy radical that quickly transform into pre-dioxins.	1.57

(table con'd)

Authors (Year)	Title	Key Findings	Ref.
M. Hirota, J. Kato, N. Saito, A. Fuwa (2001)	Catalytic Effects of Copper on Dibenzo-p-dioxins and Polychlorinated Dibenzo-p-dioxin Generations using *Ab Initio* Molecular Orbital Methods	Proposed that the role of copper in PCDD/F formation include: 1)stabilization of the total energy owing to the absorption of phenol, 2)reduction of the oxygen-hydrogen bond strength in phenol, 3)reduction of the steric effect of the hydrogen atom in the pre-dioxin.	1.119
C. Xhrouet, C. Pirad, E. Pauw (2001)	De Novo Synthesis of Polychlorinated Dibenzo-*p*-dioxins and Dibenzofurans on Fly Ash from a Sintering Process	A second maximum in PCDD/F formation was found at 400 °C on sinter fly-ash. Decomposition rxns. become important at long rxn. time. PCDD/F ratio is independent of rxn. time. PCDF are more stable than PCDD at higher temps. *De novo* synthesis explains PCDF formation, but PCDD must be formed from precursors.	1.120
P. Fermo, F. Cariati, S. Santacesari, S. Bruni, M. Lasagni, M. Tettamanti, E. Collina, D. Pitea (2000)	MSWI Fly Ash Native Carbon Thermal Degradation: A TG-FTIR Study	To act as a catalyst, copper has to be present in a free ionic form and not bound as in CuO. $CuSO_4$ is relatively inactive as a catalyst, but may be due to its stability as an ionic salt. Low-temperature carbon gasification is strongly dependent on the catalyst.	1.121
T. Hatanaka, T. Imagawa, M. Takeuchi (2000)	Formation of PCDD/Fs in Artificial Solid Waste Incineration in a Laboratory-Scale Fluidized-Bed Reactor: Influence of Contents and Forms of Chlorine Sources in High-Temperature Combustion	As the Cl content of the waste increased, CO and PCDD/F increased when PVC and NaCl was used as the Cl source. CO and PCDD/F concentrations strongly correlate.	1.122

1.2 Patnaik, P. *A Comprehensive Guide to the Hazardous Properties of Chemical Substances*; Reinhold: New York, 1992.

1.3 Mitrou, P.I.; Dimitriadis, G.; Raptis, S.A. *European Journal of Internal Medicine* **2001**, *12*, 406.

1.4 Landers J.P.; Brunce, N.J. *Biochemical Journal* **1991**, *276*, 273.

1.5 Altwicker, E.R.; Schonberg, J.S.; Ravi, K.N.V. K.; Milligan, M.S. *Hazard. Waste. Hazard Mater*. **1990**, *7*, 73.

1.6 Thomas, V.M.; Spiro, T.G. *Environ. Sci. Technol.* **1996**, *30*, 82A.

1.7 Thomas, V.M.; Spiro, T.G. *Toxicol. Environ. Chem*. **1995**, *50*, 1.

1.8 "Comments on the U.S. EPA Dioxin Exposure and Health Documents;" American Hospital Association; Chacago, IL, Jan. 13, 1995.

1.9 Cudahy, J.J.; Rigo, H. G. *J. Air & Waste Manage. Assoc.* **1998**, *48*, 1107.

1.10 Heindl, A.; Hutzinger O. *Chemosphere* **1986**, *15*, 653.

1.11 Dobbs, A.J.; Grant, C *Chemosphere* **1981**, *10*, 1185.

1.12 Lemieux, P.M.; Lutes, C.C.; Abbott, J.A.; Aldous, K.M. *Environ. Sci. Technol.* **2000**, 34, 377.

1.13 Baker, J.I.; Hites,R.A. *Environ. Sci. Technol.* **2000**, *34*, 2886.

1.14 Bumb, R.R.; Crummett, W.B.; Cutie, S.S.; Gledhill, J.R.; Hummell, R.H.; Kagel, R.O.; Lamparski, L.L.; Luoma, E.V.; Miller, D.L.; Nestrick, T.J.; Shadoff, L.A.; Stehl, R.H.; Woods, J.S. *Science* **1980**, *210*, 385.

1.15 Olie, K.; Vermeulen, P.L.; Hutzinger, O. *Chemosphere* **1977**, *6*, 455.

1.16 Huang, H.; Buekens, A. *Chemosphere* **1995**, *31*, 4099.

1.17 Fielder, H. *Environ. Eng. Sci.* **1998**, *15*, 49.

1.18 Tupporainen, K.A.; Ruokojarvi, P.H.; Asikainen, A.H.; Aatamilia, M.; Ruuskinen, J. *Environ. Sci. Technol.* **2000**, *34*, 4958.

1.19 Weber, R.; Hagenmaier, H. *Chemosphere* **1999**, *38*, 529.

1.20 Hell, K.; Stieglitz, L.; Dinjus, E. *Environ. Sci. Technol*. **2001**, *35*, 3892.

1.21 Sidhu, S.; Maqsud, L.; Dellinger, B.; Mascolo, G. *Combust. Flame* **1995**, *100*, 11.

1.22 Karasek, F.W.; Dickson, L.C. *Science* **1987**, *237*, 754.

1.23 Altwicker, E.R.; Milligan, M.S. *Chemosphere* **1993**, *27*, 301.

1.24 Evans, C.S.; Dellinger, B. *Environ. Sci. Technol.* **2003**, *37*, 1325.

1.25 Mulholland, J. A.; Akki, U.; Yang, Y.; Ryu, J.Y. *Chemosphere* **2001**, *42*, 719.

1.26 Dempsey, C.R.; Oppelt, E.T. *J. Air & Waste Manag.* **1993**, *43*, 25.

1.27 Bruce, K.R.; Beach, L.O.; Gullett, B.K. *Waste Management* **1991**, *11*, 97.

1.28 Hunsinger, H.; Jay, K.; Vehlow, J. *Chemosphere* **2002**, *46*, 1263.

1.29 Shaub, W.M.; Tsang, W. *Environ. Sci. Technol.* **1983**, *17*, 721.

1.30 Khachatryan, L.; Asatryan, R.; Dellinger, B. *Chemosphere* **2003**, *52*, 695.

1.31 Wiater, I.; Born, J.G.P.; Louw, R. *Eur. J. Org. Chem.* **2000**, 921.

1.32 Yang, Y.; Mulholland, J.A.; Akki, U. *Proc. Comb. Inst.. (27th Symposium (International) on Combustion/The Combustion Institute)* **1998**, *27*, 1761.

1.33 Khachatryan, L.; Burcat, A.; Dellinger, B. *Combust. Flame* **2003**, *132*, 406.

1.34 Tuppurainen, K.; Ruuskanen, J. *Chemosphere* **1999**, *38*, 1825.

1.35 Louw, R.; Ahonkhai, S.I. *Chemosphere*, **2002**, 1273.

1.36 Evans, C.S., dissertation for a Ph.D degree at Louisiana State University, **2004**.

1.37 Truce, W.E.; Kreider, E.M.; Brand, W.W. *Org. React.* **1970**, *18*, 99.

1.38 Milligan, M.S.; Altwicker, E.R. *Environ. Sci. Technol.* **1996**, *30*, 230.

1.39 Stieglitz, L.; Vogg, H. *Chemosphere* **1987**, *16*, 1917.

1.40 Lomnicki, S.; Dellinger, B. *J. Phys. Chem. A*, **2003**, *107*, 4387.

1.41 Kirby, C.S.; Rimstidt, J.D. *Environ. Sci. Technol.*, **1993**, *27*, 652.

1.42 Hinton, W.S.; Lane, A.M. *Chemosphere*, **1991**, *23*, 831.

1.43 Addink, R.; Olie, K. *Environ. Sci. Technol.*, **1995**, *29*, 1425.

1.44 Pekarek, V.; Grabic, R.; Marklund, S.; Puncochar, M.; Ullrich, J. *Chemosphere*, **2001**, *43*, 777.

1.45 Altwicker, E.R. *Chemosphere,* **1996**, *33*, 1897.

1.46 Stieglitz, L. *Environ. Eng. Sci*, **1998**, *15*, 5.

1.47 Addink, R.; Altwicker, E.R. *Environ. Eng. Sci.*, **1998**, *15*, 19.

1.48 Weber, P.; Dinjus, E.; Stieglitz, L. *Chemosphere,* **2001**, *42*, 579.

1.49 Addink, R.; Bakker, W.C.M.; Olie, K. *Environ. Sci. Technol.*, **1995**, *29*, 2055.

1.50 Stieglitz, L; Bautz, H.; Roth, W.; Zwick, G. *Chemosphere*, **1997**, *34*, 1083.

1.51 Hell, K.; Stieglitz, L.; Altwicker, E.R.; Addink, R.; Will, R. *Chemosphere,* **2001**, *42*, 697.

1.52 Milligan, M.S.; Altwicker, E.R. *Environ. Sci. Technol.*, **1996**, *30*, 225.

1.53 Karasek, F.W.; Dickson, L.C. *Science*, **1992**, *237*, 754.

1.54 Milligan, M.S.; Altwicker, E.R. *Environ. Sci. Technol.*, **1996**, *30*, 230.

1.55 Huang, H.; Buekens, A.; Jacobs, P. *Organohalogen Compounds*, **1999**, *41*, 125.

1.56 Farquar, G.R.; Alderman, S.L.; Poliakoff, E.D.; Dellinger, B. *Environ. Sci. Technol.* **2003**, *37*, 931.

1.57 Voncina, E.; Solmajer, T. *Chemosphere,* **2002**, *46*, 1279.

1.58 Boyd, S. A.; Mortland, M. M. *Environ.Sci.Technol.* **1986**, *20*, 1056.

1.59 Ghorishi, S.B.; Altwicker, E.R.; *Environ. Sci. Technol.*, **1995**, *29*, 1156.

1.60 Larrubia, M. A.; Busca, G. *Appl. Catal. B: Environmental* **2002**, *39*, 343.

1.61 Blumenstsock, M.; Zimmermann, R.; Schramm, K.W.; Kaune, A.; Nikolai, U.; Lenoir, D.; Kettrup *J. Anal. Appl. Pyrolysis*, **1999,** *49*, 179.

1.62 Khachatryan, L.; Dellinger, B. *J. Chem. Soc., Perkin Trans.* **2002**, *2*, 779.

1.63 Khachatryan, L.; Dellinger, B. *Chemosphere*, **2003**, *52*, 709.

1.64 Wehrmeier, A.; Lenoir, D.; Sidhu, S. S.; Taylor, P. H.; Rubey, W. A.; Kettrup, A.; Dellinger, B. *Environ. Sci. Technol.* **1998**, *32*, 2741.

1.65 Froese, K. L.; Hutzinger, O. *Environ. Sci. Technol.* **1996**, *30*, 998.

1.66 Addink, R.; Altwicker, E.R. *J. Harard. Mat*., **2004**, *114*, 53.

1.67 Addink, R.; Altwicker, E.R. *Environ. Sci. Technol*., **2004**, *39*, 5196.

1.68 Ryan, S.P.; Altwicker, E.R. *Environ. Sci. Technol*. **2004**, *38*, 1708.

1.69 Addink, R.; Altwicker, E.R. *Chemosphere*, **2001**, *44*, 1361.

1.70 Ryan, S.P.; Altwicker, E.R. *Chemosphere*, **2000**, *40*, 1009.

1.71 Hell, K.; Altwicker, E.R.; Stieglitz, L.; Addink, R. **2000**, *40*, 995.

1.72 Buekens, A.; Brown, P.; Klaus, J. *Organohalogen Cmpds*., **2003**, *63*, 175.

1.73 Huang, H.; Buekens, A. *Chemosphere*, **2001**, *44*, 1505.

1.74 Huang. H.; Buekens, A. Chemosphere, **2000**, *41*, 943.

1.75 Khachatryan, L.; Asatryan, R.; Dellinger, B. *J. Phys. Chem. A*, **2004**, *108*, 9567.

1.76 Alderman, S.L.; Farquar, G.F.; Poliakoff, E.D.; Dellinger, B. *Proc. Comb. Inst*., **2004**, *in press*.

1.77 Evans, C.; Dellinger, B. *Environ. Sci. Technol*., **2003**, *37*, 5574.

1.78 Asatryan, R.; Davtyan, A.; Khachatryan, L.; Dellinger, B. *Organohalogen. Cmpds*., **2002**, *56*, 277.

1.79 Lomnicki, S.; Dellinger, B *Proc. Comb. Inst*., **2002**, *41*, 943.

1.80 Taylor, P.H.; Sidhu, S.S.; Rubey, W.A.; Dellinger, B.; Wehrmeier, A.; Lenoir, D. Schramm, K.W. *Proc. Comb. Inst*. **1998**, *27*, 1769.

1.81 H. Fiedler, *Environ. Eng. Sci.*, **1998**, *15*, 49.

1.82 Wikstrom, E.; Ryan, S.; Touati, A.; Tabor, D.; Gullett, B. *Environ. Sci. Technol*., **2004**, *38*, 3778.

1.83 Wikstrom, E.; Rhan, S.; Touati, A. Gullett, B.K. *Environ. Sci. Technol*. **2004**, *38*, 2097.

1.84 Wikstrom, E.; Ryan, S.; Touati, A.; Telfer, M.; Tabor, D.; Gullett, B.K. *Environ. Sci. Technol*., **2003**, *37*, 1108.

1.85 Wikstrom, E.; Ryan, S.; Touati, A.; Gullett, B.K. *Environ. Sci. Technol.*, **2003**, *37*, 1962.

1.86. Ryan, S.; Touati, A.; Wikstrom, E.; Gullett, B.K. *Organohalogen, Cmpds*., **2003**, *63*, 45.

1.87 Telfer, M.; Gullett, B. *Organohalogen Cmpds*., **2002**, *56*, 353.

1.88 Iino, F.; Tabor, D.G.; Imagawa, T.; Gullett, B.K. *Organhalogen Cmpds*., **2001**, *50*, 447.

1.89 Wikstrom, E.; Touati, A.; Telfer, M.; Gullett, B.K. *Organohalogen Cmpds*., **2001**, *50*, 336.

1.90 Gullett, B.K.; Dunn, J.E.; Raghunathan, K. *Environ. Sci. Technol*., **2000**, *34*, 282.

1.91 Gullett, B.K.; Touati, A.; Lee. C.W. *Environ. Sci. Technol*., **2000**, *34*, 2069.

1.92 Iino, F.; Imagawa, T.; Gullett, B.K. *Environ. Sci. Technol*., **2000**, *34*, 3143.

1.93 Gullett, B.K.; Wikstrom, E. *Organohalogen Cmpds*., **1998**, *36*, 179.

1.94 Hunsinger, H.; Seifert, H.; Jay, K. *Organohalogen Cmpds*., **2003**, *63*, 37.

1.95 De Jong, V.; Cieplik, M.K.; Louw, R. *Environ. Sci. Technol*., **2004**, *38*, 5217.

1.96 Wiater-Protas, I.; Louw, R. *Eur. J. Org. Chem*., **2001**, 3945.

1.97 Cieplik, M.K.; Oviedo, M.C.; Louw, R. *Chemosphere*, **2000**, *40*, 195.

1.98 Wiater, I.; Louw, R. *Eur. J. Org. Chem*., **1999**, 261.

1.99 Soederstroem, G.; Marklund, S. *Environ. Sci. Technol.*, **2004**, *38*, 825.

1.100 Soederstroem, G.; Marklund, S *Organohalogen Cmpds*., **2003**, *63*, 1026.

1.101 Soederstroem, G.; Marklund, S *Environ. Sci. Technol.*, **2002**, *36*, 1959.

1.102 Ryu, J.Y.; Mulholland, J.A.; Dunn, J.E.; Iion, F.; Gullett, B.K. *Environ. Sci. Technol*., **2004**, *38*, 5112.

1.103 Oh, J.E.; Touati, A.; Gullett, B.K.; Mulholland, J.A. *Environ. Sci. Technol*., **2004**, *38*, 4694.

1.104 Ryu, J.Y.; Mulholland, J.A.; Oh, J.E.; Nakahata, D.T.; Kim, D.H. *Chemosphere*, **2004**, *55*, 1147.

1.105 Ryu, J.Y.; Mulholland, J.A.; Chu, B. *Chemosphere*, **2003**, *51*, 1031.

1.106 Ryu, J.Y.; Mulholland, J.A. *Proc. Comb. Inst*., **2002**, *29(pt2)*, 2455.

1.107 Mulholland, J.A.; Ryu, J.Y. *Combust. Sci. Technol.*, **2001**, *169*, 107.

1.108 Nakahata, D.T.; Mulholland, J.A. *Proc. Comb. Inst*., **2000**, *28(pt2)*, 2701.

1.109 Fullana, A.; Nakka, H.; Sidhu, S. *Organohalogen Cmpds*., **2003**, *63*, 147.

1.110 Sidhu, S.; Fullana, A. *Organohalogen Cmpds*. **2003**, *63*, 13.

1.111 Sidhu, S.; Edwards, P. *Inter. J. Chem. Kinetics*, **2002**, *34*, 531.

1.112 Tuppurainen, K.; Asikainen, A.; Ruokojarvi, P.; Ruuskanan, J. *Acc. Chem. Res*., **2003**, *36*, 652.

1.113 Tuppurainen, K.; Ruokojarvi, P.; Asikainen, A.; Aatamila, M. Ruuskanan, J. *Environ. Sci. Technol.*, **2000**, *34*, 4958.

1.114 Weber, R.; Nagai, K.; Nishino, J.; Shiraishi, H.; Ishidi, M.; Takasuga, T.; Konndo, K.; Hiraoka, M. *Chemosphere*, **2002**, *46*, 1247.

1.115 Weber, R.; Hagenmaier, H. *Organohalogen Cmpds*., **1999**, *41*, 297.

1.116 Weber, R.; Hagenmaier, H. *Organohalogen Cmpds*., **1998**, *36*, 337.

1.117 Grabic, R.; Pekarek, V.; Fiserova, E.; Ullrich, J.; Karban, J.; Crhova, S.; Tomsej, T. *Organohalogen Cmpds.*, **2002**, *56*, 205.

1.118 Conesa, J.A.; Fullana, A.; Font, R. *Environ. Sci. Technol.* **2002**, *36*, 263.

1.119 Hirota, M.; Kato, J.; Saito, N.; Fuwa, A. *Toxicological and Environ. Chem*., **2001**, *81*, 133.

1.120 Xhrouet, C; Pirad, C.; de Pauw, E. *Environ. Sci. Tech*., **2001**, *35*, 1616.

1.121 Fermo, P; Cariati, F.; Santacesaria, S.; Bruni, S.; Lasagni, M.; Tettamanti, M.; Collina, E.; Pitea, D. *Environ. Sci. Technol.*, **2000**, *34*, 4370.

1.122 Hatanaka, T.; Imagawa, T.; Takeuchi, M. *Environ. Sci. Technol*., **2000**, *34*, 3920.

CHAPTER 2: EXPERIMENTAL

2.1 Temperature Controlled Dosing Cell

A temperature controlled dosing cell designed for transmission studies was used in all FTIR and XANES experiments and is similar to that described by Basu *et al.*[2.1] Specifically, the cell was used to collect *in situ* the infrared spectra of potential PCDD/F precursors adsorbed to solid fly-ash surrogate substrates and to study, using X-ray spectroscopy, the fate of CuO in a surrogate fly-ash during thermal exposure to the precursors. Several features which make the dosing cell ideal for such studies are: high vacuum operation, random gas transport to all parts of the solid substrate surface, uniform substrate deposition, a sample temperature range from ambient to 900 °C, and very rapid sample heating and cooling rates that permit kinetic studies. The cell was made from a standard stainless steel cube that accepts 2.75-inch conflat (CF) flanges at each face and has an internal volume of 215 cm^3. A schematic of the cell and its components is shown in Figure 2.1.

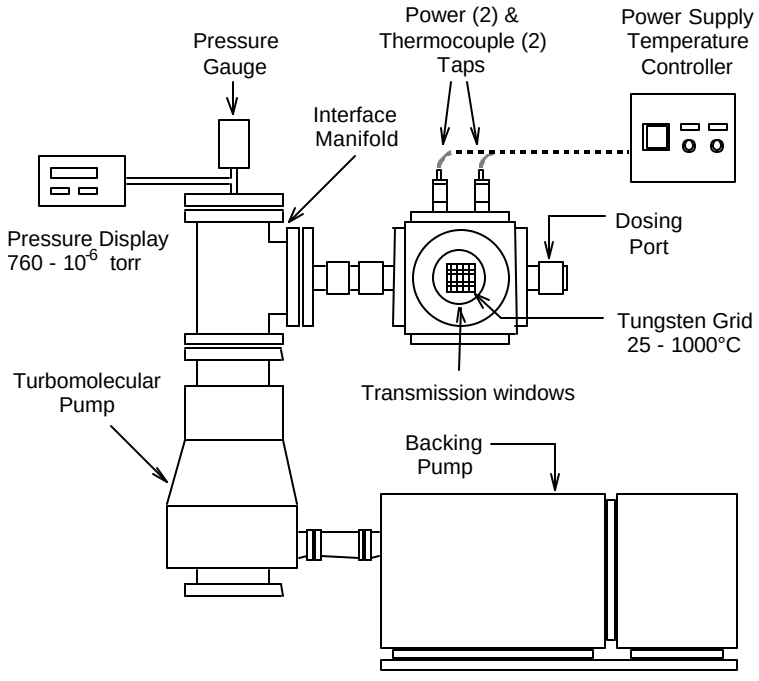

Figure 2.1 A schematic of the dosing cell and its accessories.

Accessory components bolted to each face of the cube include a modified electrical/thermocouple feedthough that makes up the sample holder and heating element, two transmission windows, one vacuum interface manifold, one dosing port flange and one blank bottom flange. The dimensions of the cell are such that it can be directly placed into the FTIR spectrometer sample compartment or between two ion chambers for X-ray absorption studies. A rotary vane and turbomolecular pump are connected to the cell and permit evacuation down to 10^{-6} Torr.

An air-to-vacuum feedthough, with two solid tubular copper power pins and type K thermocouple connector, was modified so that it serves as a sample holder and heating element and is referred to as the grid assembly. To fashion the grid assembly, the copper posts were cut to the necessary length and a vertical slice of each post was removed 25 mm up the length of the post so that the cut out piece was in the shape of a half cylinder. The now flat faces of the copper posts of the feedthrough were drilled and tapped in two places, while the cutout pieces were drilled though. The tungsten grid is securely fastened across the posts between the cut out pieces and faces of the copper posts with Alan head bolts and can be resistively heated. This modification was performed in a manner so that when the grid assembly is bolted to the cell cube, the grid is centered in the cell perpendicular to the transmission windows and normal to the incident infrared or X-ray radiation.

The powder substrate sample under investigation was deposited onto the tungsten grid. This procedure will be described in section 2.2.1. The grid is composed of 0.05 mm diameter wire and is spaced in 0.22 mm intervals and has an infrared transmission of approximately 80 %. Spectra were taken of the portion of sample covering the voids in the grid. The temperature of the grid and substrate was measured with a pre-fabricated 0.08 mm type K (chromel/alumel)

thermocouple spot-welded to the top center of the grid. The tungsten was cleaned by soaking it in a 0.1 M NaOH solution prior to attaching the thermocouple. Each lead of the thermocouple was spot-welded to the corresponding thermocouple pins of the feedthrough. The grid assembly and the dosing cell are shown in Figure 2.2.

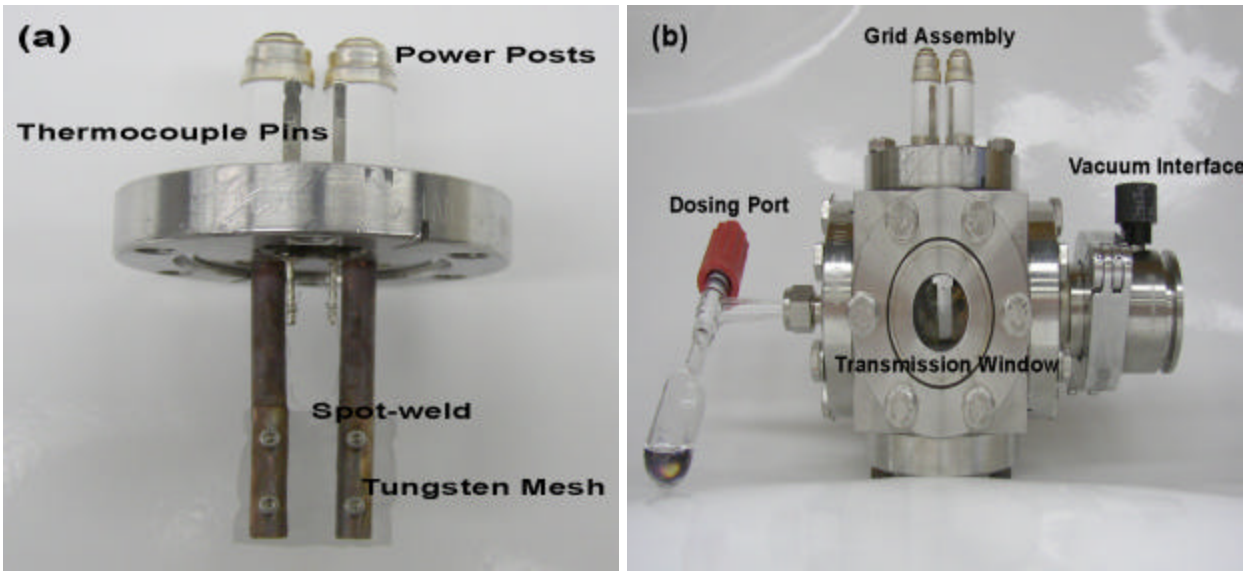

Figure 2.2 (a) The grid assembly that serves as a sample holder and heating element and (b) the dosing cell.

The copper posts of the grid assembly act as heat sinks, thus causing a temperature gradient across the grid. To ensure that the IR beam was intersecting the sample in the center of the grid, where the temperature gradient across the grid is minimal,[2.1] very thin sheet metal blinds were added to the grid assembly that covered all but the center 4 mm of the grid. This was not a requirement for X-ray absorption studies, as the beam position on the grid was determined with X-ray sensitive paper.

Power for heating the grid, and in turn the sample deposited on it, was supplied from a standard AC transformer. A temperature controller and solid-state relay maintained the reaction temperature once it had been approximately set by manually adjusting the voltage setting of the transformer. A high voltage 0.5-ohm edge wound resistor was placed in the circuit to supply the

resistance needed to initiate heating of the grid. A block diagram showing the wiring of electrical components is shown in Figure 2.3.

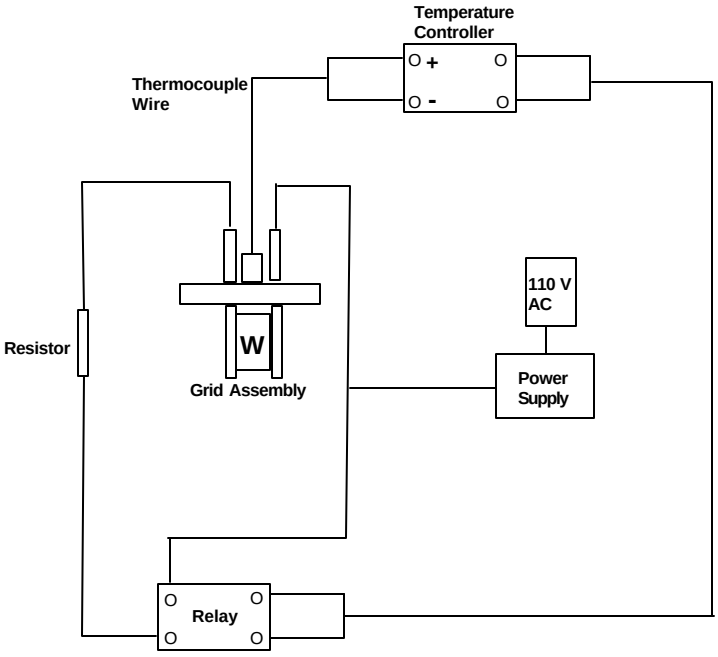

Figure 2.3 The grid assembly and its electrical components.

For FTIR experiments, the transmission windows were hermetically sealed CaF_2 windows embedded in CF flanges. The infrared cutoff of CaF_2 is near 1000 cm^{-1}. Since the silica and silica based substrates under study strongly adsorb incident IR radiation below approximately 1200 cm^{-1}, no advantage was taken from using KBr windows, whose hydroscopic nature make them prone to fogging. For the XANES experiments the transmission windows were made from 100-μm thick Kapton film sealed between two open flanges, with flat Viton gaskets making a vacuum-tight seal between the flange bolted on the cell and the side opposite the knife-edge of the outer flange.

The PCDD/F precursor, or dosant, to be studied was placed in a Pyrex side-arm dosing port that fits a ¼ inch swagelok to CF flange. The sample loaded dosing port had to be evacuated thoroughly prior to performing experiments to remove headspace air. For kinetic measurements, liquid precursors with a vapor pressure of at least 0.8 Torr gave the best results. Under these conditions, the gas phase concentration of the dosant was that of its vapor pressure. Solid phase precursors could be used to obtain qualitative spectra of the adsorbed species, given long reaction times. A high vacuum Teflon valve separated the bulk dosant from the cell interior.

One significant feature of the dosing cell critical to the experiments to be described was the ability to rapidly heat and cool the sample, owing to the low heat capacity of the tungsten grid. The sample could be heated or cooled quickly, thus allowing one to rapidly initiate and quench the reaction. This allowed for time-dependent spectral studies since the reaction could be stopped at known reaction time and a spectrum acquired.

2.2 FTIR Experiments

All FTIR spectra were collected using a Midac M2000 series Fourier transform infrared spectrometer. Spectra were collected in absorbance mode from 4000-1200 cm^{-1} with 2 cm^{-1} resolution. The region below 1275 cm^{-1} could not be examined due to strong absorption by the silica. For most applications, each spectrum consisted of 40-50 scans co-added scans. Depending on the goal of the work to be performed, either the FTIR background was taken of the bare tungsten mesh or of the substrate once it had been supported on the grid, with the latter resulting in a difference absorption spectrum. The first scenario was used in situations such as determining reaction kinetics based on loss of surface hydroxyl groups due to precursor adsorption. Difference spectra were preferred for qualitative analysis since adsorption due to the

substrate was negated. This resulted in a flat baseline, which made it easier to discern subtle spectral features. Midac software was used for peak height analysis and Origin graphing software was used to determine peak frequencies.

2.2.1 Time-Dependent Chemisorption of 2-Chlorophenol on a Silica Surface

Time-dependent adsorption of 2-chlorophenol onto pure silica was monitored *in situ* from 200-500 °C in 50 °C increments. The silica substrate studied was a moderately high surface area silica sold under the trade name Cabosil. Cabosil is a high purity, fumed silica with a surface area of approximately 250 m^2/g, with a particle size on the order of 0.1µm.

To support the substrate on the tungsten grid, an acetone slurry containing 0.25 g of Cabosil and 125 ml of acetone was prepared using an ultrasonic bath. An atomizer was then used to evenly coat the entire tungsten mesh with a fine mist of the suspension. For pure silica, there was no disadvantage to preparing the silica/acetone slurry directly in the atomizer flask. Approximate sonication time was on the order of 45 minutes. Best results were obtained with low air flow though the atomizer and light thumb pressure on the atomizer trigger. Quick bursts of the suspension were used to coat the grid rather than a continuous stream of material. A heat gun was used to evaporate the acetone after every few seconds of application until a uniform layer of the substrate formed over the voids in the grid. The total amount of powder deposited on the grid was typically 10-15 mg. It was important to support an amount of silica on the grid that will give good IR spectra, but not so much to impede transmission due to increase scattering.

For this particular experiment, the IR background was taken over a clean tungsten grid with a cell base pressure of 10^{-6} Torr. Once supported on the grid and placed in the dosing cell, the silica was placed under vacuum to remove of any remaining acetone. The cell was then vented and the sample held at 375 °C for 20 minutes in air to remove organic impurities in the

material before again being placed under vacuum. The Cabosil surface is rich in surface hydroxyl groups and their relative abundance and type can be altered by different thermal treatment.[2.2]

Prior to dosing with 2-chlorophenol, the silica sample was heated under vacuum at 800 °C for 20 minutes. This procedure removed all bound and molecular water and converted all hydrogen bonded, surface hydroxyl groups to siloxanes. Isolated, freely vibrating hydroxyl groups remained on the surface and gave rise to a sharp absorption band at 3747 cm^{-1}. Shoulders on each side of this absorption band at 3743 cm^{-1} and 3751 cm^{-1} are due to freely vibrating geminal hydroxyl groups that are spaced far enough apart as not to mutually hydrogen bond, thus they are not converted to siloxanes during the thermal pre-treatment.[2.3] This method of surface pretreatment facilitates kinetic measurement, as the rate of 2-chlorophenol chemisorption will be determined by measuring the rate of disappearance of surface hydroxyl groups. This technique has been used to measure the rate of adsorption of chlorosilanes on Cabosil. [2.4]

Prior to dosing with 2-chlorophenol, a spectrum was taken of the pretreated, undosed silica to serve as the t = 0 point. The sample was brought up to the desired reaction temperature and 2-chlorophenol vapor was introduced to the cell by opening the dosing port valve. Due to the increased heat transfer from the surface to its surroundings brought about by introduction of the dosant, the surface temperature generally dropped by approximately 20 °C, which made it necessary to slightly increase the voltage across to the grid. The time interval from the introduction of 2-chlorophenol to the cell until the temperature was stabilized was approximately 5-15 seconds. The reaction was allowed to proceed for the desired time and terminating current flow across the grid quickly quenched activated chemisorption.

Before acquiring the spectrum, the supply of 2-chlorophenol was isolated and the cell was evacuated to 5 x 10^{-6} Torr and held for 10 minutes. The surface temperature was held at 150 °C during cell evacuation. This ensured that all free and physisorbed chlorophenol was removed from the cell, thus leaving only chemically adsorbed species on the surface. After collecting the spectrum, the dose/evacuate/acquire spectrum cycle was repeated until the reaction was at or near equilibrium surface coverage.

Since 2-chlorophenol vapor was introduced to the cell from the bulk, and because the cell was evacuated prior to collecting each IR spectrum and fresh 2-chlorophenol admitted to the cell before proceeding to the next time point, the concentration of 2-chlorophenol was essentially constant throughout any given run. Additionally, it has been estimated that a silica surface dehydroxylated at 800 °C will have a hydroxyl surface coverage of less than 1.2 OH groups/100 Å^2.[2.5] Under these conditions, this corresponds to approximately 4 x 10^{18} available surface hydroxyl groups, which are shown to be the sites of adsorption, while the 2-chlorophenol molecular density remains constant an order of magnitude higher, ensuring pseudo-first order conditions.

2.2.2 Time-Dependent Chemisorption of Chlorophenol and Chlorobenzenes on CuO/SiO_2

Time-dependent adsorption spectra of 2-chlorophenol, 1,2-dichlorozenzene and chlorobenzene reacting with a CuO/SiO_2 surface at 350 °C, as well as temperature dependent spectra between 200-500 °C of 2-chlorophenol after 3 minutes of reaction, were collected using procedures similar to those described above.

Copper oxide was supported on Cabosil by the method of incipient wetness, with a copper loading of 5%, on a mass basis. The first step in this preparation was to determine the amount of water needed to achieve incipient wetness for a given amount of Cabosil. Incipient

wetness is the term used when the water added to the silica is either contained within the pore structure and/or bound to adsorption sites on the surface, i.e. no bulk water is present. For Cabosil, this typically corresponded to 7.8 ml/g. Once the correct volume of water had been determined, an aqueous solution of copper(II) nitrate hemipentahydrate ($Cu(NO_3)_2 \cdot 2.5\ H_2O$) of the concentration necessary so as to yield 5% Cu in the CuO/SiO_2 substrate mixed with the correct amount of Cabosil, for instance, 2.26 g of Cabosil would require 0.45 g $Cu(NO_3)_2 \cdot 2.5\ H_2O$. The resulting gel was allowed to stand for 2 hours with occasional stirring before being dried for 7 hours at 100 °C. The blue-green powder was then calcined at 450 °C for 12 hours to convert all $Cu(NO_3)_2$ to CuO. The resulting grey black powder was thoroughly ground with a mortar and pestle before use.

This substrate was then suspended in acetone and applied to the tungsten grid as described above. Sonication times of around 90 minutes were required to achieve a good suspension. For this material, it was best to prepare the slurry in a separate beaker and then decant only the acetone containing the suspended material into the atomizer flask, since the act of supporting the copper on the silica resulted in the formation of some heavier, larger particles that were not sufficiently crushed in the mortar and they will clog the atomizer nozzle. To support enough sample on the tungsten mesh the entire contents of the flask was generally consumed. It was generally more time consuming to prepare copper supported samples than pure Cabosil samples.

After being supported on the grid, the substrate was heated in air at 450 °C to remove any organic impurities before being pumped down to a base pressure of 10^{-6} Torr. The FTIR background spectra were recorded over the substrate, which resulted in the collection of

difference spectra. Operation of the dosing cell and spectral acquisition procedures were identical to that described in the previous section.

2.3 X-ray Absorption Near-Edge Structure Spectroscopy Studies

XANES spectra were collected using the double crystal monochromator beam line[2.6] at the synchrotron radiation source at the Center for Advanced Microstructures and Devices (CAMD), at Louisiana State University.[2.7] At injection, the electron storage ring operates with a beam current ca. 150 mA and typically has a lifetime of 4-8 hours. The photon flux after the monochromator is estimated to be approximately 10^8 s^{-1}. Absorption spectra were collected from 8930-9400 eV. The photon bandwidth was 2 eV and the step size in the region of the Cu K-edge was ~ 0.3 eV. For these experiments, the synchrotron radiation was monochromatized using a pair of Ge(220) crystals.

2.3.1 Data Collection

The time-dependent reduction and speciation of Cu(II) in a CuO/SiO_2 fly-ash was monitored from 275-375 °C in the presence of 2-chlorophenol, 1,2-dichlorobenzene, and chlorobenzene. For these experiments, the surrogate fly-ash substrate was composed of a mixture of Cabosil and < 5 micron particle size CuO. 0.17 g of each component was added to the atomizer flask and sonicated for approximately 90 minutes. A “more is better” approach was used when supporting the sample for X-ray adsorption analysis. The entire contents of the flask were atomized equally onto both sides of the grid to achieve desired spectral intensity. The Cu concentration of this substrate was approximately 40 % by weight. While this value is higher than typical fly-ash copper concentrations, the attenuation of the X-ray beams provides for high quality XANES spectra, thereby permitting precise determinations of chemical speciation in the substrate.

The substrate was heated in air at 375 °C for 20 minutes to remove any remaining solvent and organic impurities in the material. A previous XANES study that utilized this particular substrate demonstrated that consistent results were obtained when the copper oxide was first reduced to completion via thermal exposure to the aromatic dosant then re-oxidized back to Cu(II) by heating the substrate in air.[2.8] This pretreatment technique was also employed for the work described here. Some insight into why this procedure resulted in consistent results will be demonstrated with Scanning Electron Microscopy (SEM) images.

Control experiments showed that heating or vacuum alone did not reduce any Cu(II). Dosing of the sample was carried out using methods analogous to those used in the FTIR work, with the reaction rapidly initiated and quenching for the reaction time intervals between spectral acquisitions. However, since XANES is an elementally-specific technique, the dosant did not have to be evacuated from the cell before collecting spectra.

A three ion chamber arrangement[2.9] was used to monitor the incident and absorbed photon flux across the sample and an internal standard. The dosing cell was placed between the first and second chamber with the sample normal to the incident beam. The cell was bolted though its bottom blank flange onto a stainless steel slotted plate, which was bolted to an optical jack that was firmly fastened to the CAMD endstation optics table. The slotted plate and optical jack allowed continuous horizontal and vertical translation of the sample through the beam path. The cell was adjusted until the portion of the sample probed was approximately 3-5 mm directly below the thermocouple spot weld. Proper sample position was determined using X-ray sensitive paper.

An internal standard, Cu(0) metal foil, was placed between the second and third ion chambers thereby allowing simultaneous collection of sample spectra and well-defined reference

spectra. The ion chamber currents were collected using electrometers (Keithley model 428) and recorded with an analog to digital interface.

2.3.2 Data Analysis

The first step involved in the data analysis was to energy correct the sample spectra for small deviations in monochromator calibration. This was done by comparing the sample spectra with the simultaneously collected Cu metal internal standard spectra. The reference energy, the position of the Cu(0) K-edge (8979 eV), was determined from the maximum of the first derivative of each reference spectra and the sample spectra were corrected accordingly. The next step in the data analysis was normalization of the sample spectra. The aim of normalization is to produce a spectrum exhibiting a pre-edge region with no slope and a value of zero, while having its post-edge oscillations equally divided above and below the normalized value of one. These first two steps were conducted using WinXas.[2.10]

The next steps involved in the data analysis were required to determine the resultant oxidation state and chemical speciation of the CuO after thermal reaction with the PCDD/F precursors. This was quantified by fitting the experimental spectra to a 3-component linear combination of standard spectra. Obviously, the compounds chosen for reference standards must contribute to the experimental spectra. A prior experiment had demonstrated that CuO reduced by 2-chlorophenol at 375 ° C resulted in the formation of $Cu(I)_2O$ and Cu metal.[2.8] On this basis, the reference standards used were Cu(II)O, $Cu(I)_2O$ and Cu(0). Since Cu(II)O was the initial copper containing component, it was used as the Cu(II) reference standard. Because CuO was reduced by chlorinated organics, it would be possible to form Cu(I)Cl. However, the Cu_2O reference resulted in superior spectral fitting compared to that of CuCl. The data fitting procedures were developed by Farquar using two custom Visual Basic programs.[2.11] The first

takes energy-corrected, normalized spectra and interpolates the values of the energy axis to standard, pre-determined intervals. This was necessary because the energies probed between each monochromator step were at irregular intervals and the data reduction procedure requires consistency in the energy values between the experimental and simulated spectra. The same Visual Basic software package also truncates the energy range in the far post-edge XANES region since it is not critical for spectral fitting. However, this region was crucial for proper spectral normalization, so it should be collected.

The second program was used to determine the percentage of each component compound in the sample. This was accomplished by calculating a series of linear combinations of the reference spectra. A theoretical spectrum was generated for every reasonable three component combination of copper in each of the oxidation states. The program calculates a reduced c^2 value for each possibility by comparing each data point in the spectra. The equation used is shown below, where O is the theoretical value and E is the experimental value.[1.11]

$$c^2 = \frac{(O-E)^2}{E}$$

The percent compositions of the reference standards making up the simulated spectra having the lowest c^2 value, or best fit, corresponds to the percentage of each copper component observed experimentally.

2.4 SEM Analysis of 2-Chlorophenol Reaction with CuO

An Scanning Electron Microscopy (SEM) study was conducted to investigate any morphological changes of CuO at various points in the thermal reduction/re-oxidation cycle. This was done in an effort to investigate the effects of the pre-treatment procedure described in section 2.3.1.

CuO samples were treated to a procedure designed to replicate the samples used in the XANES studies. 6 mg of CuO powder was placed in a 5 mm quartz tube and heated in a tube furnace. The sample was oxidized at 375 °C for 15 minutes then evacuated to ~ 10^{-4} Torr. The sample was exposed to 2-MCP at 375 °C for 15 min. Previous studies with XANES indicate that this procedure will reduce approximately 70% of the CuO.[2.8] Following reduction, 2-MCP was evacuated, and the sample was heated in air at 375 °C for 20 minutes. XANES analysis had previously confirmed that this procedure would return all of the reduced copper back to its fully oxidized form. SEM analysis was performed on samples prior to exposure to 2-MCP, after reaction with 2-MCP but before re-oxidation, and after re-oxidizing the exposed sample back to CuO. Images were taken with a JEOL JSM-840 A Scanning Electron Microscope.

2.5 References

2.1 Basu, P.; Ballinger, T.H.; Yates, J.T. *Rev. Sci. Instrum.* **1988**, *59*, 1321.

2.2 Hair, M.L. *J. Non-Crystl. Solids*, **1975**, *19*, 299.

2.3 Hair, M.L.; Hertl, W. *J. Phys. Chem.* **1969**, *72*, 2372.

2.4 Hair, M.L.; Hertl, W. *J. Phys. Chem.* **1968**,

2.5 Peri, J.B.; Hensley, A.L. *J. Phys. Chem*. **1968**, *72*, 2926.

2.6 Schilling, P.; Morikawa, E.; Tolentino, H.; Tamura, E.; Kurtz, R. L.; Cusatis, C. *Rev. Sci. Instrum.* **1995**, *66*, 2214.

2.7 Stockbauer, R. L.; Ajmera, P.; Poliakoff, E. D.; Craft, B. C.; Saile, V. *Nuclear Instruments and Methods in Physics Research* **1990**, *291*, 505.

2.8 Farquar, G.R.; Alderman, S.L.; Poliakoff, E.D.; Dellinger, B. *Environ. Sci. Technol.* **2003**, *37*, 935.

2.9 West, J. B. Vacuum Ultraviolet Spectroscopy II; Academic Press: San Diego, 1998; Vol. II.

2.10 Ressler, T. *Journal of Synchrotron Rad.* **1998**, *5*, 118.

2.11 Farquar, G.R., dissertation for a Ph.D degree at Louisiana State University, **2003**.

CHAPTER 3: FTIR STUDY OF CHLORINATED AROMATIC PCDD/F PRECURSOR CHEMISORPTION ON MODEL FLY-ASH SURFACES

3.1 Introduction

FTIR spectroscopy was used to measure the rate of 2-chlorophenol chemisorption from 200-500 °C onto a silica surface using a pseudo-first order kinetic reaction scheme. Adsorption products were observed and characterized and a chemisorption pathway was inferred. A second FTIR study was undertaken which explored the time and temperature dependent absorption of 2-chlorophenol, 1,2-dichlorobenzene, and chlorobenzene on a surrogate fly-ash surface composed of 5 % CuO supported on silica. It was demonstrated that chemisorption of 2-chlorophenol and 1,2-dichlorobenzene results in the formation of identical surface bound species, an observation that could place much greater emphasis on chlorinated benzenes and PCDD/F precursors.

3.2 2-Chlorophenol Chemisorption on a Silica Surface from 200-500 °C

Most heterogeneous catalytic reactions require chemisorption of at least one reactant to the surface, and this is the probable first step in surface-mediated formation of PCDD/F from chlorinated aromatic precursors. Here, FTIR spectroscopy was used to study the adsorption of 2-chlorophenol, a known dioxin precursor, onto a well defined silica surface that serves as a surrogate for more complex incinerator fly-ash. Silica surfaces are rich in various types surface hydroxyl groups, e.g. vicinal, geminal, isolated. The O-H stretching vibrations of these silanol groups appear in infrared adsorption spectra in the region between approximately 3700-3500 cm^{-1}. The exact stretching frequency is dependent on the type of hydroxyl group and any interaction with neighboring sites. The types and stretching frequencies of hydroxyl groups present on the surface of the silica used for this study, Cabosil, are illustrated in Figure 3.1

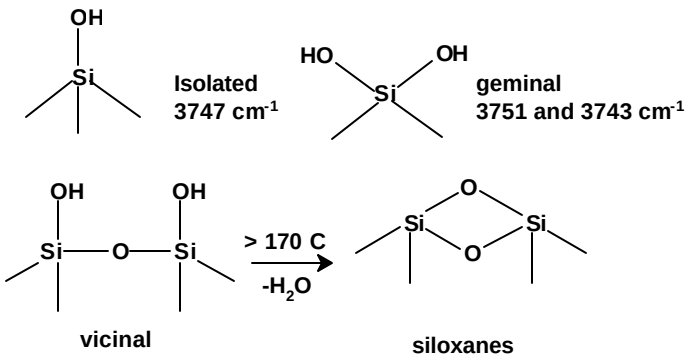

Figure 3.1 Types of hydroxyl groups on Cabosil.

Isolated, freely vibrating hydroxyl groups are present and give rise to a relatively sharp peak at 3747 cm^{-1}. Geminal hydroxyl groups are present and are manifested as shoulders at 3751 and 3743 cm^{-1} on either side of the 3747 cm^{-1} peak. Vicinal hydroxyl groups are initially present, but begin to condense, via the elimination of H_2O, when heated at about 170 °C and above 400 °C, this dehydration is irreversible. In this study, the silica was pre-treated at 800 °C. Therefore, no vicinal groups were present on the surface, only isolated groups and geminal groups which were spaced far enough apart as to not condense.

Figure 3.2 illustrates potential pathways of 2-chlorophenol chemisorption on silica.

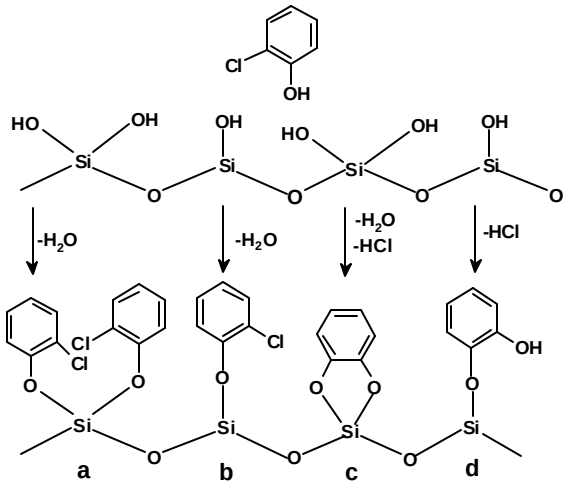

Figure 3.2 Possible adsorption mechanisms of 2-chlorophenol at geminal and isolated surface hydroxyls.

Pathway **a** depicts two molecules of 2-chlorophenol chemisorbed at geminal hydroxyl groups, while Pathway **b** shows adsorption at an isolated site, both via elimination of H_2O. Surface adsorbed chlorophenolate is the end result in each case. 2-chlorophenol also has the potential to adsorb via both ring substituents to yield a catecholic, or diphenolate type intermediate as illustrated in Pathway **c**. Additionally, adsorption may occur via ring Cl to yield a hydroxy phenolate though the elimination of HCl, as in Pathway **d**.

The ultimate yield of PCDD/F from aromatic precursors may be related to the sites at which chemisorption takes place, therefore it is beneficial to determine which pathways in Figure 3.2 are relevant. Infrared spectroscopy is ideal for studying the uptake of pollutant precursors at various silanol sites. Additionally, IR spectroscopy is amenable to characterizing the adsorbates as intermediates in surface-mediated PCDD/F formation.

3.2.1 Characterization of Adsorption Products

Figure 3.3 presents an FTIR difference spectrum resulting from exposure of Cabosil, a moderately high surface are silica, to 2-chlorophenol after 30 minutes of reaction at 325 °C. As this is a difference absorption spectrum with the FTIR background taken over the undosed silica, the negative peak at 3747 cm^{-1} indicates removal of surface hydroxyl groups on the silica, indicating that they are sites of chemisorption. For kinetic measurements, difference spectra were not employed because the peak height at 3747 cm^{-1} at a known reaction time, relative to that of the undosed sample, was used to monitor uptake of 2-chlorophenol (*vide infra*).

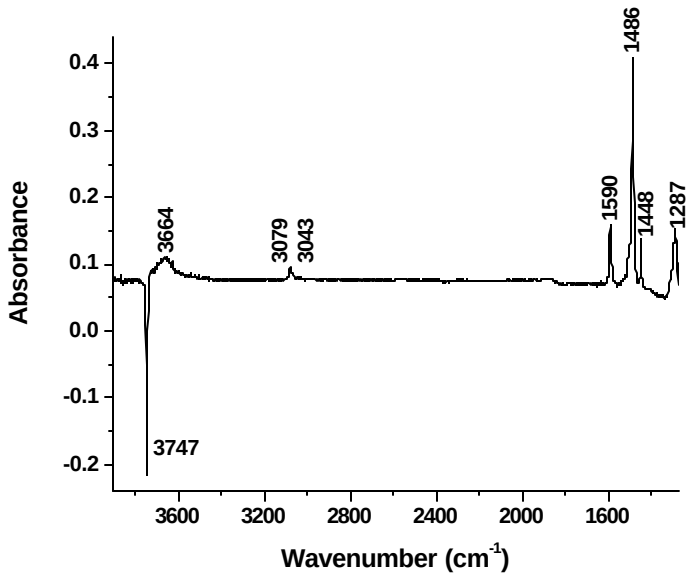

Figure 3.3 FTIR difference spectrum of silica after 30 minutes exposure to 2-chlorophenol at 325 °C. The negative peak at 3747 cm^{-1} is due to the loss of silica surface hydroxyl groups, indicating that they are sites of chemisorption. The labeled positive peaks are from 2-chlorophenol chemisorbed as chlorophenolate.

Peaks at 3079 cm^{-1} and 3043 cm^{-1} are due to aromatic C-H stretching vibrations of chemisorbed 2-chlorophenol and are shifted 7 and 15 cm^{-1} lower in energy, respectively, from their gas-phase values. Peaks at 1590 cm^{-1}, 1486 cm^{-1}, and 1448 cm^{-1} are attributed to the aromatic ring-breathing modes of chemisorbed chlorophenolate and are shifted 3-10 cm^{-1} from the gas-phase. The C-O stretch of the adsorbed chlorophenolate is observed at 1287 cm^{-1}, which is shifted 8 cm^{-1} from the gas-phase. Because these features persist after the cell had been evacuated to 10^{-6} Torr and held 10 minutes at 150 °C, the absorbing species are chemisorbed to the surface and not physically bound. These assignments are in close agreement with other 2-chlorophenol adsorption studies reported in the literature.[3.1,3.2] The broad absorption band at 3664 cm^{-1} is most likely due to hydrogen bonding between chlorine ring substituents of surface bound 2-chlorophenol and neighboring silica hydroxyl groups. Absent from the spectrum is a peak at 1338 cm^{-1} due to 2-chlorphenol O-H bending. This peak is present when 2-chlorophenol

is physisorbed and is an indication that 2-chlorophenol chemisorbs though its hydroxyl substituent.[3.2] This is consistent with Pathways **a** and **b** in Figure 3.2 and indicates that Pathway **d**, reaction though the Cl ring substituent does not occur to an appreciable extent. Additionally, there is no evidence of 2-chlorophenol O-H stretching, which is observed at 3570 cm^{-1} when physisorbed, further indicating that 2-chlorophenol chemisorbs at silica surface hydroxyl groups via its hydroxyl group.

At a reaction temperature of 300 °C (very weak at 300 °C) features begin to appear in the spectra that cannot be assigned to adsorbed 2-chlorophenol. As will be discussed, these additional features are due to surface bound carboxylates and possibly other reaction products, as well as 2-chlorophenol chemisorbed to the surface through both its hydroxyl and chlorine substituent as a catecholic-type intermediate. This is shown in Figure 3.4, which depicts the spectral region of 1625-1400 cm^{-1} for selected temperatures after 10 minutes of reaction.

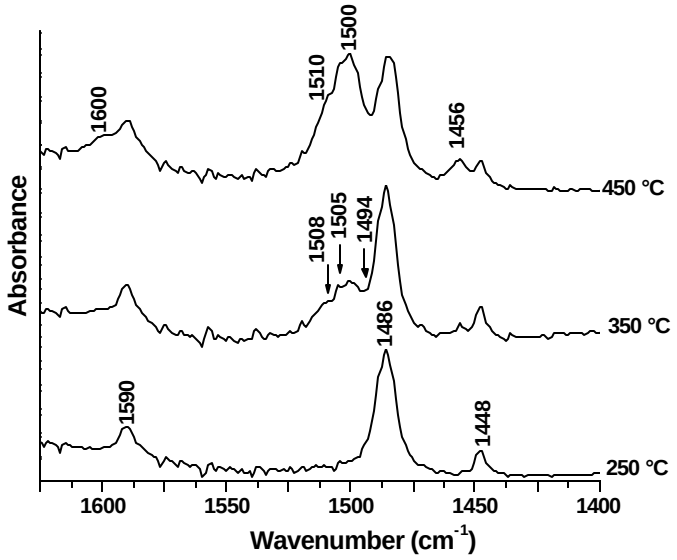

Figure 3.4 Temperature dependent IR spectra of 2-chlorophenol adsorption and oxidation after 10 minutes of reaction. For clarity, peaks attributed to chemisorbed 2-chlorphenolate are labeled in the 250 °C trace. Peaks attributed to chlorophenol bound in the bidentate form are depicted in the 350 °C trace. The carboxylate and carbonate partial oxidation products are labeled in the 450 °C trace.

The peak at 1600 cm^{-1} is assigned to the asymmetric -COO^- vibration of a surface carboxylate of the formate type, while the peak at 1456 cm^{-1} is due to asymmetric -COO^- stretching due to a surface bound carboxylate of the acetate type.[3.3-3.7] The shoulder at 1510 cm^{-1} is most likely due to the presence of surface bound carbonate.[3.6] The very intense peak at 1500 cm^{-1} is not conclusively assigned, but it is most likely also due to a surface carboxylate species,[3.8] probably of the formate type, as the adsorbing species responsible for this peak is more stable upon air oxidation versus the chlorphenolate or acetate species (*vide infra*). Surface bound carboxylates are commonly formed partial oxidation products and have been detected with FTIR in the catalytic oxidation of 1,2-dichlorobenzene over vanadia doped Al_2O_3, during the conversion of 2-chloropropane with SCR-DeNOx catalysts, and in surface-mediated methanol oxidation.[3.5,3.6,3.9] It has also been reported that carboxylate species are the dominant surface-mediated partial oxidation product of substituted benzenes.[3.9] Even though the absorption of 2-chlorophenol was carried out in the absence of gas-phase oxygen, oxidation products are still formed due to the uptake of surface oxygen.[3.3,3.6] Utilization of surface oxygen has also been proposed to take place for trichlorophenol oxidation though a Mars-van Krevelen type of mechanism.[3.10]

When 2-chlorophenol, chemisorbed at 325 °C, was exposed to 20% oxygen and held at 400 °C for 6 minutes, approximately 33% of adsorbed 2-chlorophenol was removed from the surface, based on loss of the chlorophenolate ring-breathing peak at 1486 cm^{-1}. The peaks at 1500 cm^{-1} and 1505 cm^{-1} became more resolved and were shown to be more stable toward oxidation than 2-chlorophenolate, which is the expected behavior of surface carboxylates. Oxidation at longer times caused increasing removal of surface species, both phenolate and carboxylates, with the peak at 1500 cm^{-1} most persistent. Concurrent with the removal of surface

bound phenolate and carboxylates oxidation and desorption was the re-formation of surface hydroxyl groups.

To further explore the nature of aromatic chemisorption on silica, 4-chlorophenol, phenol and chlorobenzene were separately exposed to Cabosil around 350 °C. 4-chlorophenol was adsorbed to see what effect the *para*- Cl had on the ring-breathing vibrations. 4-chlorophenol adsorbed to silica surface hydroxyl groups with aromatic ring-breathing at 1592 and 1493 cm^{-1}, which were shifted 10 cm^{-1} from the gas-phase. It was discovered that chlorobenzene did not chemisorb to any appreciable extent, although phenol did. However, some chlorobenzene chemisorption was noted following several hours of exposure. FTIR spectra of adsorbed phenol and chlorobenzene are shown in Figure 3.5 and it can be seen that identical surface bound species are formed from each dosant. These peaks are consistent with the aromatic ring-breathing modes of adsorbed phenolate.

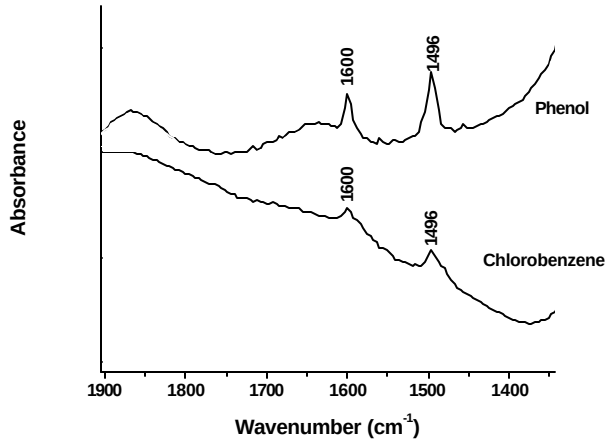

Figure 3.5 Comparison of FTIR spectra resulting from phenol and chlorobenzene chemisorption to Cabosil at 350 °C.

3.2.2 Catecholic Reaction Intermediate

It has been proposed that carboxylates are formed heterogeneously from aromatic species through a dihydroxy, or catecholic, type intermediate.[3.11] To this end, we elected to adsorb

catechol vapor from the finely ground solid onto pretreated Cabosil at room temperature. Following this procedure, adsorption bands were noted at 1604 cm^{-1} 1508 cm^{-1}, 1505 cm^{-1} and 1494 cm^{-1}. These peaks are also evident in our spectra generated from 2-chlorophenol chemisorption and are most prevalent in the 300-350 °C range and are labeled on the 350 °C trace of Figure 3.4. When adsorbed catechol is heated in air for 2 minutes, the peaks attributed to catecholic species reduce in intensity and are completely removed at 460 °C. This behavior is shown in Figure 3.5. During this thermal oxidation process, new peaks appear that are in excellent agreement with those we previously assigned to surface carboxylates (1600 cm^{-1}, 1500 cm^{-1}, 1456 cm^{-1}). The most stable peak with respect to air oxidation is again the peak at 1500 cm^{-1}. This is further evidence that carboxylate partial oxidation products formed from 2-chlorophenol and catechol proceed though a common intermediate, i.e. a bidentate bound aromatic ring structure. We observe a partial oxidation product peak from 2-chlorophenol and catechol partial oxidation at 1505 cm^{-1} and we observe this peak from ambient catechol adsorption. This may indicate that the peak observed at 1505 cm^{-1} after catechol adsorption is due to a partial oxidation product, formed at room temperature. However, another explanation is that both an oxidation product and a catecholic ring breathing mode co-exist at this frequency.

3.2.3 Rate of 2-Chlorophenol Chemisorption

Figure 3.7 depicts the expanded spectrum of the IR band due to freely vibrating surface hydroxyl groups and the time-dependent loss of intensity of the peak after exposure to 2-chlorophenol at 350 °C. Only a few of the time points measured are shown to reduce congestion in the figure.

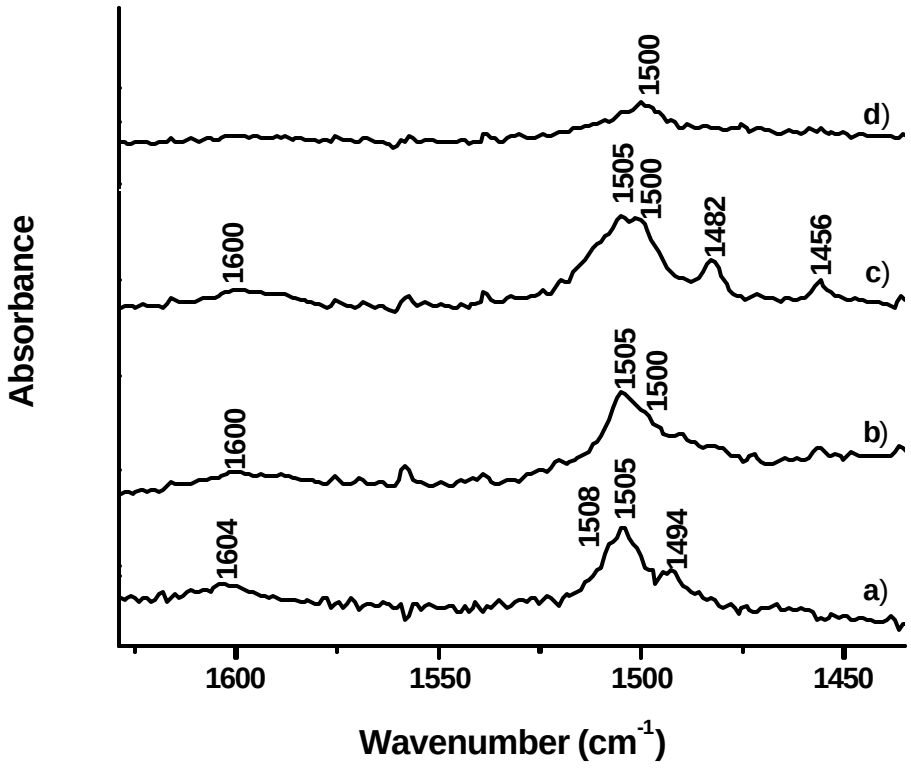

Figure 3.6 Temperature dependent spectra of catechol adsorbed onto Cabosil at 25 °C and heated in 21% O_2 for two minutes at 250 °C, 300 °C, and 460 °C.

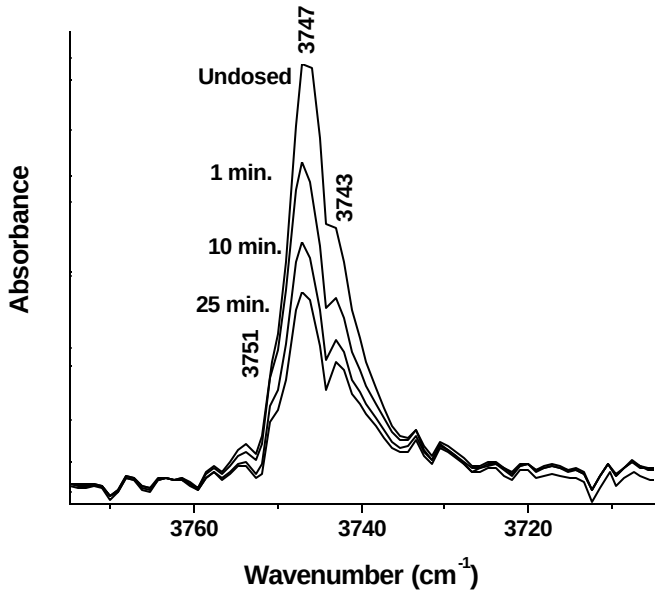

Figure 3.7 IR spectra illustrating loss of hydroxyl stretching due to adsorption of 2-chlorophenol at 350 °C for the selected times indicated in the figure.

The central peak at 3747 cm^{-1} is due to O-H stretching of isolated hydroxyl groups, and the shoulders at 3751 cm^{-1} and 3743 cm^{-1} are due to geminal hydroxyl groups that are sufficiently spaced as to not mutually hydrogen bond, thus they are not converted to siloxanes during the 800 °C pre-treatment prior to dosing. This characteristic of Cabosil has been reported by Hair and Hertl and their observations suggest that a Cabosil surface heated to 800 °C will have approximately 60 % isolated hydroxyl groups and 40% geminal groups.[3.12] As the reaction progresses, there is loss of intensity for all bands which means isolated and geminal hydroxyl groups participate in adsorption of 2-chlorophenol. The geminal bands become increasingly resolved as the reactions proceeds. The behavior depicted in Figure 3.7 is representative for all temperatures examined, which ranged from 200-500 °C in, 50 °C increments. For completeness, the time-dependent growth of phenolate absorption and carboxylate partial oxidation products is shown for same time points in Figure 3.8.

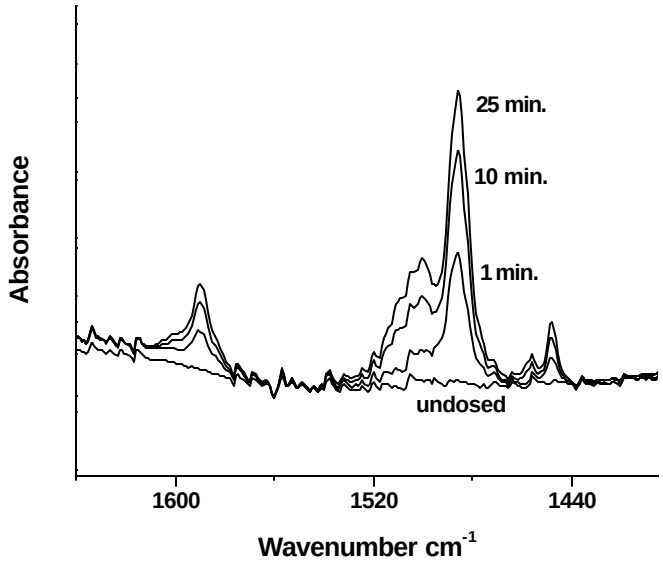

Figure 3.8 Spectra showing the increase in chlorophenolate and partial oxidation products for the time points spectra in Figure 3.7.

Since the undosed peak height is proportional to the number of available surface sites, the fractional surface coverage (θ) at any time can be determined based on the degree of reduction of the surface hydroxyl stretching peak at 3747 cm^{-1}. We can assume that all surface sites were available for 2-chlorophenol chemisorption since long reaction time at high temperature resulted in the complete disappearance of silanol stretching peak. The surface coverage was determined according to the equation shown below:

$$q(t) = \frac{peak\ \ height(0) - peak\ height(t)}{peak\ height(0)}$$

Figure 3.9 depicts the surface coverage with respect to time for all temperatures measured. For each temperature, the reaction is initially fast, and then begins to slow as equilibrium surface coverage is approached. After approximately 15 minutes of reaction at 500 °C, the surface hydroxyl sites are nearly completely removed, making a precise determination of the degree of reduction difficult.

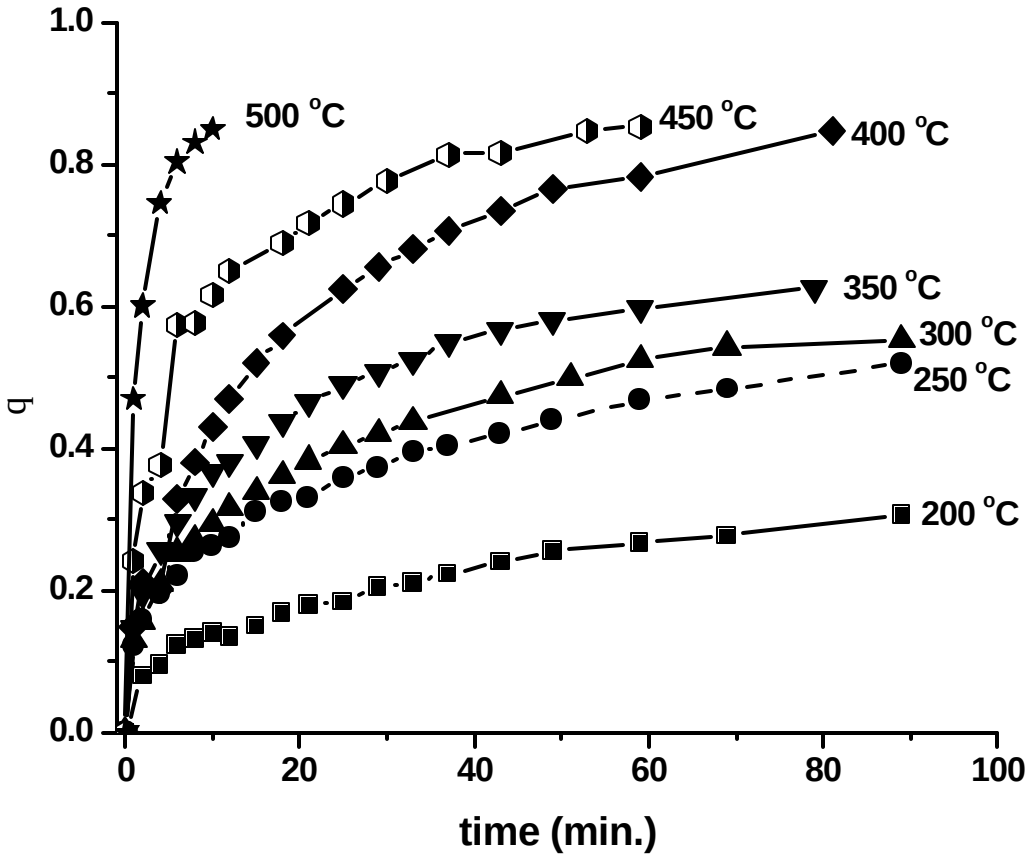

Figure 3.9 Surface coverage as a function of temperature as determined by the loss of surface hydroxyl groups upon 2-chlorophenol chemisorption on Cabosil.

Chemisorption kinetics were determined based on the following:

$$A + S \underset{k_d}{\overset{k_a}{\longleftrightarrow}} AS$$

Where *A* is vapor phase 2-chlorophenol and *S* is the silica surface and AS is

2-chlorophenol chemisorbed to the surface.

The rate of chemisorption is then:

$$\frac{d[AS]}{dt} = k_a[A][S] - k_d[AS]$$

For pseudo-first order conditions, $[A]=[A_0]$ and $k_a' = k_a[A]_0$ therefore,

$$\frac{d[AS]}{dt} = k_a'[S] - k_d[AS]$$

Since $[S]=[S]_0-[AS]$,

$$\frac{d[AS]}{dt} = k_a'([S]_0 - [AS]) - k_d[AS] = k_a'[S]_0 - (k_a' + k_d)[AS]$$

Dividing though by $[S]_0$ and defining $q = \frac{[AS]}{[S]_0}$ yields;

$$\frac{dq}{dt} = k_a' - (k_a' + k_d)q$$

Plotting $\frac{dq}{dt} vs q$ will yield a straight line with a slope of $-k_a' + k_d$ with and intercept of k_a'.

Figure 3.10 depicts these kinetic plots for a few selected temperatures. Adsorption occurs at a fast initial rate and a slower rate at higher surface coverage. The fast reaction extends to greater surface coverage with increasing temperature. For instance, at 250 °C, 350 °C, and 450 °C this fast initial reaction rate occurs up to q = 0.21, 0.28, and 0.63, respectively. Arrhenius behavior is depicted in Figure 3.11 for both the "fast" and "slow" reaction. The data were fit to the equation below:

$$k(t) = Ae^{\frac{B}{T}} \text{ where } B = \frac{-E_a}{R}$$

From 250-450 °C, the fast reaction exhibits a weak temperature dependence and relatively low activation energy of 7.1 ± 2.4 kJ mol^{-1} and B = 686 K , while the slower reaction has an activation energy of 22.0 ± 2.3 kJ mol^{-1} and B = 2,546 K in the 200-450 °C range. The rate coefficients and activation energy of adsorption are given in Table 3.1.

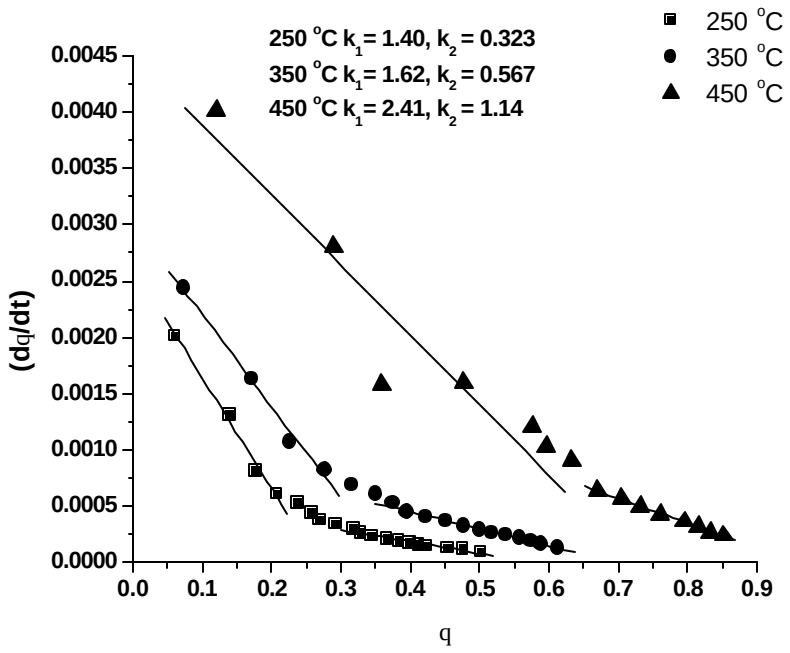

Figure 3.10 Pseudo-first order kinetic plots for the chemisorption of 2-chlorophenol on silica shown for selected temperatures. The y-intercept corresponds to the pseudo-first order rate constant. k_1 indicates the fast, initial reaction and k_2 indicates the slower reaction that occurs at higher surface coverage.

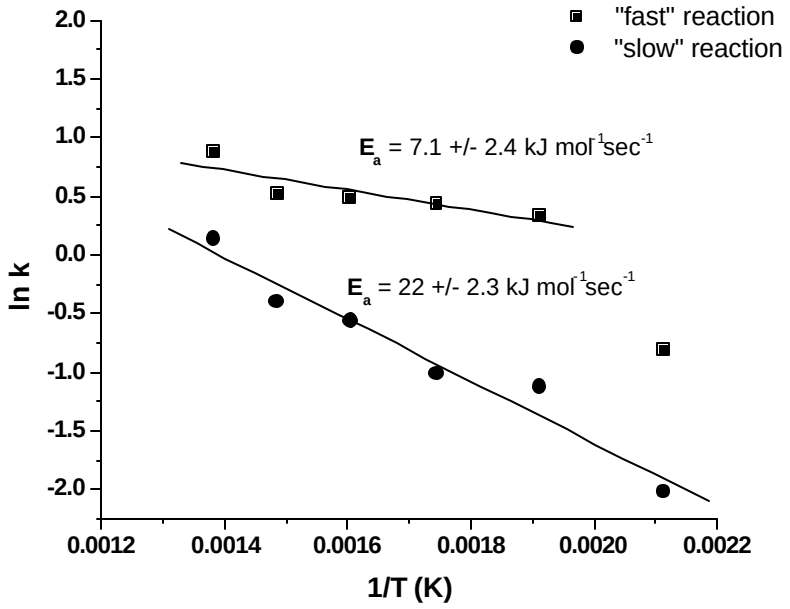

Figure 3.11 Arrhenius behavior of 2-chlorophenol chemisorption on Cabosil.

Table 3.1 Rate constants for chemisorption of 2-chlorophenol on silica. k_1 indicates the fast, initial reaction and k_2 indicates the slower reaction that occurs at higher surface coverage. E_a is the activation energy for chemisorption.

Temperature (°C)	k_1 (atm^{-1} sec^{-1})	k_2 (atm^{-1} sec^{-1})
200	0.446 ± 0.0175	0.132 ± 0.00439
250	1.40 ± .0573	0.323 ± 0.0154
300	1.55 ± .00807	0.362 ± 0.0154
350	1.62 ± .06209	0.567 ± 0.0155
400	1.68 ± 0.280	0.669 ± 0.0100
450	2.41 ± 0.283	1.14 ± 0.0172
E_a (kJ mol^{-1})	7.1 ± 2.4	22 ± 2.3 kJ

We have not included transition metals, e.g. copper oxides, in this study which are known to catalyze the formation of PCDD/F from chlorophenols. However, both silica and transition metal surfaces contain surface hydroxyl sites at which 2-chlorophenol can chemisorb. Silica was readily amenable to a kinetic study by FTIR because the different types of surface hydroxyl sites are well resolved. This is not true for copper oxide. The reaction with silica can be considered a model, albeit at a slower reaction rate, for reaction with transition metal oxides. Adsorption of PCDD/F precursors to a surface of copper oxide supported on silica is described in the following section.

3.3 Reaction of 2-Chlorophenol, 1,2-Dichlorobenzene and Chlorobenzene with CuO/SiO_2

3.3.1 Comparison of Adsorption Products

Figure 3.12 compares FTIR spectra in the region of 1645 cm^{-1} to 1265 cm^{-1} resulting from the reaction of 2-chlorophenol, 1,2-dichlorobenzene and chlorobenzene with a CuO/SiO_2 surface at 350 °C. Copper is present at 5% by weight and was prepared by the method of incipient wetness using silica in the form of Cabosil as the support, which was described in Chapter 2. The grey-black sample turned to a reddish-brown during thermal exposure to each

dosant which indicates that CuO was reduced, most likely to a mixture of $Cu(I)_2O$ and Cu(0). This will be the scope of the next chapter.

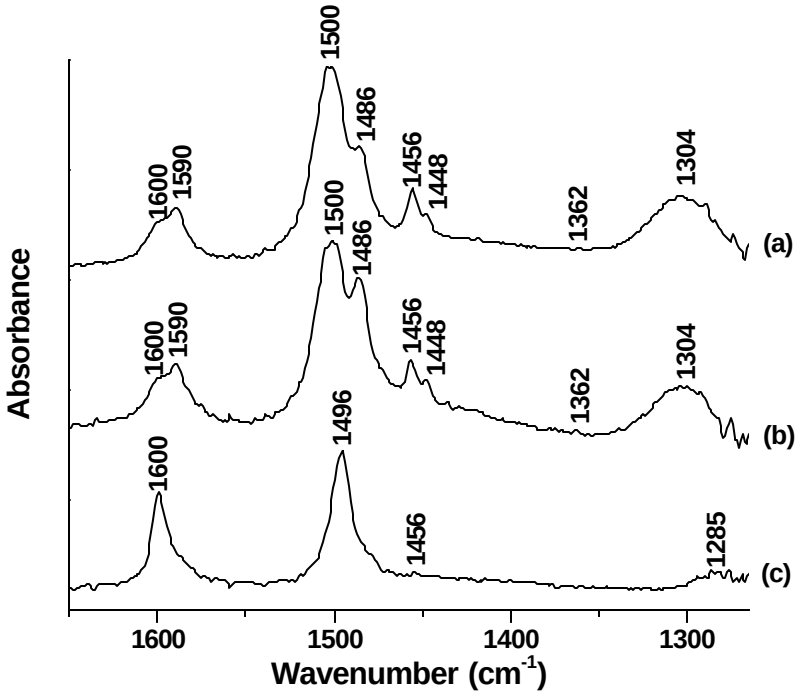

Figure 3.12 FTIR spectra comparing the chemisorbed reaction products after exposure of (a) 2-chlorophenol, (b) 1,2-dichlorobenzene and (c) chlorobenzene to CuO/SiO_2 at 350 ºC.

Based on the FTIR spectra, 2-chlorophenol and 1,2-dichlorobenzene adsorb to the surface to produce identical species. Peaks at 1590 cm^{-1}, 1486 cm^{-1}, and 1448 cm^{-1} are attributed to aromatic ring-breathing modes of 2-chlorophenol and 1,2-dichlorobenzene adsorbed as a chlorophenolate. These bands are shifted 8-10 cm^{-1} lower in energy than the analogous gas-phase bands of 2-chlorophenol and 13-24 cm^{-1} to lower energy for those of 1,2-dichlorobenzene. As will be shown later in this discussion, surface hydroxyl groups of primarily silica and possibly those of CuO are removed from the surface during reaction, indicating that they are sites of adsorption. Absent from the 2-MCP spectrum is a peak at 1338 cm^{-1} due to 2-MCP phenolic hydroxyl bending. This peak is present when 2-chlorophenol is physically adsorbed at room

temperature and indicates that 2-MCP adsorbs to surface hydroxyl sites though its phenolic O-H substituent. Although the C-Cl stretching bands of 1,2-DCBz could not be examined, it must chemisorbs though its chlorine substituent since the phenolate species observed is identical to that formed from 2-chlorophenol chemisorption. Larrubia and Busca have reported this behavior for the adsorption of 1,2-dichlorobenzene on SCR-DeNO$_x$ catalysts.[3.13] The chemisorption pathways of 2-chlorophenol and 1,2-dichlorobenzene to yield chlorophenolate is depicted at isolated CuO hydroxyl sites in the upper half of Figure 3.13.

In the previous section, when 2-chlorophenol was chemisorbed to silica, also as Cabosil, but with no copper present, the phenolate ring breathing bands were in the exact agreement with the present results. However, 1,2-dichlorobenzene did not chemisorb to the silica in the absence of CuO. A control experiment in which the silica was treated to the incipient wetness preparation procedure, with the exception of the addition of the CuO precursor, revealed that the wetting, drying and calcination steps alone involved in supporting CuO on silica did not alter reactivity of surface silanol groups with regard to the uptake of 1,2-dichlorobenzene; therefore, the presence of CuO seems to be critical for 1,2-dichlorobenzene chemisorption to take place. Silica hydroxyl groups are, however, removed from the surface following 1,2-dichlorobenzene adsorption. This indicates that 1,2-dichlorobenzene adsorption initially takes place at copper sites before migrating across the surface to the less active silica hydroxyl sites. Although we depicted 2-chlorophenol and 1,2-chlorophenol reacting at surface hydroxyl sites of CuO in Figure 3.13, it is possible that these compounds adsorb at other active sites on CuO, such as oxygen vacancies.

Also evident in the 2-chlorophenol and 1,2-dichlorobenzene spectra in Figure 3.12 is an absorption band centered around 1304 cm^{-1}. This seems to be a superimposed with an additional

peak at 1289 cm^{-1}. In the previous study of 2-chlorophenol adsorption on pure Cabosil, a peak was observed at 1287 cm^{-1} which was assigned to the C-O stretching vibration of phenolate adsorbed to a silica hydroxyl site. This is also the assignment given here for the peak at 1289 cm^{-1}. It is possible that the absorption 1304 cm^{-1} is the due to C-O stretching of phenolate adsorbed to CuO hydroxyl sites, but this cannot be confirmed at this time. Although not shown, peaks attributed to aromatic C-H stretching vibrations of the adsorbed phenolate are also present at 3079 and 3046 cm^{-1} following 2-chlorophenol and 1,2-dichlorobenzene adsorption.

Absorption bands at 1600, 1511, 1505, 1500, 1456 and 1362 cm^{-1} are evident in the spectra and are again due to the formation of surface bound carboxylates of the formate and acetate types, which were assigned and described in section 3.1.1. It was previously shown that the surface-mediated partial oxidation of aromatic precursors occurs through a bidentate adsorbed catecholic type intermediate. The lower half of Figure 3.13 illustrates the proposed chemisorption pathways of 2-chlorophenol and 1,2-dichlorobenzene to yield catecholic intermediate at geminal hydroxyl sites.

Reaction of chlorobenzene yields absorption bands due to phenolate ring-breathing at 1600 cm^{-1} and 1496 cm^{-1}, shown in the lower trace of Figure 3.12. Peaks not shown at 3080 cm^{-1} and 3053 cm^{-1} are due to aromatic C-H stretching. These are in exact agreement with phenol and chlorobenzene chemisorbed to pure silica at 350 °C, thus phenol and chlorobenzene adsorb in a manner analogous to that shown in the upper half of Figure 3.13, via H_2O and HCl elimination, respectively. As with 1,2-chlorobenzene, chlorobenzene did not chemisorb to any appreciable extent in the absence of CuO. Surface bound partial oxidation products make a very small contribution to the chlorobenzene spectrum, with only a weak peak at 1456 cm^{-1} that is attributed to acetate species. However, it is possible that other oxidation products are formed, but not

chemically bound to the surface and are removed during the cell evacuation procedure. Perhaps the lack of a second ring substituent other than H prevented the formation of the catecholic intermediate.

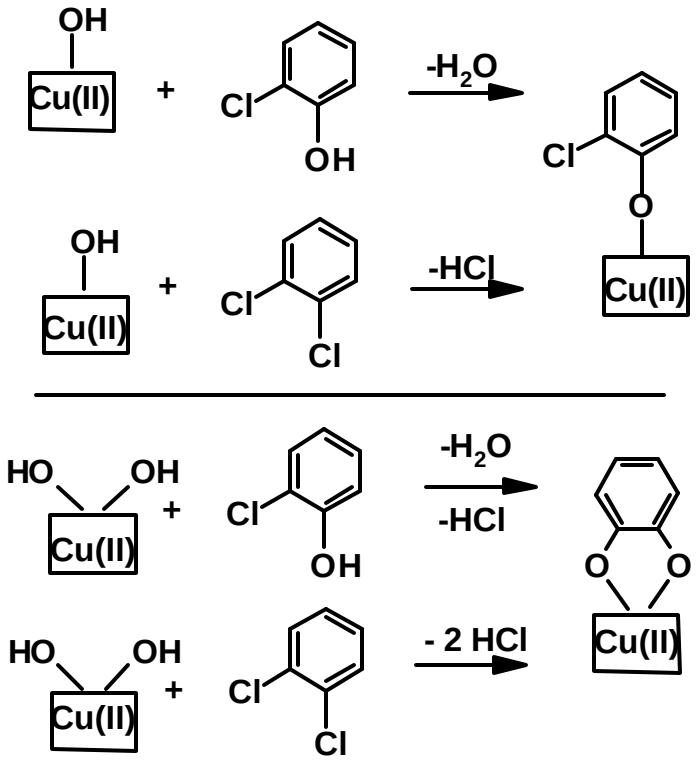

Figure 3.13 Chemisorption of 2-chlorophenol and 1,2-dichlorobenzene to yield the same surface species. Adsorbed chlorophenolate, upper drawing, was observed directly by FTIR, while the formation of the catecholic intermediate was inferred based on the observation of carboxylate partial oxidation products.

3.3.2 Temperature-Dependence of 2-Chlorophenol Chemisorption

Figure 3.14 depicts the temperature dependence of 2-chlorophenol chemisorption and oxidation after 3 minutes exposure to the CuO/SiO_2 surface. At 200 °C peaks due to adsorbed chlorophenolate at 1486 and1590 cm^{-1} are evident. A relatively small concentration of a surface bound formate is also observed. By 350 °C, the relative absorbance due to partial oxidation products is greater than that of the chlorophenolate bands. The carboxylate:phenolate ratio continues to increases with increasing temperature. In this study, when CuO is dispersed on the

silica, carboxylates are formed at approximately 100 °C lower temperature and much higher carboxylate:phenolate ratios are observed for any given temperature vs. that of pure silica, illustrating the promoting effect of CuO on 2-chlorophenol oxidation.

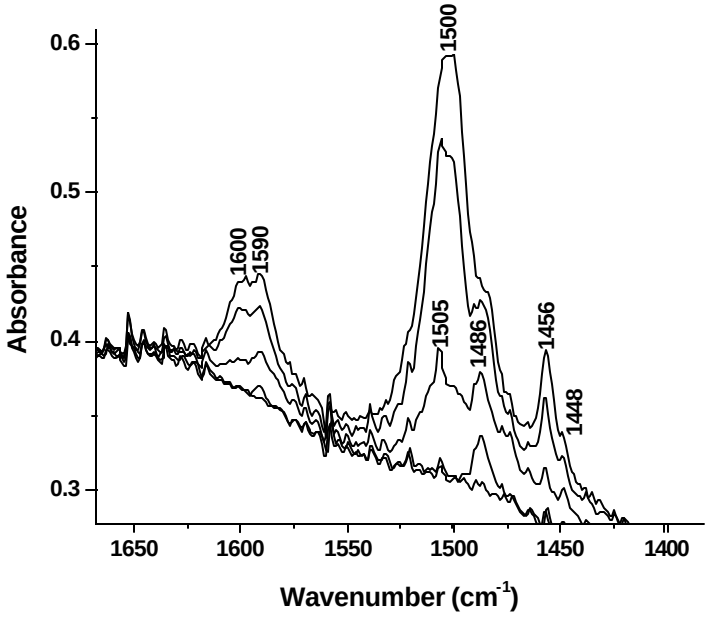

Figure 3.14 Temperature dependence of 2-chlorophenol chemisorption onto CuO/SiO_2 after 3 minutes of reaction. The baseline is shown, and in order of increasing absorbance are spectra taken at 200 °C, 350 °C, 400 °C, 500 °C.

Concurrent with the growth of the peaks due to adsorption and oxidation of the dosants is the removal of surface hydroxyl groups, evidenced by a sharp decrease in adsorption in at approximately 3745 cm^{-1}, which is consistent with that of silica surface hydroxyl groups.[3.12] This is shown at a few time points of 2-chlorophenol chemisorption in Figure 3.15 and suggests that surface hydroxyl groups are one of the sites of chemisorption. As this is a difference absorption spectra, the more negative the peak, the more hydroxyls groups removed from the surface, i.e., the longer the reaction time. Also evident are peaks at 3742 and 3737 cm^{-1}, indicating that more than one type of surface hydroxyl participates in the adsorption process. These additional absorptions may be due to either vicinal or geminal silanols, or possibly

hydroxyl groups of CuO and could explain the observation of multiple phenolate C-O vibrations due to chlorophenolate adsorption at sites of different energy, also shown in Figure 3.15, along with time-dependent growth of 2-chlorophenol adsorption and partial oxidation products.

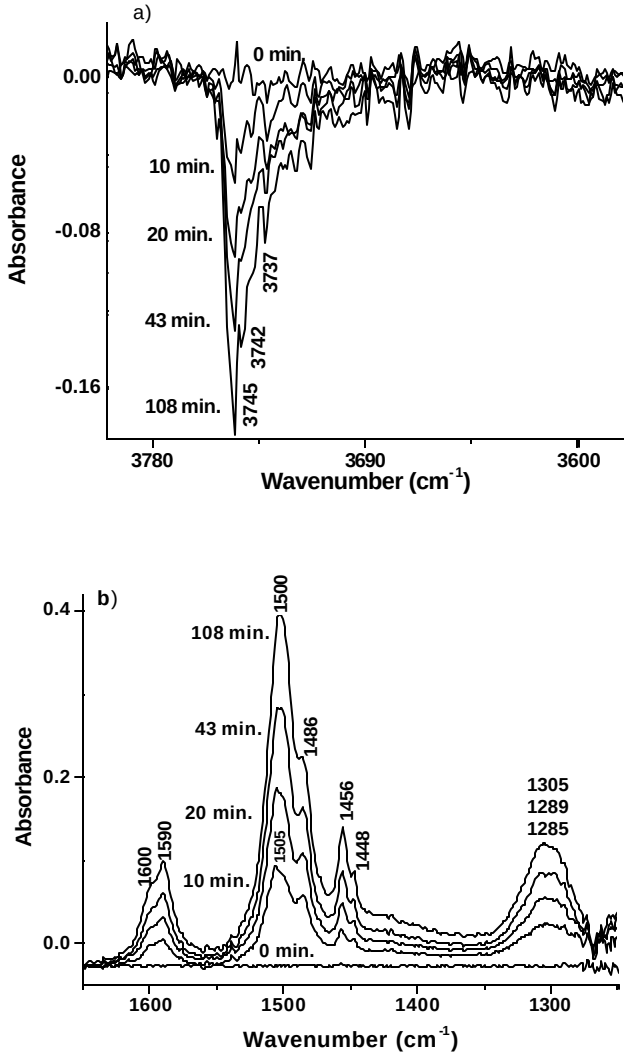

Figure 3.15 IR spectra depicting: a) loss of surface hydroxyl groups after reaction of 2-chlorophenol at 350 ºC. The peak becomes more negative (more –OH removed from the surface) as the reaction proceeds. b) growth of adsorption and partial oxidation products.

Surface hydroxyl groups are also removed in the same manner after adsorption of 1,2-dichlorobenzene and chlorobenzene. The time-dependent growth of 1,2-dichlorobenzene adsorption and oxidation products is qualitatively identical to that shown for 2-chlorophenol, but

adsorption and oxidation occur at a slower rate. Spectra taken after the dosed substrates were oxidized at 400 °C in 21% O_2 for 5 minutes revealed no adsorbed surface species and re-hydroxylation of the surface, indicating complete oxidation and desorption of adsorbed species.

3.3.3 Rate of 2-Chlorophenol and 1,2-Dichlorobenzene Chemisorption

The vapor pressures of 2-chlorophenol and 1,2-dichlorobenzene are sufficiently close that the relative rates of adsorption and oxidation can be compared by plotting the peak heights of a phenolate absorption and oxidation product with respect to time, as shown in Figure 3.16. The peak at 1486 cm^{-1} is an aromatic ring-breathing mode of the adsorbed phenolate, while the peak at 1500 cm^{-1} corresponds to surface bound formate. The growth in intensity of these bands was fit to an exponential of the form: $I_t = I_\infty(1-e^{-kt})$; where I_t is the peak height at reaction time t, I_8 is the asymptotic value of the peak height, k is the rate coefficient for chemisorption (k_{cs}) and oxidation (k_{ox}). The fit of the phenolate band resulting from 2-chlorophenol adsorption gives I_∞ = 0.245 and $k_{cs} = 6.6x10^{-4}$ s^{-1}. For 1,2-dichlorobenzene, I_∞ = 0.304 and $k_{cs} = 6.0x10^{-5}$ s^{-1}. Fitting of the growth of the formate peak at 1500 cm^{-1} results in I_∞ = 0.424, $k_{ox} = 5.5x10^{-4}$ s^{-1} and I_∞ = 0.269 and $k_{ox} = 1.0x10^{-4}$ s^{-1} for 2-chlorophenol and 1,2-dichlorobenzene, respectively. These analyses indicate that adsorption and partial oxidation is approximately 11 and 6 times faster, respectively, for 2-chlorophenol than 1,2-dichlorobenzene. This is expected, as 2-chlorophenol adsorption requires breaking of the phenolic O-H bond, which has a bond dissociation energy of 82 kcal/mol, compared to a bond dissociation energy of 97 kcal/mol for the C-Cl bond in 1,2-dichlorobenzene.[3.14,3.15]

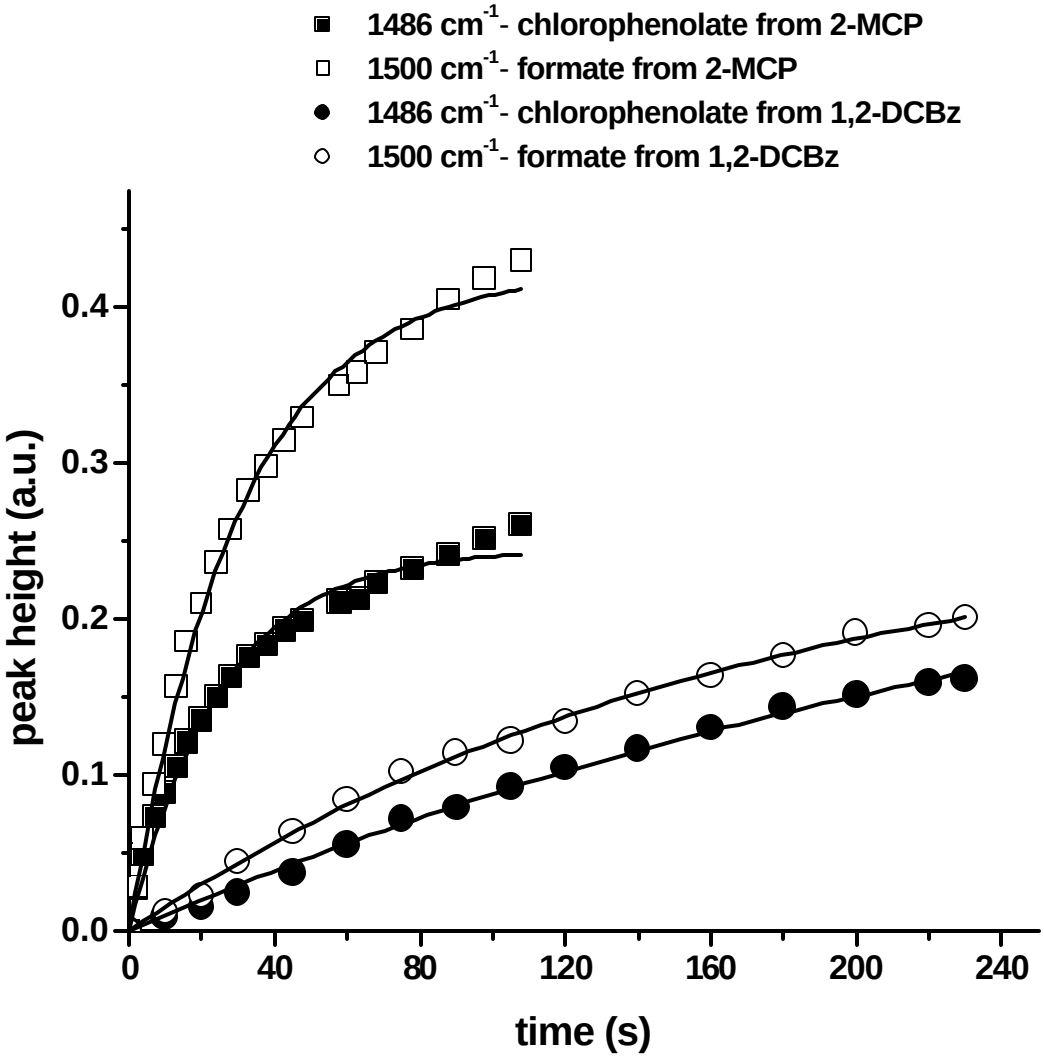

Figure 3.16 A comparison of the rates of chemisorption and oxidation of 2-chlorophenol and 1,2-dichlorobenzene at 350 °C by plotting the peak height of a common phenolate ring breathing mode (1486 cm^{-1}) and formate COO^- stretch (1500 cm^{-1}).

3.4 Chapter Summary and Relevance for PCDD/F Formation

The formation of PCDD/F is a marginal process of chlorophenol oxidation, evidenced by the fact that yields of PCDD/F from reactions of chlorophenols on fly-ash and surrogate fly-ash are typically less than 1%.[3.16,3.17] However, the heterogeneous oxidation of chlorophenols to

their most thermodynamically stable end-products, i.e., CO_2, and HCl, and their incomplete oxidation to form such species as PCDD/F involves chemisorption at active surface sites. Therefore, knowledge of the rates and geometries of precursor adsorption at potentially active sites is beneficial in developing a detailed model of PCDD/F formation from chlorinated phenols.

In this chapter, it was demonstrated that 2-chlorophenol chemisorbs at isolated and geminal surface hydroxyl groups of silica to form surface-bound phenolates. Above 300 °C carboxylate partial oxidation products are formed though a catecholic intermediate. Initial adsorption to the surface is accomplished through reaction of the phenolic hydroxyl, following by reaction through the chlorine substituent to form catecholate at geminal sites. The rate of chemisorption was measured over the temperature range of heterogeneous PCDD/F formation and the Arrhenius behavior described. Chlorobenzene and 1,2-dichlorobenzene did not chemisorb to pure silica to an extent that would permit kinetic analysis.

An additional FTIR study showed that 2-chlorophenol and 1,2-dichlorobenzene adsorb to a silica surface impregnated with CuO to yield the same products. The presence of CuO caused partial oxidation products to be formed at lower temperature and lower phenolate:oxidation product ratios were observed at equivalent temperatures. Table 3.2 summarizes the FTIR results presented in this chapter.

One of the suggested roles of transition metal species in the formation of PCDD/F is that of an electron acceptor, in which upon chemisorption of the chlorophenol to a metal cation site (M^{n+}), an electron is transferred from chlorophenolate to the metal, resulting in the formation of a surface associated chlorophenoxyl radical and a $(M^{n+})^{-1}$. Evidence of this has been provided using EPR[3.17] and X-ray adsorption spectroscopy. [3.18] The following chapter will address this to

a greater extent. Since reactions of chlorophenols on both catalytic copper oxide surfaces and silica surfaces involved initial chemisorption of chlorophenols, future studies will focus on the differences in the distribution and reactivity of isolated, vicinal, and geminal hydroxyl sites associated with mixed copper oxide/silica surfaces. This distribution may well control the absolute and relative yields of PCDD and PCDF by determining whether they are oxidized, react with another surface-bound PCDD/F precursor, or react with a gas-phase precursor.

In the upper pathway of Figure 3.17, we depict the chemisorption of 2-chlorophenol at single isolated surface hydroxyl site to form the surface-bound 2-chlorophenolate. Phenolates at isolated sites are capable of reacting with gas-phase species via an Eley-Rideal pathway. The Eley-Rideal reaction of a surface-bound chlorophenolate and a gas-phase chlorinated phenol has been proposed to be responsible for formation of PCDDs. [3.17]

In the middle pathway in Figure 3.17, chemisorption of 2-chlorphenols at two neighboring isolated sites is depicted. The chlorophenolates at these sites can react further via a Langmuir-Hinshelwood pathway. The Langmuir-Hinshelwood reaction of two surface-bound chlorphenolates has previously been proposed to be responsible for the formation of PCDFs. [3.17] This pathway would also be applicable to adsorption at vicinal hydroxyl sites, however these were removed during the 800 °C thermal silica pre-treatment.[3.12]

In the lower pathway of Figure 3.17, 2-chlorophenol reacts with geminal, surface hydroxyl sites to form a surface-bound catecholate species. Oxidation of the catecholate results in the formation of the observed carboxylates. However, free catechols have previously been observed in the CuO/silica catalyzed oxidation of 2-chlorophenol which suggests that they participate in other reactions or are desorbed from the surface.[3.17]

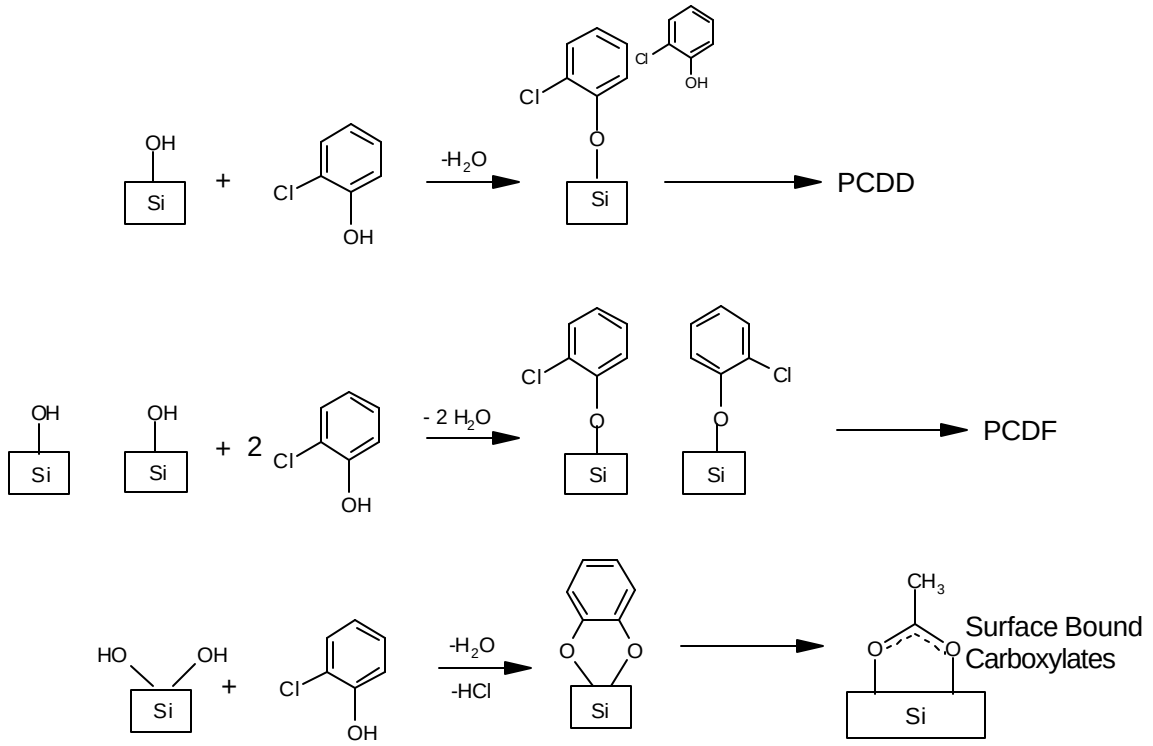

Figure 3.17 Chemisorption of 2-chlorophenol onto silica. The upper pathway illustrates chemisorption of 2-chlorophenol at an isolated hydroxyl via H_2O elimination to form 2-chlorophenolate. The middle pathway depicts adsorption at neighboring isolated sites. The lower pathway illustrates 2-chlorophenol adsorbed at a geminal site through both the phenolic hydroxyl and chlorine substituent resulting in a bidentate bound diphenolate, which is believed to be an intermediate in the formation of carboxylate partial oxidation products.

Our FTIR study demonstrates that 1,2-dichlorobenzene chemisorbs to the surface to produce the same species as 2-chlorophenol. If reactions of adsorbed phenolate (phenoxy radicals) are responsible for PCDD/F formation, it stands to reason that chlorinated benzenes will contribute to total yields, especially PCDF formation, which is proposed to take place by coupling of adsorbed chlorophenoxy radicals.

Our measurements indicate that the rate of reaction of 1,2-dichlorobenzene is ~ 11x slower than 2-chlorophenol. This suggests that since the concentrations of chlorinated benzenes are 100x greater[3.19] than chlorinated phenols in incinerator effluent, the number of surface-bound

PCDD/F phenolate precursors that result from chlorinated benzenes is approximately 9x greater than those from chlorinated phenols. Additional research on the role of chlorinated benzenes as precursors in PCDD/F formation is clearly indicated.

3.5 References

3.1 Kung, K.H.S.; McBride, M.B. *Environ. Sci. Technol.* **1991**, *25*, 702.

3.2 Bandara, J.; Mielczarski, J.A.; Kiwi, J. *Appl. Catal. B: Environmental* **2001**, *34*, 307.

3.3 Krishnamoorthy, S.; Rivas, J.A.; Amiridis, M.D. *J. Catal* **2000**, *193*, 264.

3.4 Angevaare, P.A.J.M.; Grootendorst, E.J.; Zuur, A.P.; Ponec, V. *New Developments in Selective Oxidation* Centri, G. and Trifiro, F. (eds.) **1990**, Elsevier, Amsterdam, pg. 861.

3.5 Busca, G. *Catal. Today* **1996**, *27*, 457.

3.6 Krishnamoorthy, S.; Amiridis, M.D. **1999**, *51*, 203.

3.7 Little, J.H. "Infrared Spectra of Adsorbed Species" 1966 Academic Press London New York.

3.8 Sambeth, J.E.; Centeno, M.A.; Paul, A.; Briand, L.E.; Thomas, H. J.; Odriozola, J.A. *J. Mol Catal. A: Chemical* **2000**, *161*, 89.

3.9 Larrubia, M. A.; Busca, G. *Appl. Catal. B: Environmental* **2002**, *39*, 343.

3.10 Lomnicki, S.; Lichtenberger, J.; Xu, Z.; Waters, M.; Kosman, J.; Amiridis, M.D. *Appl. Catal. B: Environmental* **2003**, *46*, 105.

3.11 Lichtenberger, J.; Amiridis, M.D. *J. Catal.* **2004**, *223*, 296.

3.12 Hair, M.L.; Hertl, W. *J. Phys. Chem.* **1969**, *72*, 2372.

3.13 Larrubia, M. A.; Busca, G. *Appl. Catal. B: Environmental* **2002**, *39*, 343.

3.14 Khachatryan, L.; Asatryan, R.; Dellinger, B. *Chemosphere* **2003**, *52*, 695.

3.15 Tsang, W. *Combust. Sci. and Tech.* **1990**, *74*, 99.

3.16 Weber, R.; Hagenmaier, H. *Chemosphere* **1999**, *38*, 529.

3.17 Lomnicki, S.; Dellinger, B. *J. Phys. Chem. A* **2003**, *107*, 4387.

3.18 Farquar, G.R.; Alderman, S.L.; Poliakoff, E.D.; Dellinger, B. *Environ. Sci. Technol.* **2003**, *37*, 931.
3.19 Blumenstsock, M.; Zimmermann, R.; Schramm, K.W.; Kaune, A.; Nikolai, U.; Lenoir, D.; Kettrup *J. Anal. Appl. Pyrolysis*, **1999,** *49*, 179.

Table 3.2 Summary of FTIR studies of chemisorption of aromatic PCDD/F precursors on surrogate fly-ash surfaces.

Dosant/ Temp.	Surface	Surface O-H removed (cm^{-1})	Phenolate modes (cm^{-1})	Carboxylate modes (cm^{-1})	Comments
2-MCP/ 200-500 °C	SiO_2	3747 (isolated) 3751 (geminal) 3753 (geminal)	1590, 1486, 1448 ring C=C 3079, 3043 ring C-H 1287 C-O	1600, 1520, 1510, 1500, 1505, 1500, 1456 @ T>300 °C	E_a 7 kJ mol^{-1} (fast) E_a 22 kJ mol^{-1} (slow); Observed catecholic intermediate
4- MCP/ 350 °C	SiO_2	3747 (isolated) 3751 (geminal) 3753 (geminal)	1592, 1493 ring C=C	n.d.	Rate of adsorption same as 2-MCP
Phenol/ 350 °C	SiO_2	3747 (isolated) 3751 (geminal) 3753 (geminal)	1600, 1496 ring C=C	n.d	Reacts via H_2O elimination analogous to 2-MCP
MCBz/ 350 °C	SiO_2	3747 (isolated) 3751 (geminal) 3753 (geminal)	1600, 1496 ring C=C	n.d	Same surface phenolate formed as from phenol, HCl elimination
2- MCP/ 200-500 °C	CuO/SiO_2	3745 (silica) 3742 3737	1590,1486,1448 ring C=C 3079, 3046 ring C-H	1600, 1511, 1505, 1500, 1456, 1362	All features identical to 1,2-DCBz
MCBz 350 °C	CuO/SiO_2	3745 (silica) 3742 3737	1600, 1495 ring C=C 3080, 3053 ring C-H	1456 (weak)	Trace partial oxidation evident; yields same species as phenol
1,2-DCBz 350 °C	CuO/SiO_2	3745 (silica) 3742 3737	1590,1486,1448 ring C=C 3079, 3046 ring C-H	1600, 1511, 1505, 1500, 1456, 1362	Adsorbs 11x slower than 2-MCP

CHAPTER 4: XANES SPECTROSCOPIC STUDY OF AROMATIC PCDD/F PRECURSOR REACTIONS WITH CU(II)O FROM 275-375 °C

4.1 Introduction

In order to address the issues of how metal oxide species might participate in the uptake of pollutant precursors, XANES spectroscopy was used to study the fate of copper(II) oxide, with respect to reduction and speciation, in a silica mixture when exposed to 2-chlorophenol, 1,2-dichlorobenzene and chlorobenzene. Reduction kinetics were measured from 275-375 °C and reduction products of CuO, i.e., chemical speciation, were determined. A scanning electron microscopy study was conducted to examine the morphology of the copper particles at various stages during the course of reaction, which helped explain how different thermal pre-treatment of CuO effects reactivity.

4.1.1 Potential Reactions of Chlorinated Aromatics with CuO

In the preceding chapter, it was demonstrated using FTIR spectroscopy that chlorinated phenols and benzenes adsorb to isolated and geminal surface hydroxyl groups of silica and CuO supported on silica to yield surface adsorbed phenolate species. This is the likely first step in surface-mediated PCDD/F formation. It is well known that copper species promote heterogeneous PCDD/F, although the mechanism is not clear. Experimental and theoretical studies in the literature implicate transition metal reduction or oxidation as being key steps in PCDD/F formation;[4.1-4.4] however, the actual redox reaction has not been studied extensively. A surface-stabilized phenoxyl radical has been identified as an intermediate in the formation of PCDD/F when 2-chlorophenol is adsorbed to CuO/silica and the existence of the radical implies electron transfer resulting in reduction of the copper.[4.1]

Figure 4.1 depicts some potential adsorption geometries of 2-chlorophenol onto Cu(II)O to form phenolate and subsequent electron transfer from the phenolate to the metal

center to form the phenoxyl radicals. Based on packed-bed flow reactor studies,[4.1] it is suspected that PCDF form via reaction of two neighboring, surface associated phenols, which is shown in both Pathways **a** and **b** of Figure 4.1. Pathway **a** illustrates two molecules chemisorbed to a geminal copper site. In this case, the formation of two phenoxyl radicals would result in reduction of Cu(II)O to Cu(0). If only one 2-chlorophenol is chemisorbed to each copper, as in Pathway **b**, reduction to Cu(I) is implied.

An Eley-Rideal mechanism in which adsorbed phenol reacts with a gas-phase molecule is believed to form PCDD.[4.1] This is shown in the right side of Pathway **c,** where adsorption is at one hydroxyl of a geminal cupric site. Electron transfer to produce the phenoxyl radical would result in Cu(I). Although not shown, this would also be the case for the analogous reaction at an isolated, single hydroxyl site. The existence of a catecholic reaction intermediate at geminal sites of silica following uptake of 2-chlorophenol was demonstrated in Chapter 3. If this occurs at copper sites, a double electron transfer to the metal center from the bidentate bound phenol would result in the reduction to Cu(0), illustrated in the left hand side of Pathway **c**. In this chapter, XANES spectroscopy is utilized to better characterize these potential reactions at active sites of CuO.

4.1.2 A Brief Introduction to XANES Spectroscopy

Some background will be given since XANES spectroscopy is not one of the more common spectroscopic techniques. A more thorough discussion of XANES spectroscopy can be found in the following reference.[4.5] XANES is an acronym for X-ray absorption near-edge structure spectroscopy and is an elementally specific probe using X-ray absorption. Because this is an element specific technique, it is capable of probing the local environment of the Cu atoms of interest in this study; secondly, it does not require any special sample

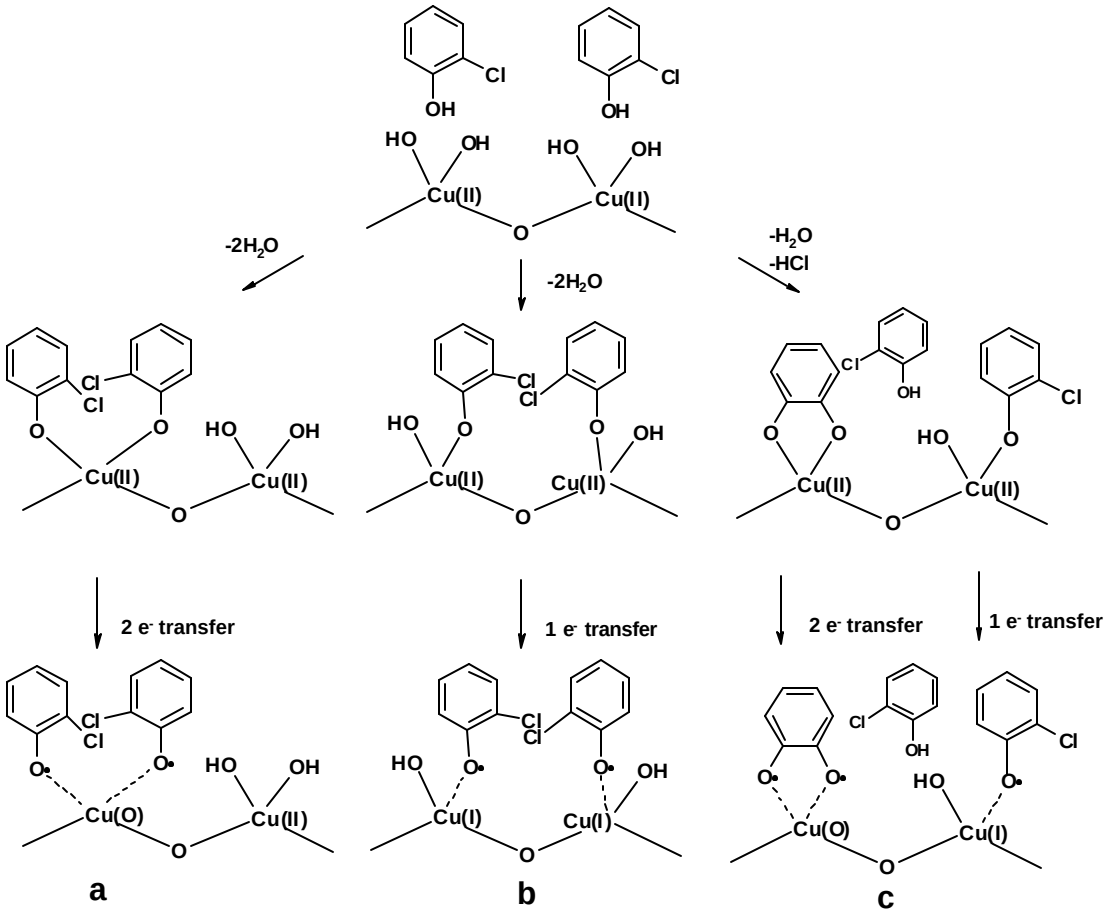

Figure 4.1 Possible mechanisms for the adsorption of 2-chlorophenol and reduction of Cu(II)O.

preparation procedures (e.g., high vacuum or low temperatures), so it can be used with the surrogate systems used to mimic a real combustion environment. XANES is a technique that is in wide use for many studies of complex, disordered, and heterogeneous systems,[4.5-4.7] but has only recently been used to study surface-mediated dioxin formation.[4.8]

XANES spectroscopy is made possible by high intensity X-rays that are produced by synchrotron radiation. Synchrotron radiation is generated though relativistic acceleration of charged particles.[4.9] Electrons are the particles of choice for synchrotrons since they are readily available and are the lightest of the charged particles, which results in higher power radiation. The resulting radiation contains a continuous spectrum that must be monochromatized to the

target energy. For this work, light was monochromatized with a double crystal monochromator.[4.10]

Ions chambers coupled with electrometers were used to measure the incident radiation before and after passing through the sample and the relative change in photon intensity before and after the sample, described by the ratio of transmitted to incident light. Current from the ion chambers was recorded with and analog to digital interface. The adsorption at any given energy is given by the equation below, where A is the absorbance value, I_0 is the incident photon intensity and I_f is the intensity after passing though the sample.

$$A = -\log\frac{I_o}{I_f}$$

Absorption arises when the energy of an incident photon reacting with the sample is equal to the energy needed to excite a core electron to unoccupied valence orbitals or into the continuum. This study was conducted at the Cu K-edge, therefore the absorption resulted from ejecting degenerate 1s electrons.

Figure 4.2 shows a XANES absorption spectrum of CuO taken at the Cu K-edge. There are typically two types of information encoded into such spectra. First, the edge, or white line, will shift according to the oxidation state of the atom, owing to changes in the local electron density (i.e., the same effect which induces chemical shifts in XPS spectroscopy). The edge position on the energy axis is the precise energy in which the binding energy of the electron and incident photon is equal, resulting in a zero kinetic energy photoelectron. The precise position of the edge, the point of no slope, is the maximum of the first derivative of the spectrum. Secondly, the shape of the near edge structure (local maxima above and below the ionization threshold, or edge) will frequently be characteristic of particular local chemical geometries, or speciation. Our experimental spectra were made up of copper compounds in three oxidation states. The method

employed to determine the percent contribution each species made to our experimental spectra was given in Chapter 2, Section 2.3.

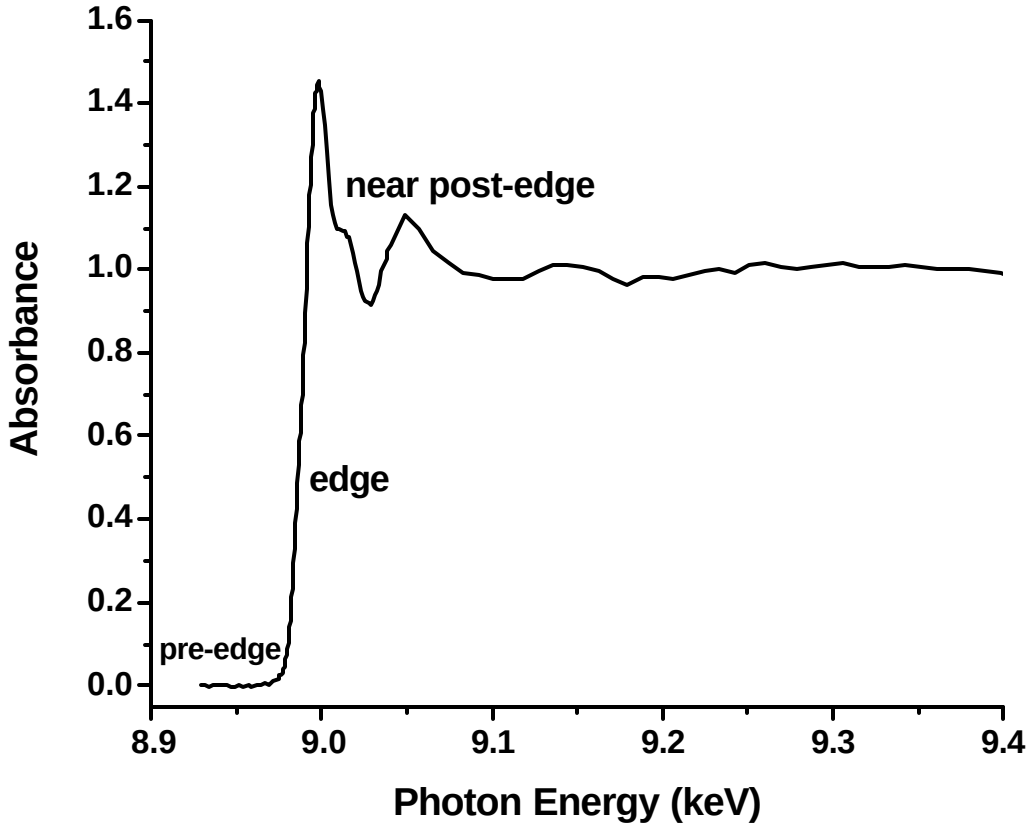

Figure 4.2 XANES spectrum at the Cu K-edge of CuO.

4.2 The Effect of Redox Cycling on the Reactivity of 2-Chlorophenol with CuO: XANES and SEM Analysis

It was noted during the course of a previous experiment that the reactivity of CuO in a silica mixture depended on its thermal history.[4.8] Specifically, it was determined that consistent data resulted, with respect to the rate of Cu(II) reduction, if the CuO substrate was first sent though a redox cycle. First, the substrate was exposed to 2-chlorophenol at 375 °C for 20

minutes. This treatment was known to covert approximately 70 % of Cu(II)O to $Cu(I)_2O$. The substrate was then re-oxidized completely back to CuO by heating it in air at 350 °C for 20 minutes. To investigate the effects of this thermal pre-treatment, the rate of reduction of a previously unexposed or “virgin” sample was compared with that of a sample that had undergone one redox cycle, or had been "recycled". SEM images were taken of CuO treated under the same conditions at various stages of the reaction to assist the investigation.

XANES transmission spectra resulting from CuO reaction with 2-chlorophenol at 375 °C are depicted in Figure 4.3, and data sets from two samples are shown: a) a previously unexposed, virgin sample, and b) a recycled sample. A comparison of the spectra at t = 120 s shows that the Cu K-edge has shifted to substantially lower energy for the recycled sample relative to the shift for virgin sample. This is empirical evidence that more of the Cu was reduced in the recycled sample than the virgin sample during the same time interval, i.e., the reaction rate is enhanced via this recycling procedure. This trend is also observed for the other time points.

Figure 4.4 depicts the experimental compositions of Cu(II) and Cu(I) as a function of time for each sample. $Cu(I)_2O$ is the primary reaction product, with Cu(0) formed in low concentrations. Because Cu(0) is a minor component (< 5%) of the reaction, and to reduce congestion in the figure, it is not shown in Figure 4.4. It was determined that Cu_2O was the major Cu(I) product and not another Cu(I) species as the Cu_2O reference standard resulted in qualitatively superior fits compared to other standards, e.g. Cu(I)Cl.

It is apparent from Figure 4.4 that most, but not all of the copper is reduced. Subsequent experiments have revealed that the amount of copper ultimately available for reaction is temperature dependent. For example, as shown in Figure 4.4, at 375 °C the reaction reaches

apparent completion when approximately 70% of the copper has been reduced. However, we have determined that dosing at 425 °C for 120 s is sufficient to reduce all Cu(II) present.

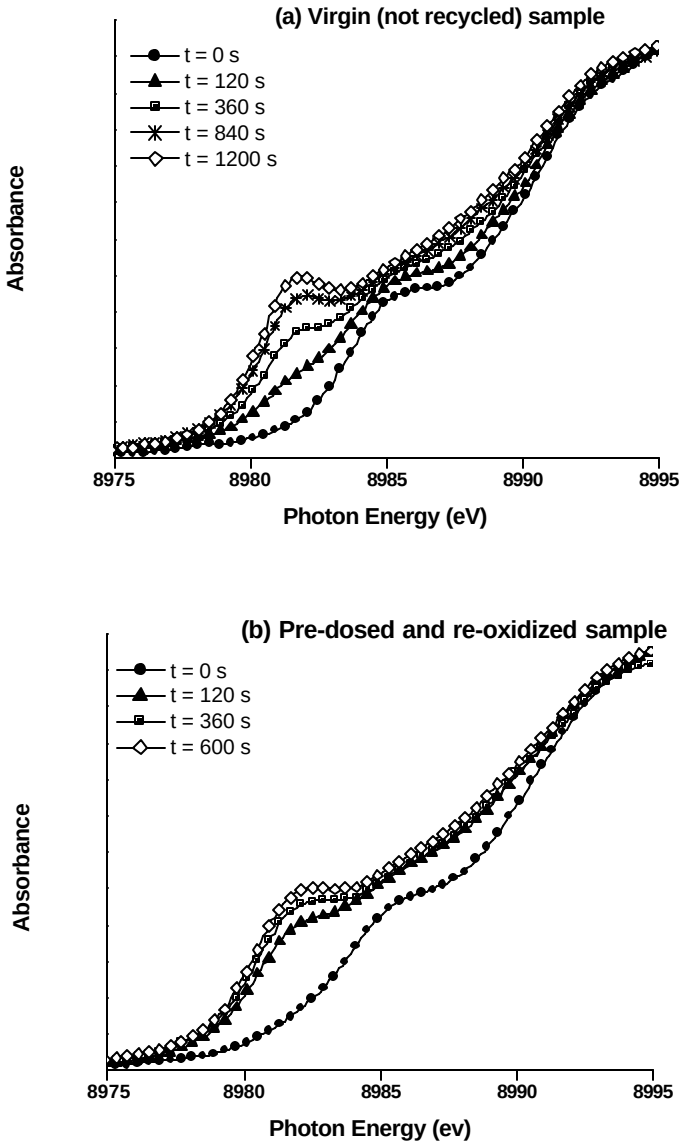

Figure 4.3 Absorption spectra of the CuO/SiO_2 mixture acquired at the Cu K-edge as a function of time following exposure to 2-chlorophenol at 375 °C of: a) a previously unexposed sample and b) a sample that had been reduced to completion then re-oxidized.

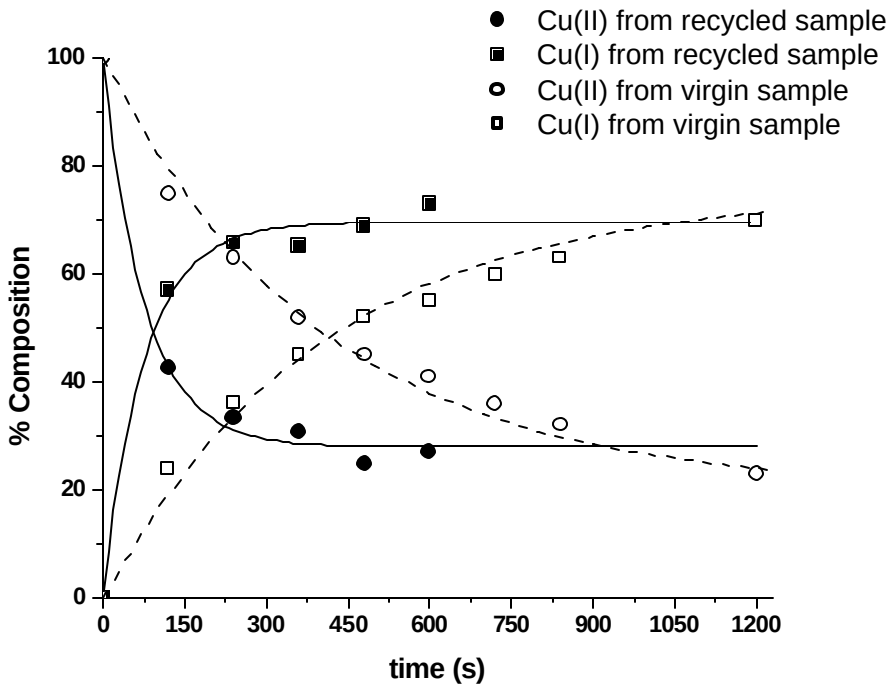

Figure 4.4 Comparison of the rate of reduction of Cu(II) and the formation of Cu(I) for a virgin sample and a recycled sample resulting from 2-chlorophenol exposure at 375 °C.

XANES measures the bulk, not surface properties of the sample. Since over 70% of the Cu(II) in the bulk of the sample is reduced, it is obvious that more copper is undergoing reduction than is originally available on the surface. This large extent of reaction implies that as 2-chlorophenol reduces the surface sites, additional oxides migrate from the interior to replenish the reactive surface oxide sites. This is corroborated by the SEM data.

The SEM images in Figure 4.5 depict grains of copper: a) before exposure to 2-chlorophenol, b) after reaction with 2-chlorophenol, and c) after re-oxidation. The white bar in each frame represents 6 μm. From comparison of Figures 4.5a and 4.5b, it is clear that following reaction with 2-MCP that the copper oxide grains have been reduced in mean diameter by more than an order of magnitude. The right-hand frame of Figure 4.5 reveals that following re-oxidation, the mean particle size has increased and possibly become more crystalline but is

still clearly smaller than the original particles. This difference in particle morphology must be responsible for the increased reaction rate of the cycled samples.

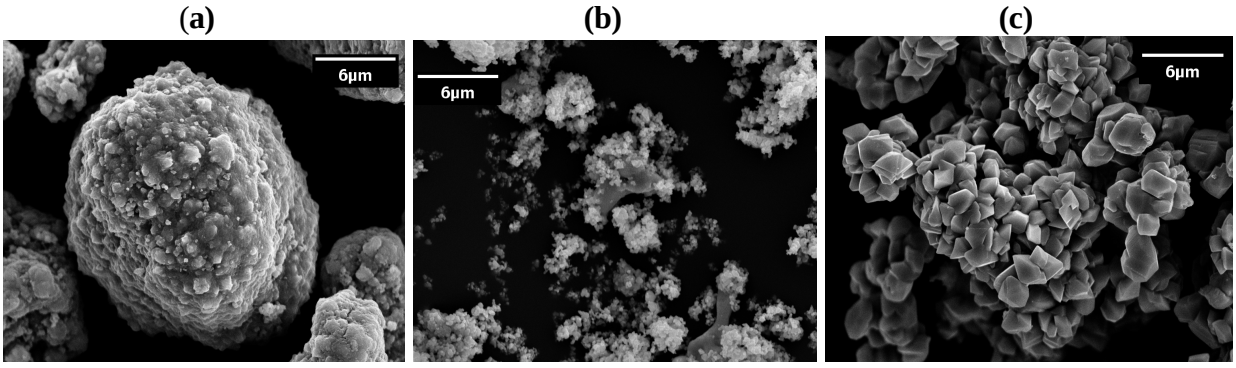

Figure 4.5 SEM images of CuO: a) before reaction ("virgin"), b) after exposure to 2-chlorophenol at which point mostly Cu_2O is present, and c) after the sample has been re-oxidized back to CuO ("recycled"). The white bar near the top of each frame represents 6 µm.

4.3 Reactions of 2-Chlorophenol, 1,2-Dichlorobenzene, and Chlorobenzene with CuO

4.3.1 Chemical Speciation of Reaction Products

Chapter 3 of this dissertation demonstrated that 2-chlorophenol and 1,2-dichlorbenzene each chemisorb to CuO/SiO_2 at surface hydroxyl groups to yield identical chlorophenolate species. In this section, their reactivity's with respect to Cu(II) reduction are examined. Chlorobenzene was included in this study to examine the rate of reduction of a mono- substituted chlorinated aromatic. Figure 4.6 illustrates the reduction of CuO and the formation of Cu_2O and Cu(0) when the CuO/silica mixture is exposed to each dosant at 350 °C. In each case, the major reduction product is Cu_2O. This held true for all temperatures examined (275-375 °C). Reduction to metallic copper is a minor reaction product, ranging from 0-5%, with a 2% average over the complete data set. The time-dependent speciation for each temperature and dosant can be found in Appendix 1.

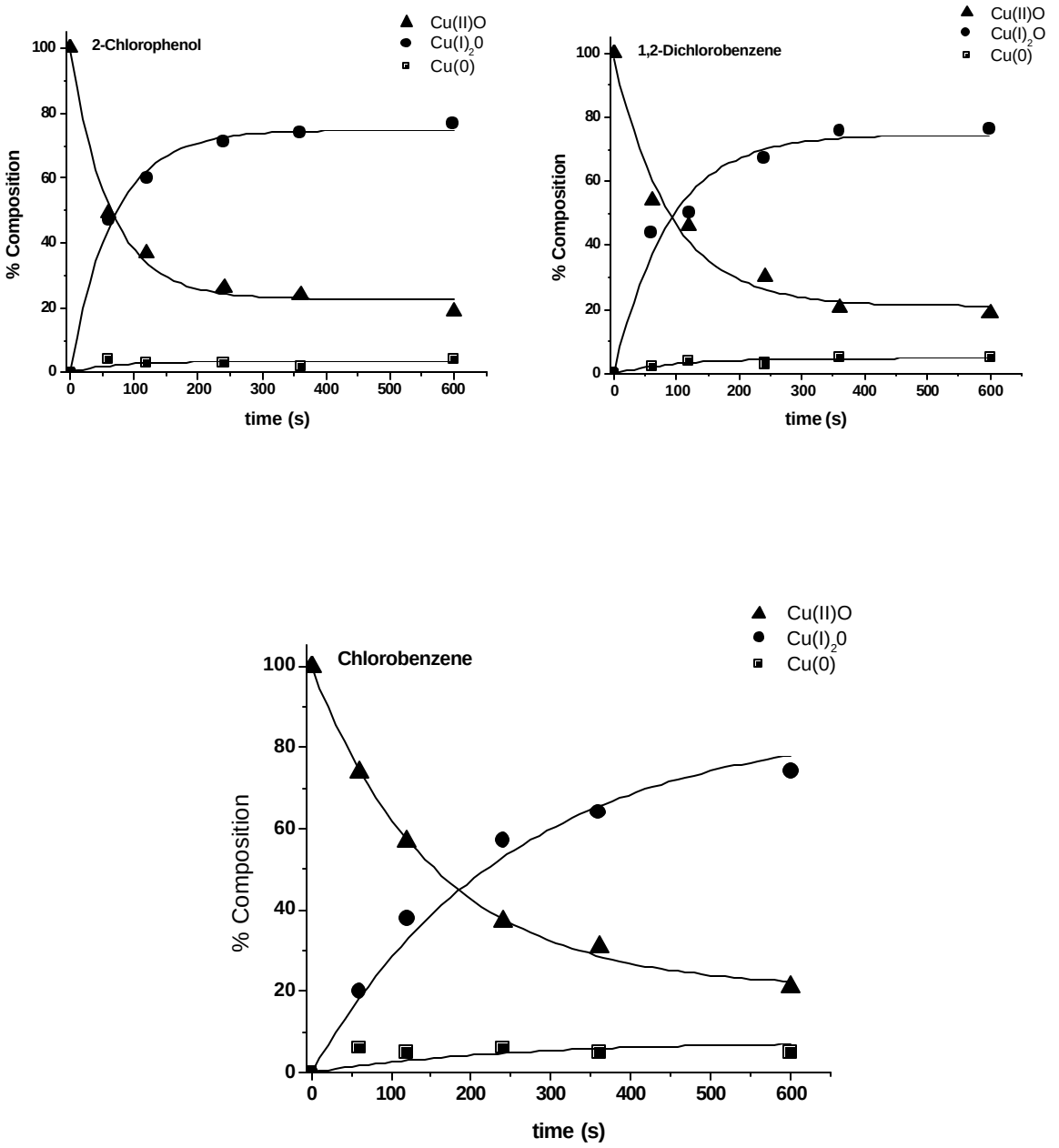

Figure 4.6 Time-dependent reduction of Cu(II)O and formation of $Cu(I)_2O$ and Cu(0) for reactions of 2-chlorophenol, 1,2-dichlorobenzene and chlorobenzene at 350 °C.

4.3.2 Kinetics of CuO Reduction

A general reaction scheme for 2-chlorophenol adsorption onto the copper oxide surface to form surface bound chlorophenolate (CP---CuO) is represented by Rxn. 1. This is followed by reduction of Cu(II) to Cu(I) and Cu(0) and the formation of 2-chlorophenol oxidation products (Rxn. 2).

Rxn. 1 2-MCP + CuO $\rightarrow$ CP---CuO

Rxn. 2 CP---CuO $\rightarrow$ Cu_2O + Cu(0) + 2-MCP oxidation products

The rate of Cu(II) reduction can measured using a pseudo-first order kinetic reaction scheme, with the rate law depicted in the equation below, where f_r is the amount of Cu(II) remaining *unreacted* at time, t, and $(D)_0$ is the vapor-phase concentration of the 2-chlorophenol.

$$\ln f_r(\mathrm{Cu(II)}) = -k_{bi}(D)_0 t$$

The percent composition of Cu(II) vs. time was fit to an exponential decay of the form shown below:

$$\mathrm{Cu}_{\mathrm{II}(t)} = \mathrm{Cu}_{\mathrm{II}(\infty)} + (100 - \mathrm{Cu}_{\mathrm{II}(\infty)})e^{\frac{-t}{t}}$$

$Cu_{II(t)}$ denotes the percent composition of Cu(II) in the substrate at reaction time t. $Cu_{II(\infty)}$ denotes the asymptotic value of the decay curve. The inverse of the decay constant, τ, yields a pseudo-first order rate coefficient, k', where $k' = k_{bi}(D)_o$. Examples of this are shown for 2-chlorophenol and chlorobenzene in Figure 4.7. Fits are generally good over the time interval measured at lower reaction temperatures, but begin to degrade at higher temperatures and longer reaction times, probably due to competing reactions of secondary reaction products. The calculated values of k_{bi} for each dosant at each temperature are given in Table 4.1.

Arrhenius plots of ln k_{bi} versus 1/T yields the two-parameter Arrhenius activation energy (E) and pre-exponential factor (A). These are shown in Figure 4.8. The activation energy of Cu(II) reduction is found to be 112 ± 6.4 kJ/mol, 101 ± 1.21 kJ/mol, and 88 ± 3.3 kJ/mol by 2-chlorophenol, 1,2-dichlorobenzene, and chlorobenzene, respectively. The A-factors are 9.7 x 10^9, 1.2x10^9, and 5.6x10^6 atm^{-1} sec^{-1}, respectively.

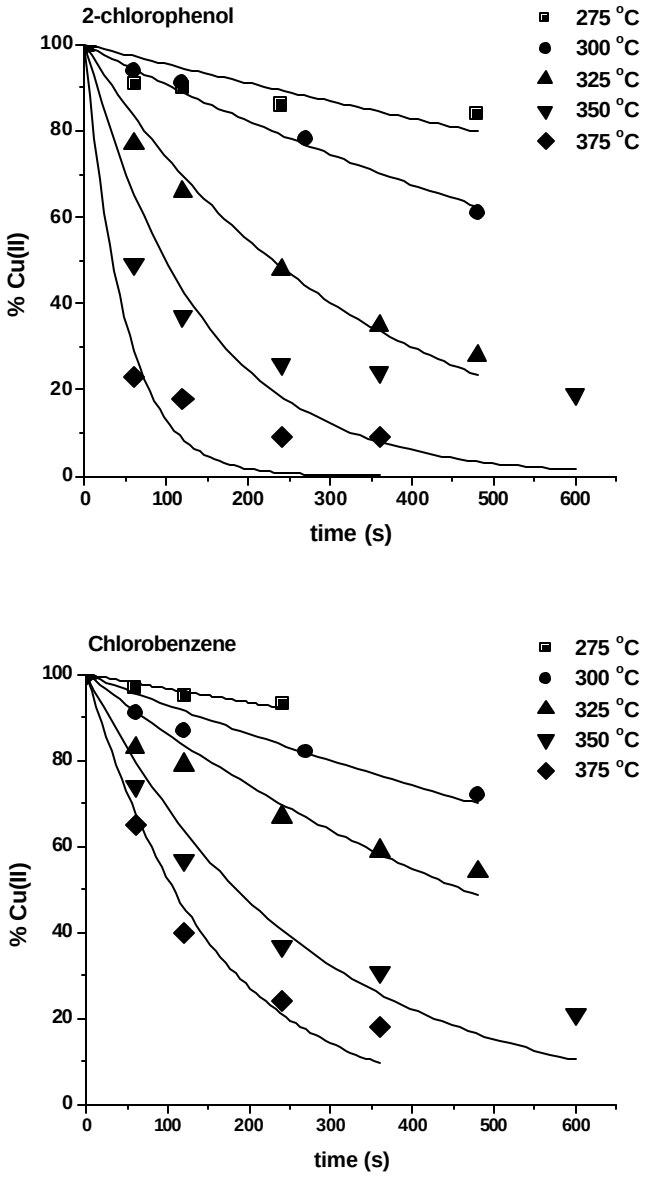

Figure 4.7 Exponential decay fits of Cu(II) reduction for 2-chlorophenol and chlorobenzene.

Table 4.1 Bimolecular rate coefficients, k_{bi}, for the reduction of Cu(II).

Temperature (°C)	2-MCP k_{bi} (atm^{-1} sec^{-1})	1,2-DCBz k_{bi} (atm^{-1} sec^{-1})	MCBz k_{bi} (atm^{-1} sec^{-1})
275	0.251	0.125	0.022
300	0.524	0.573	0.048
325	1.62	1.25	0.096
350	3.77	2.93	0.24
375	10.93	2.73	0.415
E_a (kJ mol^{-1})	112 ± 6.4	101 ± 1.21	88 ± 3.3
A (atm^{-1} sec^{-1})	$9.7x10^9$	$1.2x10^9$	$6.6x10^6$

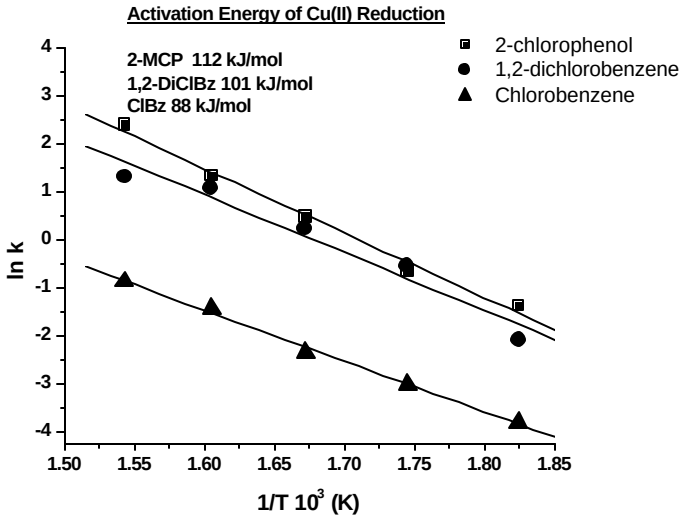

Figure 4.8 Arrhenius plots showing the temperature dependence of reaction from 275-375 °C.

4.4 Chapter Summary and Relevance for PCDD/F Formation

Low temperature formation of PCDD/F in the post-combustion, cool-zone of combustion systems requires the presence of a transition metal whether formation is from a chemical precursor (chlorinated phenols or chlorinated benzenes) or elemental carbon as a chemical reagent in the so-called *de novo* process.[4.11-4.13] The function of the catalyst is not explicitly clear, but it has been suggested that in the precursor pathway, the catalyst facilitates the coupling of aromatic ring structures, stabilizes a Smiles type dioxasipiro intermediate, and participates in PCDD/F chlorinating reactions.[4.3] Specifically, it has been proposed that the metal substrates

can serve as electron transfer oxidants that in turn facilitate ring coupling.[4.4] The formation of surface associated chlorophenoxyl radicals as intermediates in PCDD/F formation has also been attributed to electron transfer from surface bound chlorophenols to metal cation sites.[4.1]

A detailed investigation was conducted by Lomnicki and Dellinger, who used 2-chlorophenol as a model for PCDD/F precursor and CuO supported on silica as a model fly-ash.[4.1] Their results suggested that PCDD are formed through an Eley-Rideal mechanism and that PCDF are form via the Langmuir-Hinshelwood pathway. The main PCDD/F products formed from their experiments were the same products expected based on gas-phase radical-molecule and radical-radical reactions.[4.14,4.15] Based on this, it was suspected that surface associated phenoxyl radicals may form PCDD/F in a manner similar to that of gas-phase formation. Using EPR spectroscopy, they found solid evidence supporting the existence a carbon-centered phenoxy radical when 2-chlorophenol is adsorbed onto CuO/SiO_2. They went on to suggest that chlorophenol adsorbs to a Cu(II) site as chlorophenolate and a surface associated radical is formed following electron transfer from chlorophenolate to the metal cation site, thus reducing Cu(II) to Cu(I), illustrated in Figure 4.9.

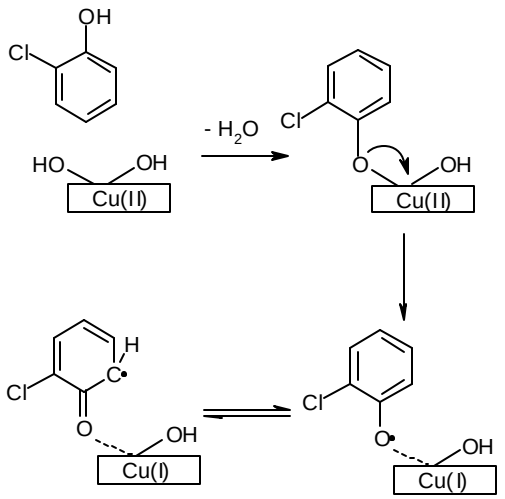

Figure 4.9 Adsorption of 2-chlorophenol on copper(II) oxide and formation of the resonance stabilized chlorophenoxyl radical.

It had been previously demonstrated that CuO is reduced to primarily Cu_2O in the presence of 2-MCP vapor at 375 °C.[4.8] These new results shown this to be the case for reduction over the temperature range of heterogeneous PCDD/F formation. This is also the case for reactions of 1,2-dichlorobenzene and chlorobenzene. These results are consistent with the proposal that phenoxyl radical formation occurs following a 1 e^- transfer to Cu(II) sites, i.e. the same behavior shown in Figure 4.9. These results are supported by complementary observations of CuO reduction during the catalytic oxidation of 2-chlorophenol with CuO doped zeolites.[4.16,4.17]

We have successfully measured pseudo-first order reaction rate coefficients and calculated Arrhenius parameters for our model system. Our results indicate that the thermal and reaction history of the particle affects its rate of reaction and reduction by subsequent exposure to 2-chlorophenol, as it was evident that the reaction rate varied as the particle parameters were changed by the history of thermal exposure. This is likely related to the change in surface area and rate of diffusion of internal reactive oxide groups to the surface.

These XANES data provide critical information, and can help in understanding the detailed microscopic mechanism of PCDD/F formation via surface-mediated processes. While the current data do not definitively prove a particular mechanism, they do provide useful guideposts for informed speculation regarding likely reaction pathways.

4.5 References

4.1 Lomnicki, S.; Dellinger, B. *J. Phys. Chem. A* **2003**, *107*, 4387.

4.2 Weber, P.; Dinjus, E.; Stieglitz, L. *Chemosphere* **2001,** *42*, 579.

4.3 Tuppurainen, K.; Asikainen, A.; Ruokojarvi,P; Ruuskanen, J. *Acc. Chem. Res.* **2003**, 652.

4.4 Tuppurainen, K.; Ruuskanen, J. *Chemosphere* **1999**, *38*, 1825.

4.5 D. C. Koningsberger and R. Prins, X-ray Absorption - Principles, Applications, Techniques of EXAFS, SEXAFS and XANES, Wiley and Sons, New York, 1988.

4.6 Sinfelt, J.H.; Meitzner, G.D. J. H. *Acc. Chem. Res*. **1993**, *26*, 1.

4.7 Knop-Gericke, A; Havecker, M; Schedel-Niedrig, T; Schlogl, R. *Topics in Catalysis* **2001**, *15*, 27.

4.8 Farquar, G.R.; Alderman, S.L.; Poliakoff, E.D.; Dellinger, B. *Environ. Sci. Technol.* **2003**, *37*, 935.

4.9 Thompson, A.; Attwood, D; Gullikson, E.; Howells, M.; Kim, K.-J.; Kirz, J.; Kortright, J; Landau, I.; Piannetta, P.; Robinson, A.; Scofield, J.; Underwood, J.; Vaughan, D.; Williams, G.; Wilnick, H. *Center for X-Ray Optics and Advanced Light Souce X-Ray Data Booklet*, Second ed.; Lawrence Berkeley National Laboratory: Berkeley, CA, 2001.

4.10 Schilling, P.; Morikawa, E.; Tolentino, H.; Tamura, E.; Kurtz, R. L.; Cusatis, C. *Rev. Sci. Instrum.* **1995**, *66*, 2214.

4.11 Fiedler, H. *Environ. Eng. Sci.* **1998**, *15*, 49.

4.12 Stieglitz, L. *Environ. Eng. Sci*. **1998**, *15*, 5.

4.13 Addink, R.; Altwicker, E.R. *Environ. Eng. Sci*. **1998**, *15*, 19.

4.14 Weber, R.; Hagenmaier, H. *Chemosphere* **1999**, *38*, 529.

4.15 Sidhu, S.; Maqsud, L.; Dellinger, B.; Mascolo, G. *Combust. Flame* **1995**, *100*, 11.

4.16 Lin, K.S.; Wang,H.P. *Langmuir* **2000**, *16*, 2627.

4.17 Lin, K.S.; Wang,H.P. *J. Phys. Chem. B* **2001**, *105*, 4956.

CHAPTER 5: CORRELATING PCDD/F EMISSIONS WITH CHLOROPHENOL CONCENTRATIONS

5.1 Introduction

As part of the EPA program entitled, "Real-Time Monitoring of Dioxins and Other Trace Organics," our group was asked to examine the possibility of correlating isomer specific emissions of PCDD/F with the concentrations of chlorinated phenols in the gas phase. Establishing such a correlation is beneficial since gas-phase concentrations of chlorinated phenols in combustion systems are much higher that those of PCDD/F. Thus, a continuous emission monitor could presumably more readily detect chlorinated phenols than PCDD/F. If it can be established that knowledge of the concentration of individual chlorinated phenols can be used to predict PCDD/F isomer emissions, then real-time monitoring of chlorinated phenols may suffice as a surrogate for PCDD/F emissions.

The results of this study also provided an interesting look at the role chlorinated phenols as PCDD/F precursors. The coupling reactions of specific chlorophenol isomers yield specific PCDD/F isomers though both gas-phase and heterogeneous pathways.[5.1-5.6] Therefore, PCDD/F isomer and homologue class distributions could, in theory, be predicted based on chlorophenol isomer distributions. However, for this to hold true, it is required that chlorinated phenols be the sole PCDD/F precursor, that PCDD/F chlorination, de-chlorination, and/or isomerization reactions not occur after initial formation and that *de novo* formation in which PCDD/F are directly released from the carbon matrix not make a contribution to emissions. Since these theoretical constraints are not met in reality, positive or negative correlations between the observed and predicted have the potential to provide additional means of interrogating PCDD/F formation mechanisms.

This project was divided into four tasks: 1) Experimental studies and literature review of PCDD/F formation from chlorophenols; 2) Determination of which PCDD/F isomers are formed from all 19 chlorophenol isomers based on the pathways developed in Task 1; 3) Development of a predictive model, and 4) Correlation of model predictions with field data. Task 1 was undertaken, in part, to determine the relative yield of each pathway suspected in PCDD/F formation from chlorinated phenols. Multiple sets of yields were employed to take into account gas-phase and surface-mediated reactions under oxidative and pyrolytic conditions. Task 2 was necessary in order to determine which PCDD/F isomers are formed from specific chlorinated phenol isomers reacting with themselves and with every other chlorophenol isomer. Task 3 was accomplished though the development of an Excel spreadsheet model into which measured chlorinated phenol isomer concentrations can be entered and PCDD/F congener concentrations predicted, thus making Task 4 possible.

Task 1 has been completed; however, since this author was not the principal experimental investigator, a description of Task 1 will only include the details necessary for an understanding of the rest of the chapter. This chapter presents the completed results for Tasks 2 and 3. Task 4 is described within the context of the data currently available. After studying the available field data, it was apparent that meaningful correlations between laboratory models and field data could not be realized with the limited and incomplete data currently available in the literature; therefore, Task 4 cannot be fully described. However, additional data are anticipated from the EPA study of continuous monitoring of chlorophenols and PCDD/F and will be critical to the success of this project. Recommendations are made concerning what additional laboratory and field data are needed to successfully complete the project.

5.2 Task 1: Experimental Measurement and Assignment of PCDD/F Yields

In order to successfully predict PCDD/F formation from chlorinated phenols, it is obvious that one must have an understanding of the possible reaction pathways. Review of the literature indicates that multiple pathways are possible that give different PCDD/F congener distributions.[5.1-5.6] Proposed gas-phase pathways may be broadly grouped as radical-molecule and radical-radical reactions of phenoxy radicals. Prior work in our group and in the literature had made clear the role of *ortho*- chlorines versus *ortho*- hydrogens in determining weather PCDD, PCDF, or both are formed from chlorophenol condensation reaction. Thus, it was decided to experimentally investigate the simplest chlorinated phenol for which all pathways were available, e.g. 2-chlorophenol. Since it was unknown how reaction atmospheres and surfaces affected congener profiles and yields, the reactions were investigated the gas-phase reaction under oxidative (21 % oxygen) and pyrolytic conditions (no oxygen). The reaction was also studied over a CuO/silica bed to generate surface-mediated yields.

Experimental studies of the reactions of 2-chlorophenol were performed under various conditions at temperatures between 200 °C and 1000 °C. All studies were performed using a high-temperature flow reactor system, the STDS (System of Thermal Diagnostic Studies), which utilizes a fused silica flow reactor equipped with an in-line GC/MS analytical system.[5.7] The flow reactor is housed inside a furnace that is housed inside a Varian GC where the temperatures to and from the reactor can be controlled. The furnace maintains the experimental temperature range of 200 °C to 1000 °C. Pressure inside the reactor is maintained at 1.15 +/- 0.15 atmospheres. The gas-phase reactor is a quartz tube with a diameter of 0.1 cm and a volume of 4.7×10^{-7} m^3. The reactor used in the heterogeneous studies simple 1 mm i.d. fused-silica

reactor. The experimental protocol and a complete discussion of 2-chlorophenol reactions in the gas-phase and with the CuO/silica substrate have been reported elsewhere.[5.6,5.8]

It was discovered from the literature and during the completion of Task 1 that two pathways produce PCDD and one pathway produces PCDD/F.[5.1-5.6,5.9] These reaction pathways are described in Chapter 1, Section 1.2, and are again illustrated here, based on the PCDD/F isomers formed from the gas-phase condensation reactions of 2-chlorophenol. The gas-phase and surface reaction of 2-chlorophenol yields 3 major PCDD/F products: dibenzo-*p*-dioxin (DD), 1-monochlorodibenzo-*p*-dioxin (1-MCDD), and 4,6-dichlorodibenzo furan (4,6-DCDF).[5.5,5.6]

A radical-molecule and radical-radical pathway has been developed to account for DD formation, both illustrated in Figure 5.1.

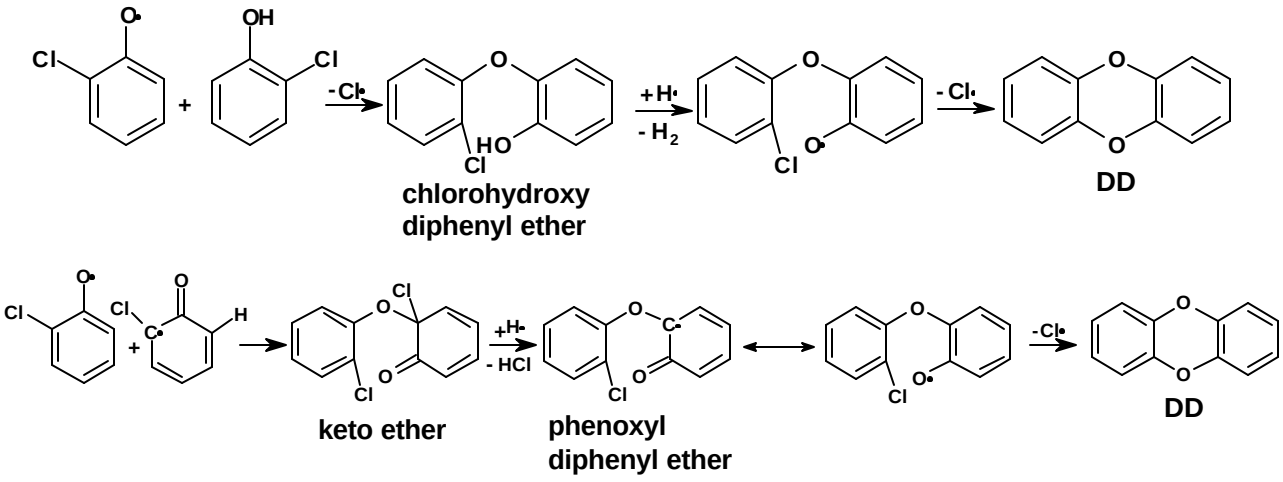

Figure 5.1 Radical-molecule (top) and radical-radical reaction of dibenzo-*p*-dioxin.

At this time, it is unclear which pathway dominates and the significance of the radical-molecule reaction is often questioned;[5.10,5.11] however, for the purposes of this study the relative yield of DD from 2-chlorophenol versus the yield of 1-MCDD and 4,6-DCDF was the more important

parameter. Therefore, for descriptive purposes, the reaction responsible for DD formation will be referred to as the radical-molecule pathway.

The formation of 1-MCDD though the radical-radical reactions is drawn in Figure 5.2 and Figure 5.3 illustrates the radical-radical reaction to 4,6-DCDF.

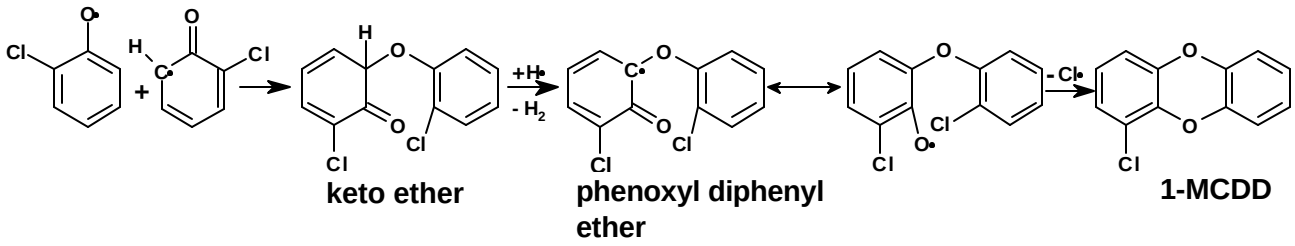

Figure 5.2 Radical-radical route to 1-MCDD.

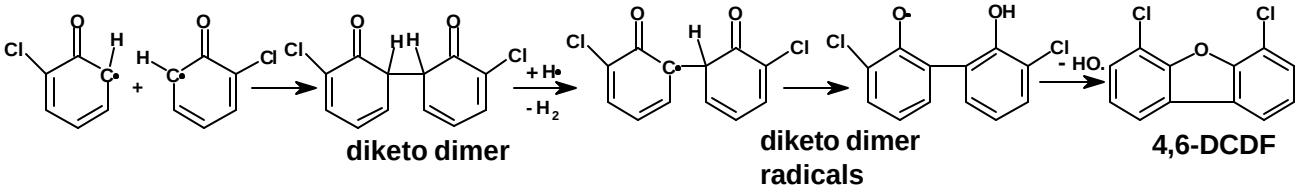

Figure 5.3 Radical-radical pathway to 4,6-dichlorodibenzofuran.

The experimental results for 2-chlorophenol were different depending on reaction conditions, with the relative ratios of DD, 1-MCDD and 4,6-DCDF varying significantly from conditions to condition. However, the relative yields could be grouped into three categories:

1) 1-MCDD>DD>>4,6-DCDF in the gas-phase oxidation and surface oxidation,

2) DD≈4,6-DCDF >1-MCDD under gas-phase pyrolysis, and

3) DD>1-MCDD>>4,6-DCDF under surface pyrolysis.

Relative yields of the PCDD/F products of interest were calculated from mass spectrometer peak area counts. Table 5.1 lists the relative yields assigned to each of the three reaction pathways considered and these yields were utilized in the spreadsheet model.

Table 5.1 Assigned relative yields of PCDD and PCDF from chlorinated phenols.

Reaction	Yields			
	Oxidation		Pyrolysis	
	Gas-phase	Surface	Gas-phase	Surface
Radical-Molecule to PCDD	0.4	0.4	1.5	2.0
Radical-Radical to PCDD	1.0	1.0	1.0	1.0
Radical-Radical to PCDF	0.15	0.15	1.3	0.1

The relative yields listed in Table 5.4 may be readily modified in the spreadsheet calculation as additional data become available.

5.3 Task 2: Determination of PCDD/F Isomers Formed from Chlorophenols

The above reaction mechanisms were all worked out for chlorinated phenols as a class to determine which PCDD/F isomers are formed via the gas-phase condensation of chlorinated phenols. The relative yields for each pathway observed for 2-chlorophenol were applied to all other chlorinated phenol isomers in the predictive model with the assumption that additional chlorines were passive participants in the reaction and did not directly affect relative yields.

Surface-mediated pathways are less well understood. A useful classification scheme for surface-mediated pathways would be: surface-mediated condensation reactions and surface-mediated chlorination/dechlorination/isomerization. The condensation step seems to results in predictable PCDD/F congener distributions, as it was observed that the major PCDD/F products formed during CuO mediated formation from 2-chlorophenol were the same as those observed in

gas-phase formation[5.6]. However, the chlorination/dechlorination/isomerization reactions may give very complex distributions that are difficult to predict unless they achieve equilibrium and give a thermodynamically predictable distributions. However, it is possible that given short reaction times, the surface-mediated condensation pathways and gas-phase pathways will dominate and give a predictable PCDD/F congener distribution, while at longer reaction times, the surface-mediated "scrambling" will occur. A superposition of all these pathways most likely occurs in a full-scale combustor.

Although this is a rather depressing scenario, some progress on simplification has been achieved. A major advance comes from evidence that the relatively well-developed gas-phase pathways can be applied to the surface-mediated condensation reactions.[5.6] Chemisorption of a chlorophenol on a metal surface, followed by one electron transfer yields a surface bound radical that would have very similar reaction properties to those of a gas-phase radical. The preceding chapters of this dissertation all provide experimental evidence that this occurs. This means that the surface-mediated condensation reactions would be qualitatively similar to the gas-phase reactions, although the relative yields may differ. Thus, our consideration of predictable PCDD/F congener distributions can be reduced to consideration of radical-radical and radical-molecule reactions illustrated above.

5.3.1 Results of Mechanistic Investigations

The possible reactions of every chlorinated phenol isomer with every other chlorinated phenol isomer were considered. This adds up to 190 potential reaction pairs, some of which produce only PCDD, some of which PCDF and some combinations produce both isomers. A table listing each chlorophenol combination and the PCDD/F isomers predicted from each applicable pathway makes

up Appendix 2. Upon completion of this task, several general observations could be made that were relevant to the prediction of PCDD/F congener distributions.

In order for a successful coupling of two chlorinated phenols to form PCDD from the radical-molecule pathway, both reactants must contain, at least, one *ortho*- chlorine. In addition, reactants with both *ortho*- sites chlorinated also participate in PCDD formation from this pathway. All of the possible PCDD congeners are formed from this pathway. There are a total of 104 combinations to produce PCDD from this pathway. The majority of radical-molecule combinations results in the formation of more than one PCDD isomer since ring closure to form PCDD proceeds though a Smiles rearrangement that produces isomer pairs.[5.2,5.3,5.12] Table 5.2 summarizes some aspects of the radical-molecule pathway to PCDD.

Table 5.2 Radical-molecule reactions to PCDD

Isomer	# of Possible Isomers	# of Possible Isomers Formed	Total Combinations Contributing to Homologue Total
MCDD*	2	2	4
DCDD	10	10	15
TrCDD	14	14	23
TeCDD	22	22	28
PeCDD	14	14	19
HxCDD	10	10	11
HpCDD	2	2	3
OCDD	1	1	1
		Total Combinations to PCDD	104

*monochlorodibenzo-*p*-dioxin = MCDD, dichlorodibenzo-*p*-dioxin = DCDD, trichlorodibenzo-*p*-dioxin = TrCDD, tetrachlorodibenzo-*p*-dioxin = TeCDD, pentachlorodibenzo-*p*-dioxin = PCDD, hexachlorodibenzo-*p*-dioxin = HxCDD, heptachlorodibenzo-*p*-dioxin = HpCDD, octachlorodibenzo-*p*-dioxin = OCDD

In order for a successful coupling of two chlorinated phenols to form PCDD from radical-radical pathway, at least one of the reactants must be unchlorinated in the *ortho*- position to allow formation of the carbon-centered radical. However, this species may combine with a

chlorinated phenol not containing an *ortho*- chlorine to yield PCDD. This is not the case with the radical-molecule pathway to PCDD and is the reason that there are 50 more combinations to yield PCDD from the radical-radical pathway, as can be seen in Table 5.3. Another difference in the radical-molecule and radical-radical pathway is that in the radical-radical route, different isomers are formed depending on which partner takes on the role of carbon-centered radical and which acts as the oxygen-centered radical. With the radical-molecule pathway to PCDD, the same PCDD isomer is always formed regardless of which chlorophenol is assigned the role of the molecule.

Table 5.3 Radical-radical reactions to PCDD

Isomer	# of Possible Isomers	# of Possible Isomers Formed	Total Combinations Contributing to Homologue Total
MCDD	2	2	3
DCDD	10	10	14
TrCDD	14	14	33
TeCDD	22	22	41
PeCDD	14	14	36
HxCDD	10	10	19
HpCDD	2	2	7
OCDD	1	1	1
		Total Reactions to PCDD	154

In order for a chlorinated phenol to participate in the radical-radical formation of PCDF, it must posses at least one *ortho*- hydrogen to facilitate formation of the carbon-centered phenoxy radical, just as in the radical-radical pathway to PCDD. Because phenol was not included in the reaction pathway, none of the mono-chlorinated isomers were formed. This also explains the omission of some possible di-tetra chlorinated congeners, as can be seen from Table 5.4. 117 PCDF of the possible 135 are formed from this pathway. The reactions of

asymmetrical phenoxy radicals result in the formation of more individual PCDF isomers than symmetrical radical. For example, a 2,4,-dichlorophenol only form one PCDF isomer, whereas, 3-chlorophenol and 3,4-dichlorophenol have been observed to form the three separate, predicable, dibenzofuran isomers and TeCDF, respectively.[5.3]

Table 5.4 Radical-radical reactions to PCDF

Isomer	# of Possible Isomers	# of Possible Isomers Formed	Total Combinations Contributing to Homologue Total
MCDF	4	0	0
DCDF	16	9	6
TrCDF	28	24	15
TeCDF	38	36	27
PeCDF	28	27	19
HxCDF	16	16	15
HpCDF	4	4	4
OCDF	1	1	1
		Total Reactions to PCDF	87

5.4 Task 3: Development of Excel Spreadsheet Model

An Excel spreadsheet model was constructed into which measured chlorinated phenol isomer concentrations can be entered and PCDD/F congener concentrations predicted. Contained within the spreadsheet are 190 rows corresponding to the 190 chlorophenol reaction pairs. The concentration of reactants must be provided as an input parameter. An effective concentration taking into account both reactants' concentration is automatically calculated. The relative yields for each reaction pathway to PCDD/F must also be included as an input parameter. Each of the 210 PCDD/F congeners is assigned a column in the spreadsheet. Within each column equations are entered into the cells corresponding to the reaction pair and PCDD/F congeners generated from that reaction pair. This equation automatically takes into account the

reactants' concentrations and the relative yield of the pathway that produced the PCDD/F congener. At the bottom of each congener column, the contribution that each reaction makes to the congener total is summed.

To the right-hand side of the congener columns are cells dedicated to displaying the homologue totals for PCDD and PCDF, the 2,3,7,8-substitued PCDD/F isomer yields, and the tetra-chlorinated dioxin isomer yields. All of this information is included in easy to read histogram format via labeled charts within the spreadsheet. The spreadsheet is configured so that should an input parameters (chlorophenol concentrations and/or relative yields) need to be modified, the change in PCDD/F yields is automatically calculated and reflected in the accompanying histograms.

5.5 Task 4: Correlation Between Calculated and Full-Scale Emissions

Table 5.5 presents the chlorinated phenol concentrations that were used in our initial attempts at correlations. These data represent measured chlorinated phenol concentrations at various sampling points within a fluidized bed incinerator.[5.13] It was immediately obvious that the data sets were incomplete and that chlorinated phenol and PCDD/F congener data was not available for the same combustor operating under the same conditions. This resulted in an inability to observe meaningful relationships.

Figures 5.4-5.8 present calculations of the homologue class distributions and 2,3,7,8-congener distributions of PCDD and PCDF, and the tetrachlorodibenzo-*p*-dioxin. The chlorophenol isomers concentration utilized in these calculations came from the furnace outlet sampling point from Table 5.5. The PCDD/F yields utilized came from the gas-phase oxidation of 2-chlorophenol in Table 5.1. The overall correlations are poor with published field data; however, some interesting trends are noticeable that may point to improved future predictions.

It is immediately evident that our current data base/model has some shortcomings regarding the PCDD and PCDF homologue distributions and the PCDD/F ratio seen in actual incinerator emissions. It is known that PCDD homologue class distributions usually peak at octa- chlorinated homologues.[5.14] However, Figure 5.4 shows the tetra- and penta- chlorinated

Table 5.5 Concentration of chlorophenols at the furnace outlet, the inlet and outlet of ESP, and the concentration measured in fly-ash. Taken from Weber and Hagenmaier, *Chemosphere*, Vol. 38, No. 11, pp. 2643-2654, 1999.

Congener	Furnace out mg/Nm^3	ESP inlet mg/Nm^3	ESP outlet mg/Nm^3	Fly-ash ng/g
2-MCP	1.0	5	7.00	0.00
3-MCP	0.03	0.2	0.50	0.00
4-MCP	0.5	0.4	4.00	0.00
2,3-DCP	0.03	0.15	0.10	0.40
2,4-DCP	1.4	12.2	39.00	48.00
2,5-DCP	0.06	1.3	0.20	0.60
2,6-DCP	0.15	2.6	4.50	7.20
3,4-DCP	n.d.	n.d.	0.00	0.00
3,5-DCP	n.d.	n.d.	0.00	0.00
2,3,4-TrCP	0.07	0.05	0.35	11.50
2,3,5-TrCP	0.05	0.20	0.10	5.80
2,3,6-TrCP	0.03	0.08	0.20	17.60
2,4,5-TrCP	0.1	0.12	0.80	11.50
2,4,6-TrCP	1.8	9.50	161.00	254.00
3,4,5-TrCP	0.01	0.02	0.09	5.8
2,3,5,6-TeCP	n.m.	0.07	0.7	7.3
2,3,4,6-TeCP	1.2	0.75	20.4	103
2,3,4,5-TeCP	0.1	0.06	0.9	8.2
PCP	3.0	0.65	23.5	251

isomers to be dominant using our model and available chlorinated phenol data. In this model, there exist only 2 reaction pairs that yield OCDD from both PCDD pathways combined vs. 69 combinations to yield TeCDD. In order to improve our current prediction, available field data needs to show the higher chlorinated phenols (penta- and tetra- isomers) to be in great abundance as compared to the mono-tri- chlorinated phenols.

A similar, although not as drastic, deviation from field data for PCDF is shown in Figure 5.5. Actual PCDF homologue distributions tend to peak at hexa- and hepta- chlorination, whereas our distributions peak at tri- to tetra-chlorination. Again, the relative abundance of di- and tri-chlorinated phenols leads to this problem.

However, there is an encouraging note. Our mechanisms do suggest why field data usually result in PCDF distributions to be less chlorinated than PCDD by one to two chlorines. As proposed by our mechanism, PCDF formation requires at least one *ortho*- site to not be chlorinated. Moreover, our laboratory data on 2-chlorophenol suggests that PCDF formation may not be dominant until both *ortho*- sites are non-chlorinated. This eliminates pentachlorophenol, 2,3,4,6-, and 2,3,5,6- chlorophenol as PCDF precursors and indicates that PCDFs will routinely have one to two fewer chlorines than PCDDs. Thus, although our model does not successfully predict the correct homologue class distributions, it is in the right direction to explain the differences in PCDD and PCDF distributions. Perhaps more complete chlorophenol distributions will improve the fit between our predictions and field data.

Figures 5.6 and 5.7 depict the calculated relative yields of the 2,3,7,8-substituted PCDD and PCDF congeners, respectively. For PCDF, very little tetra- through penta- congeners are formed. This is because our chlorophenol concentration data contains no 3,4-dichlorophenol. This presence of this chlorophenol isomer is necessary to form the omitted isomers.

Figure 5.8 depicts the calculated isomer distribution for the tetra-chlorinated dibenzo-*p*-dioxins. The most obvious feature of the histogram is the dominance of the 1,3,6,8- and 1,3,7,9- isomers. These isomers are produced in approximately equal yields since they are Smiles intermediate reaction pairs resulting from self-recombination of 2,4,6- trichlorophenol.[5.15] The reason for their extreme abundance can be traced back to the concentration of 2,4,6-TCP,

which is 4 times more abundant than the next highest concentration chlorophenol. These calculations are in qualitative, if not quantitative, agreement with the results published by Zimmerman *et al.*[5.16] The most glaring difference is the low concentration of 2,3,7,8-TCDD predicted by our model. This is due to the very low concentration of 2,4,5- trichlorophenol in Hagenmaier's field measurement that is needed to from 2,3,7,8-TCDD.

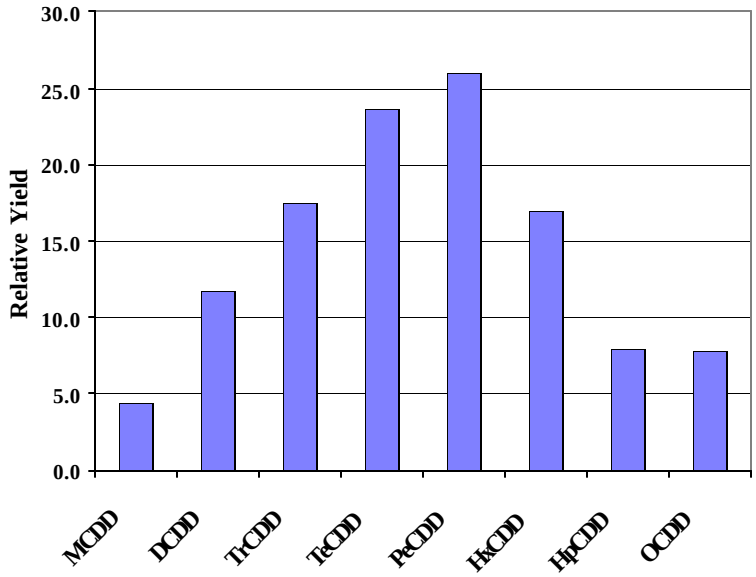

Figure 5.4 Predicted PCDD homologue class distribution.

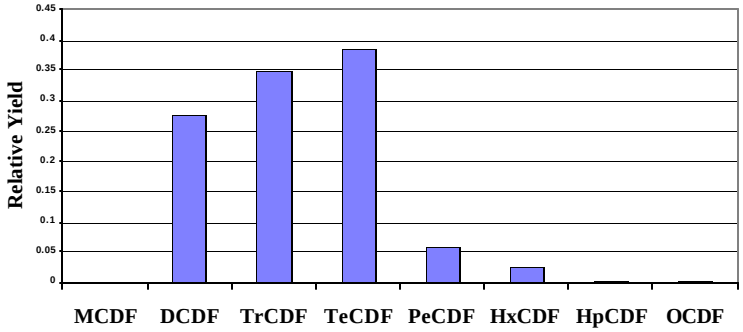

Figure 5.5 Predicted PCDF homologue class distribution.

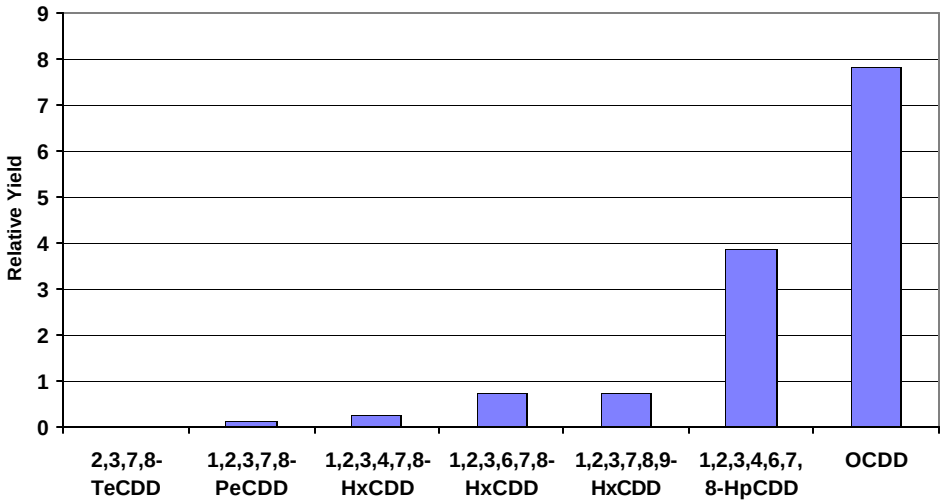

Figure 5.6 Predicted 2,3,7,8-substituted PCDD congeners.

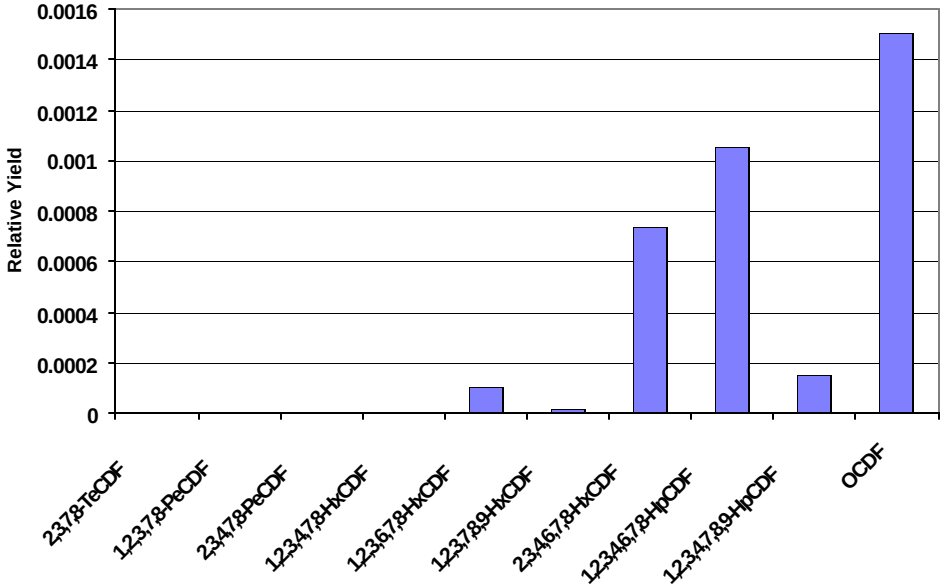

Figure 5.7 Predicted 2,3,7,8-substituted PCDF congeners.

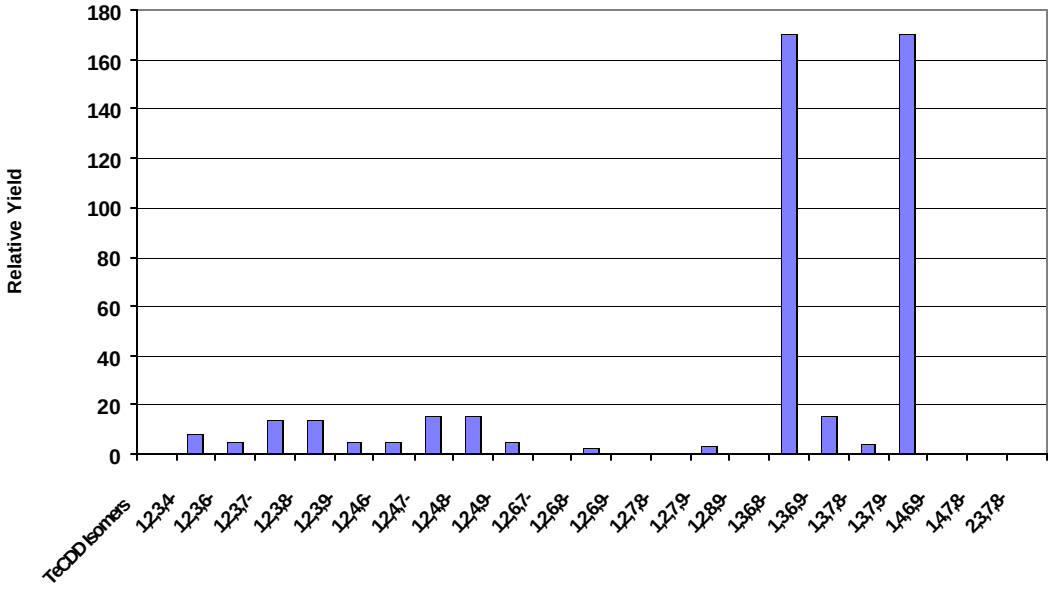

Figure 5.8 Predicted tetra-chlorinated dibenzo-*p*-dioxin isomer distribution.

5.6 Conclusions

In this work, it was determined which PCDD/F isomers could be formed via radical-molecule and radical-radical self-reactions and cross combinations of each of the 19 chlorophenol isomers. Relative yields that were based on experimental observations were applied to each reaction pathway to predict the relative abundance of PCDD/F isomers formed from the reactions. An intuitive spreadsheet model was developed that accepts chlorophenol concentrations and yields as input parameters and calculates individual congener and homologue distributions of PCDD/F. The model was tested against well-established field PCDD/F emissions, *i.e.*, the homologue class distribution of PCDD and PCDF and PCDD to PCDF ratios. Key gaps in field emissions data and laboratory mechanistic data were identified that are needed to establish correlations between laboratory-based calculations and field emissions data. Although the field data are incomplete and the model cannot be fully evaluated at this time, it

does appear that the current model has shortcomings. We recommend that the following considerations be addressed to improve the model.

5.6.1 Proposed Studies to Improve Model Predictions

- **Generate yields based on reaction of other chlorophenol isomers**

In this work, it was assumed that the relative yields of PCDD/F across the reaction pathways considered would be the same for higher chlorinated congeners as they are for 2-chlorophenol. It may be the higher chlorinated phenols produce PCDD/F at higher yields than lower chlorinated congeners. If this is the case, both predicted PCDD and PCDF yields will be shifted to the higher chlorinated homologues, thus agreeing better with actual emission data. Therefore, additional surface- and gas-phase laboratory studies of the reactions of higher polychlorinated phenols are required. These studies are needed to extend the mechanistic understanding gained from the study of 2-chlorophenol and to generate relative yields which are dependent on the number of chlorines.

In addition, Mulholland *et al.* have investigated product distributions of the 3 different furan isomers formed from the asymmetrical 3-chlorophenol and 3,4-dichlorophenol and determined that steric constraints control their relative yields.[5.3] This is an important finding and likely impacts the isomer distributions within a given homologue class. Therefore, additional experiments are needed to further explore steric effects that the number and position of Cl has on phenoxy radical coupling and ring closure reactions.

- **Investigate the possibility of PCDD/F chlorination/dechlorination reactions**

In the model, there are many more chlorophenol reaction pairs resulting in less chlorinated PCDD/F congeners than the higher chlorinated congeners, and this also leads to incorrect predicted PCDD and PCDF homologue distributions. It could be that in

actual systems, lower chlorinated PCDD/F undergo multiple chlorination reactions after initial formation. To address this, future studies should also consider reactions occurring at long reaction times on surfaces. Our data indicate that the gas-phase PCDD/F products formed as a result of surface reactions are relatively predictable. However, precursors that remain adsorbed to the surfaces for longer times can undergo chlorination/dechlorination/isomerization reactions that may also make a significant contribution to the total PCDD/F yield. Thus total PCDD/F yields in a full-scale system may be a combination of thermodynamically equilibrated PCDD/F formed at long reaction times and kinetically controlled isomers formed at shorter reaction times. For instance, Iino *et al.* have demonstrated that CuO dechlorinates fully chlorinated PCDD/F giving isomer patterns similar to those found in actual systems.[5.17] This behavior seems especially important for PCDF, but it is thought that the observed PCDD isomer pattern is the ultimate result of chlorophenol coupling reactions.[5.18]

- **Investigate and include reactions of chlorinated benzenes**

In our model, there are many more pathways to PCDD than PCDF, which is in contradiction to the observed field ratio of PCDD to PCDF which is <<1. In order to produce the "correct" PCDD to PCDF ratios, the relative yield of the pathway to PCDF would have to be much higher that those of PCDD. Our laboratory data has not shown this to be the case for reactions of chlorophenols. It could be that an accurate model will have to take into account other PCDD/F precursors. Chapters 3 and 4 of this dissertation give solid evidence that chlorinated benzenes may be overlooked dioxin precursors and a hypothesis based on those finding is presented in Chapter 6, which if true, would lead to more PCDF being formed if chlorinated benzenes are indeed viable PCDD/F precursors.

A logical starting point to explore this would be to compare the surface reactions of 1,2-dichlorbenzene and compare them with the results of the 2-chlorphenol studies.

· **Temperature dependence of reactions**

The model predictions presented in this chapter were based on the yields obtained at maximum PCDD/F formation. Ultimately, the yields used in the model should reflect PCDD/F formation rates from chlorophenol precursors over the complete temperature range that they are formed.

· **Better field data**

In order to make properly correlate PCDD/F homologue distributions, isomer distributions and PCDD/F ratios with chlorinated phenols, and to explore the role of chloroinated benzenes, complete sets of chlorinated phenol, chlorinated benzene, and PCDD/F emissions data for a pilot- or full-scale combustor are needed.

5.7 References

5.1 Born, J.G.P.; Louw, R.; Mulder, P. *Chemosphere* **1989**, *19*, 401.

5.2 Sidhu, S.; Maqsud, L.; Dellinger, B.; Mascolo, G. *Combust. Flame* **1995**, *100*, 11.

5.3 Mulholland, J. A.; Akki, U.; Yang, Y.; Ryu, J.Y. *Chemosphere* **2001**, *42*, 719.

5.4 Akki, U.; Mulholland, J.A. *Organohalogen Cmpds.* **1997**, 31, 475.

5.5 Weber, R.; Hagenmaier, H. *Chemosphere* **1999**, *38*, 529.

5.6 Lomnicki, S.; Dellinger, B. *J. Phys. Chem. A*, **2003**, *107*, 4387.

5.7 Rubey, W.A.; Grant, R.A. *Rev. Sci. Instrum.* **1988**, *59*, 265.

5.8 Evans, C.S.; Dellinger, B. *Environ. Sci. Technol*. **2003**, *37*, 1325.

5.9 Lomnicki, S.; Dellinger, B.; *Proc. Comb. Inst.* **2002**, *29*.

5.10 Khachatryan, L.; Asatryan, R.; Dellinger, B. *Chemosphere* **2003**, *52*, 695.

5.11 Louw, R.; Ahonkhai, S.I. *Chemosphere*, **2002**, 1273.

5.12 Truce, W.E.; Kreider, E.M.; Brand, W.W. *Org. React.* **1970**, *18*, 99.

5.13 Weber, R.; Hagenmaier, H. *Chemosphere* **1999**, *38*, 2643.

5.14 Zimmerman, R.; Blumenstock, M., Heger, H.J., Schramm, K.W.; Kettrup, A. *Environ. Sci. Technol.* **2001**, *35*, 1019.

5.15 Sidhu, S.; Dellinger, B. *Organohalogen Cmpds.* **1997**, *31*, 469.

5.16 Zimmerman, R.; Wehrmeier, A.; Lenoir, D.; Schramm, K.-W.; Kettrup, A. *Organohalogen Cmpds.* **1996**, *27*, 237.

5.17 Iino, F.; Tabor, D.G.; Imagawa, T.; Gullett, B.K. *Organhalogen Cmpds*., **2001**, *50*, 447.

5.18 Oh, J.E.; Touati, A.; Gullett, B.K.; Mulholland, J.A. *Environ. Sci. Technol*., **2004**, *38*, 4694.

CHAPTER 6: SUMMARY

6.1 Advances in a Unified Pathway to PCDD/F

In Chapter 1 (Section 1.4, Figure 1.8), a unified pathway to PCDD/F was presented, which incorporates both "*de novo*" and "precursor" concepts to described PCDD/F formation. In the unified pathway, carbon contained in incinerator fly-ash is the initial reagent and through surface reactions with reactive molecular species and/or radical species, acetylenic and olefinic hydrocarbons and chlorocarbons are liberated, which undergo molecular growth, cyclsation, and chlorination. This results in the formation of chlorinated aromatic hydrocarbons. These PCDD/F precursors then react further with the fly-ash to yield PCDD/F. However, the nature of precursor chemisorption to catalytic sites and the role of transition metals in the surface-mediated conversion of chlorinated aromatics to PCDD/F were not clear. The work presented in this document has focused on clarifying these reaction steps, i.e., the nature of chemisorption of PCDD/F precursors to potentially active surface sites and the role of CuO in promoting dioxin formation.

6.1.1 Reaction of 2-Chlorophenol with SiO_2

Infrared spectroscopy was used to examine surface reactions of 2-chlorophenol with SiO_2 in the temperature range of 200-500 ºC. The silica served as a simple surrogate for incinerator fly ash. 2-chlorophenol was found to chemisorb at isolated and geminal hydroxyl groups of silica. Chemisorption occurred at isolated sites via the elimination of H_2O, which resulted in chemically adsorbed chlorophenolate. This is shown in line **a** of Figure 6.1. Phenols adsorbed in such a manner are known to form PCDD via reaction with gas-phase phenols via an Eley-Rideal mechanism.[6.1] Adsorption of 2-chlorophenol also occurred at geminal surface

hydroxyl sites. Two molecules of the precursor can chemisorb adjacently, as depicted in line **b** of Figure 6.1. This configuration is known to lead to the formation of PCDF.[6.1]

Additionally, surface bound carboxylate partial oxidation products were detected and FTIR spectra comparing adsorbed catechol with 2-chlorophenol gave strong evidence which suggests that carboxylate formation proceeds though a surface adsorbed, catecholic intermediate. The formation of this intermediate is believed to take place at geminal hydroxyl sites of silica by reaction through both the phenolic hydroxyl and Cl ring substituents. This is demonstrated in line **c** of Figure 6.1.

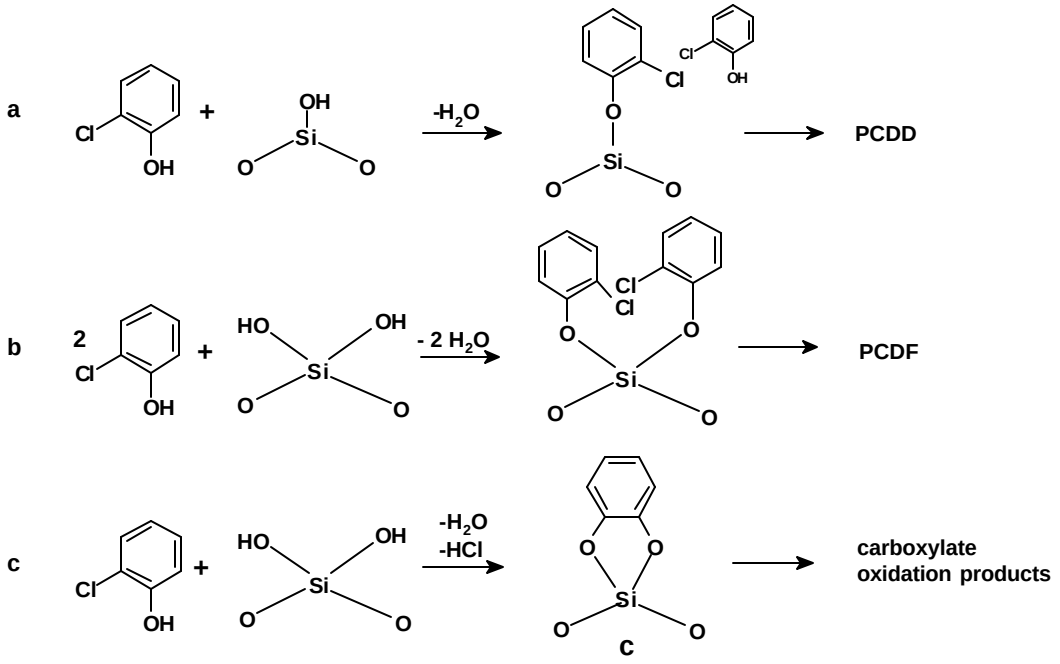

Figure 6.1 Chemisorption of 2-chlorophneol at isolated and geminal silanol groups.

IR spectra of 4-chlorophenol and phenol confirmed that phenolic aromatics chemisorb via the hydroxyl substituent to yield phenolate species. Chlorobenzene did not react to an appreciable extent with the pure silica surface, but enough adsorption occurred to confirm that it does chemisorb via HCl elimination to yield the same phenolate species as phenol. Also, 1,2-dichlorobenzene did not adsorb to the silica surface.

The kinetics of 2-chlorophenol adsorption were measured using a pseudo-first order reaction scheme. The reaction was characterized by two kinetic regimes, a fast initial reaction with an activation energy of chemisorption of 7 kJ mol^{-1}, and a slower, more activated reaction at higher surfaces coverage with an activation energy of 22 mol^{-1}. In summary, we can now say that:

- Adsorption of PCDD/F chlorophenol precursors at isolated reactive sites favors Eley-Rideal formation of PCDD.
- Adjacent adsorption of PCDD/F chlorophenol precursors at geminal sites favors PCDF formation via a Langmuir-Hinshelwood pathway. Although the silica under study here was pretreated in a manner than removed vicinal hydroxyl sites, adsorption at vicinal sites would also be amenable to PCDF formation.
- Carboxylate partial oxidation products, such as formates and acetates, form through a catecholic intermediate, which forms via bidentate adsorption at geminal surface hydroxyl groups.

6.1.2 FTIR Comparison of 2-Chlorophenol and 1,2-Dichlorobenzene Chemisorption on a CuO/SiO_2 Surface

2-chlorophenol chemisorbs on the CuO/SiO_2 surface to form phenolate and partial oxidation products, as with silica alone. However, the partial oxidation products were observed to form 100 °C lower in temperature and with much higher phenolate to carboxylate ratios than with silica alone. In contrast to adsorption on pure silica, 1,2-dichlorobenzne adsorbed readily to a silica surface in which CuO had been dispersed at a loading of 5 % Cu by weight. In addition, the FTIR spectra of adsorbed 1,2-dichlorobenzene were identical to those resulting from adsorption of 2-chlorophenol. The observation that copper must be present for 1,2-dichlorobenzene (and chlorobenzene) to chemisorb to the particular silica used in these

studies is a strong indication that chemisorption at the CuO surface occurs much more readily that adsorption at silica hydroxyl sites. In addition to cupric hydroxyl groups, other active sites on CuO that would facilitate uptake of PCDD/F precursors are cation sites and surface oxide ions.[6.2] Since we still see the loss of surface silica hydroxyl groups, it must be that following adsorption at the copper surface sites, the adsorbed species, both phenolate and partial oxidation products, migrate to the less reactive surface hydroxyl groups.

2-chlorophenol was observed to adsorb approximately 10x faster than 1,2-dichlorobenzene on the CuO/silica surface. The more rapid reaction rate of 2-chlorophenol was expected, as 2-chlorophenol adsorption requires breaking of the phenolic O-H bond, which has a bond dissociation energy of 82 kcal mol^{-1}, compared to a bond dissociation energy of 97 kcal mol^{-1} for the C-Cl bond in 1,2-dichlorobenzene. However, under incineration conditions, upwards of 10x more surface bound phenolate PCDD/F precursors would being derived from chlorinated benzenes than chlorinated phenols since chlorinated benzene concentrations can be up to 100x higher than phenols in actual systems.[6.3]

This is an important observation and could be a key detail in explaining the ubiquitous observation that PCDF to PCDD ratios >> 1 for actual systems. To illustrate, Figure 6.2 shows the equivalent chlorophenolate derived from adsorption of 2-chlorophenol and 1,2-dichlorobenzene following H_2O and HCl elimination, respectively. The right hand pathway depicts these phenolates reacting with their gas-phase counterparts via an Eley-Rideal reaction. For 2-chlorophenol (lower reaction) the favored pathway is PCDD formation. This is initiated by reaction of a gas-phase phenol with surface phenolate through OH bond scission, leading to the formation of a hydroxydiphenyl ether that condenses to form PCDD. This reaction leads to low yield PCDF formation though the Langmuir-Hinshelwood route (left side, lower) due to

competitive reaction of adsorbed molecule with a gas-phase reagent.[6.1] The upper, right hand, reaction of Figure 6.2 shows the potential reaction of a gas-phase chlorinated benzene with a surface phenolate. The Eley-Rideal mechanism here would require Cl elimination, which is a less favorable process and forms a hydroxybiphenyl in low yields. Additionally, any hydroxylbiphenyl formed would undergo ring closure to form PCDF rather than PCDD. Thus, the formation of PCDF should proceed more readily from two surface adsorbed phenolates via the Langmuir-Hinshelwood pathways (to the left) with much higher yields due to lack of competitive process from gas-phase chlorophenol. Further evidence to justify this is the observation that decreasing the gas-phase 2-chlorophenol concentrations in a pack-bed flow reactor study greatly increases the yield of PCDF relative to that of PCDD, which favors the Langmuir-Hinshelwood reaction pathway to PCDF.[6.1]

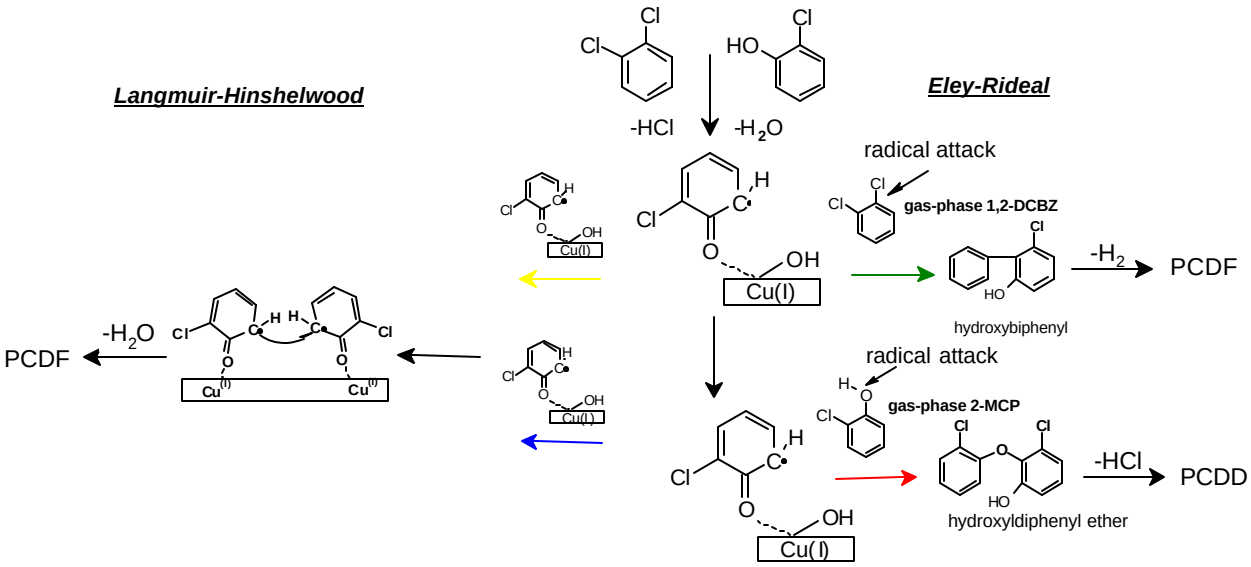

Figure 6.2 Comparison of the reaction of a chlorinated benzene (upper pathways) to reaction of chlorinated phenol (lower pathways) with a chemisorbed phenolate (formed by chemisorption of either a chlorophenol or chlorobenzene). For the reaction of a chlorinated phenol, hydroxydiphenyl ether formation by an E-R pathway (red arrow) successfully competes with PCDF formation by an L-H pathway (blue arrow). However, the analogous E-R pathway involving a gas-phase chlorobenzene to form a hydroxy biphenyl is not favorable (green arrow). Instead, PCDF formation is favored by a L-H pathway (yellow arrow) due to less competition from the L-H pathway.

An additional consideration is that the concentration of chlorinated benzenes formed *de novo* from macromolecular carbon are detected at much higher levels relative to those of chlorinated phenols[6.4,6.5] and it is well established that *de novo* PCDD/F formation results PCDF:PCDD ratios >> 1. This observation is additional evidence that chlorinated benzenes favor PCDF formation over PCDD formation. Thus, we can conclude that:

- For chemisorption of chlorinated benzenes to take place on the silica used in these studies, the presence of CuO or possibly other metal oxides is required.
- Phenolate adsorption products and partial oxidation products migrate to surface hydroxyl groups of silica following reaction at copper sites, although we cannot conclusively say that no species remain on copper sites.
- Based on our measurements, approximately 10x more chlorophenolate precursors will be derived from chlorinated benzenes than chlorinated phenols and can explain why more PCDF are formed than PCDD in actual systems.

6.1.3 XANES Study of CuO Reduction by Chlorinated Aromatics

The fate of CuO with respect to reduction and chemical speciation was determined when the metal oxide was mixed with silica and exposed to model PCDD/F precursors, 2-chlorophenol, 1,2-dichlorobenzene, and chlorobenzene. The thermal reactions were examined from 275-375 °C. In each case, the major reduction product was Cu_2O. This indicates that a 1 e^- transfer to the metal follows adsorption of the reactant to active surface sites. This supports the contention that transfer of an electron from this adsorbed phenolate to the to the surface results in reduction of the Cu(II) to form Cu(I) and a surface associated phenoxyl radical, which reacts to form PCDD/F. Bimolecular pseudo-first order reaction rate coefficients and Arrhenius parameters were calculated for our model systems. However, for clarity, it should be pointed out

that we are essentially measuring the rate of chemisorption and CuO reduction. Here, the rate of reaction seemed to depend more on the number, rather than type of ring substituents. This is based on the observation that the rate coefficients for reaction of 1,2-dichlorobenzene and 2-chlorophenol were relatively close, but substantially faster than the chlorobenzene reaction. Since, XANES is an elementally specific technique and because precursor chemisorption is a prerequisite for reduction, this leads us to conclude that the reactions at the CuO surface are much less sensitive to the nature of the aromatic ring substituent though which adsorption occurs than silica surfaces.

Additional XANES and SEM results also indicate that the thermal and reaction history of the particle affects its rate of reaction and reduction by subsequent exposure to 2-chlorophenol. This is likely related to the change in surface area and rate of diffusion of internal reactive oxide groups to the surface. This could be of consequence since it is not known how the catalytic components in fly-ash change as they are subjected to heating/cooling cycles in the pollutant formation zone of combustors as this can result in changes in the oxidation state, the chemical structure, the crystalline structure, the particle size, the surface area, and local environment of catalytic species. In summary:

- Each of the chlorinated aromatic studied reduce Cu(II)O to primarily $Cu(I)_2O$. This is consistent with a one electron transfer from the adsorbed phenolate to the metal, which would result in the formation of surface-associated chlorophenoxy radicals, which are important intermediates in PCDD/F formation.
- 2-chlorophenol and 1,2-dichlorobenzene each reduce copper at comparable rates, which are much faster than reduction by chlorobenzene. This observation places even more emphasis on chlorinated benzenes as PCDD/F precursors.

- The thermal history of the substrates has an effect on the rate of Cu(II) reduction, which is brought about by changes in CuO particle size and surface morphology after undergoing a reduction/oxidation cycle.

6.1.4 A New Unified Pathway to PCDD/F

Figure 6.3 illustrates an updated version of a unified pathway to PCDD/F incorporating the new results obtained from these studies with detailed PCDD/F mechanisms derived from a pack-bed flow reactor study.[6.1]

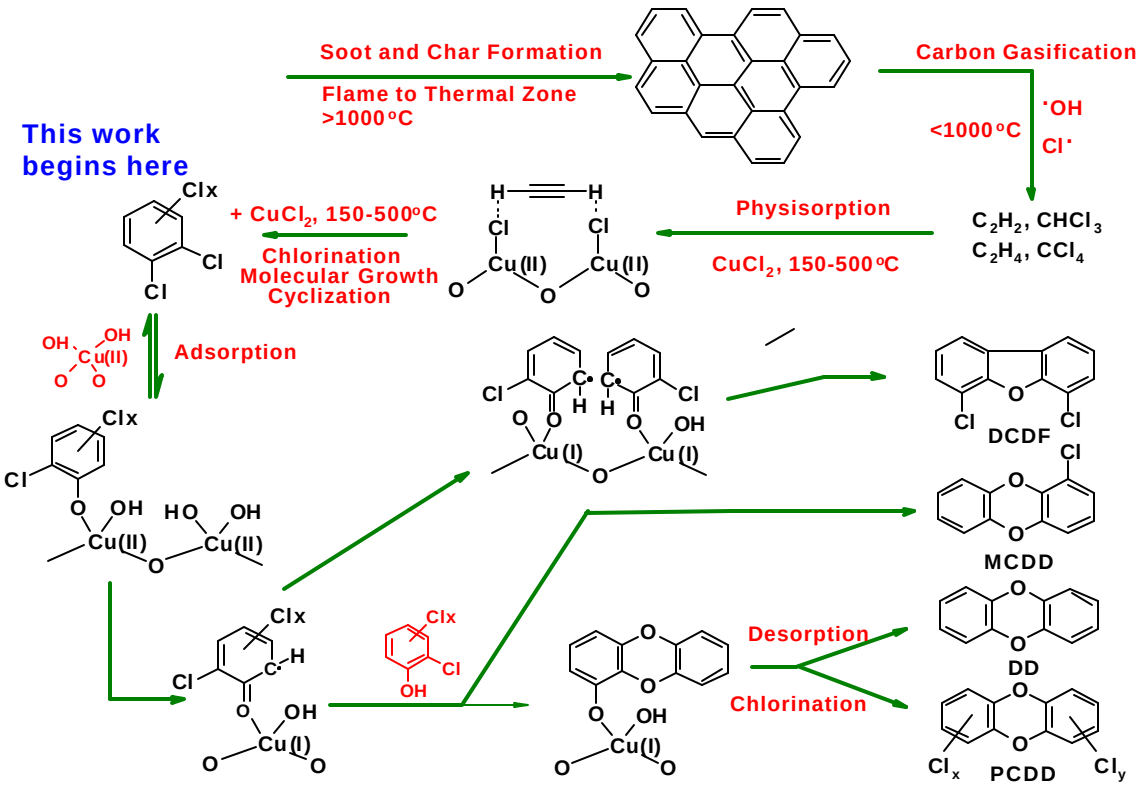

Figure 6.3 An updated unified pathway to PCDD/F formation.

From our FTIR investigation, we now know that chlorinated phenols and chlorinated benzenes both chemisorb to surface hydroxyl groups to yield chlorophenolate species. From the XANES studies, we know that the dominant pathway of CuO reduction results is a one e^-

transfer to the metal, resulting in the formation of Cu_2O. This results in the formation of a surface associated phenoxy radicals, the existence of which has been confirmed with EPR spectroscopy.[6.1] Radical character is present at both the phenolic oxygen and carbon centers. The packed-bed flow reactor study indicates that PCDF are formed via a Langmuir-Hinshelwood pathway from two adsorbed chlorophenolate entities, while PCDD are formed through one surface adsorbed phenolate and one in the gas-phase. The resulting dioxin isomer can either be immediately desorbed, or remain on the surface where it is chlorinated further before desorption.

6.2 Correlating PCDD/F Emissions with Gas-Phase Chlorophenol Concentrations

A spreadsheet model was developed to correlate gas-phase chlorophenol concentration with PCDD/F emissions. Input parameters to the model included chlorophenol concentrations and the relative yields of PCDD/F though the various pathways that had been developed. The model predictions show the PCDD homologue pattern to peak at the tetra- and penta-homologues, whereas, actual emissions data consistently show the octa- isomer to predominate. This is due to there being only 2 pathways to the octa- homologue, while 44 reactions contribute to the tetra- isomers. In order for this to approach reality, much more pentachlorophenol would have to be present than tri- or tetra- phenols, which is usually not the case. Secondly, much more PCDD is predicted to be formed than PCDF, and this is not the case in actuality. This is again related to there being many more pathways to PCDD than PCDF. In order to give the correct PCDD to PCDF ratio, the relative yield to PCDF would have to be substantially higher than those to PCDD, but this is usually not observed experimentally.

On a positive note, the model predicts that the most abundant tetra- chlorinated isomers to be 1,3,6,8- and 1,3,7,9-tetrachlorodibenzo-*p*-dioxin. These isomers are produced in approximately equal yields since they are Smiles intermediate reaction pairs resulting from self-

recombination of 2,4,6-trichlorophenol. The reason for their extreme abundance can be traced back to the concentration of 2,4,6-TCP, which is 4 times more abundant than the next highest concentration chlorophenol. This agrees well with field data.

Overall, the lack of agreement with the predictions and actual emissions could imply that lower chlorinated PCDD/F undergo multiple chlorination reactions after initial formation. Another consideration is that it was assumed that the relative yields of PCDD/F across the reaction pathways considered would be the same for higher chlorinated congeners as they are for 2-chlorophenol. It may be the higher chlorinated phenols produce PCDD/F at higher yields than lower chlorinated congeners. If this were the case, both predicted PCDD and PCDF yields would be shifted to the higher chlorinated homologues, thus agreeing better with actual emission data. Additionally, as has been demonstrated in this work, other precursors, such as chlorinated benzenes, may be an overlooked route to PCDD/F and their inclusion may make the predictions more representative of actual emissions.

6.3 Recommendations for Future Work

PCDD/F are products of incomplete combustion and their yields are miniscule compared to the major combustion products and reactants in practically all cases, i.e., laboratory and pilot plant experiments and actual combustion system. Additionally, there seems to be many PCDD/F precursors and the relationship between them is still largely unknown. These factors, coupled with the complex nature of the reaction atmosphere and other conditions have hindered the development of a mechanism to satisfactorily explain PCDD/F formation. This study addressed some these issues by using simple fly-ash surrogates in conjunction with FTIR and XANES spectroscopy. Although one type of experiment or set conditions cannot be expected to fully explain PCDD/F formation, it is hoped that these studies have advanced a more complete

understanding of surface mediated dioxin formation. The following are recommended experiments to improve our understanding of PCDD/F formation:

- Extend the FTIR studies to include reactions of higher chlorinated phenols and chlorinated benzenes. Additionally, it would be beneficial to study the adsorption of potential PCDD/F precursors on iron containing surrogate fly-ashes, and pure and metal-doped alumina-based fly ashes. Our laboratory is now equipped with Diffuse Reflectance Infrared Transmission Spectroscopy (DRIFTS) capabilities, which should expand the types of substrates that can be investigated, to possibly include actual incinerator fly-ash.

- Extended the XANES studies to investigate the reactions of higher chlorinated PCDD/F precursors and also examine their interactions with other potentially catalytic metal centers, such as Fe_2O_3. Additionally, the inclusion of Extended X-ray Absorption Fine Structure spectroscopy experiments will improve our understanding of precursor chemisorption on surfaces.

- It would be beneficial to test the model predictions against laboratory generated PCDD/F formation data. For instance, a mixture of two to five different chlorinated phenol samples could be oxidized in the gas-phase. The PCDD/F products could be collected and analyzed. By comparing the model predictions, based on the input of those isomers concentrations', and the best available yield parameters, adjustments could be made to the model to better correlate PCDD/F emissions with chlorophenol gas-phase concentrations.

6.4 References

6.1 Lomnicki, S.; Dellinger, B. *J. Phys. Chem. A*, **2003**, *107*, 4387.

6.2 Henrich, V.; Cox, P.A. "The Surface Science of Metal Oxides", **1994**, Cambridge University press.

6.3 Blumenstsock, M.; Zimmermann, R.; Schramm, K.W.; Kaune, A.; Nikolai, U.; Lenoir, D.; Kettrup *J. Anal. Appl. Pyrolysis*, **1999,** *49*, 179.

6.4 Stieglitz, L. *Environ. Eng. Sci*. **1998**, *15*, 5.

6.5 Pekarek, V.; Grabic, R.; Marklund, S.; Puncochar, M.; Ullrich, J. *Chemosphere* **2001**, *43*, 7.

APPENDIX 1: COPPER SPECIATION

2-chlorophenol, 275 °C

time(s)	% CuO	% Cu_2O	% Cu(0)
0	100	0	0
60	91	9	0
120	91	10	0
240	86	14	0
480	84	16	0

2-chlorophenol, 300 °C

time(s)	% CuO	% Cu_2O	% Cu(0)
0	100	0	0
60	94	5	1
120	91	9	0
270	78	22	0
480	61	38	1

2-chlorophenol, 325 °C

time(s)	% CuO	% Cu_2O	% Cu(0)
0	100	0	0
60	77	19	4
120	76	31	3
240	48	51	1
360	35	62	3
480	28	67	5

2-chlorophenol, 350 °C

time(s)	% CuO	% Cu_2O	% Cu(0)
0	100	0	0
60	49	47	4
120	37	60	3
240	26	71	3
360	24	74	2
600	19	77	4

2-chlorophenol, 375 °C

time(s)	% CuO	% Cu_2O	% Cu(0)
0	100	0	0
60	23	75	2
120	18	80	2
240	9	88	3
360	9	87	4

1,2-dichlorobenzene, 275 °C

time(s)	% CuO	% Cu_2O	% Cu(0)
0	100	0	0
60	95	4	1
120	95	5	0
240	91	8	1
480	90	10	0

1,2-dichlorobenzene, 300 °C

time(s)	% CuO	% Cu_2O	% Cu(0)
0	100	0	0
60	86	11	3
120	80	20	0
270	70	30	0
480	65	32	3

1,2-dichlorobenzene, 325 °C

time(s)	% CuO	% Cu_2O	% Cu(0)
0	100	0	0
60	82	13	5
120	72	26	2
240	55	39	6
360	41	54	5
480	34	62	4

1,2-dichlorobenzene, 350 °C

time(s)	% CuO	% Cu_2O	% Cu(0)
0	100	0	0
60	54	44	2
120	46	50	4
240	30	67	3
360	20.5	75.5	5
600	19	76	5

1,2-dichlorobenzene, 375 °C

time(s)	% CuO	% Cu_2O	% Cu(0)
0	100	0	0
60	70	26	4
120	34	60	6
240	17	77	6
360	13	82	5

Chlorobenzene, 275 °C

time(s)	% CuO	% Cu_2O	% Cu(0)
0	100	0	0
60	97	0	3
120	95	1	4
240	93	3	4

Chlorobenzene, 300 °C

time(s)	% CuO	% Cu_2O	% Cu(0)
0	100	0	0
60	91	0	9
120	87	10	3
270	82	14	4
480	72	27	1

Chlorobenzene, 325 °C

time(s)	% CuO	% Cu_2O	% Cu(0)
0	100	0	0
60	83	12	5
120	79	19	2
240	67	30	3
360	59	35	6
480	54	44	2

Chlorobenzene, 350 °C

time(s)	% CuO	% Cu_2O	% Cu(0)
0	100	0	0
60	74	20	6
120	57	38	5
240	37	57	6
360	31	64	5
600	21	74	5

Chlorobenzene, 375 °C

time(s)	% CuO	% Cu_2O	% Cu(0)
0	100	0	0
60	65	31	4
120	40	55	5
240	24	70	6
360	18	78	4

APPENDIX 2: PCDD/F ISOMERS FROM CHLOROPHENOL REACTIONS

Reactant A	Reactant B	Reaction Pathways to PCDD/F		
		Rad.-Mol. To PCDD	Rad.-Rad. To PCDD	Rad.-Rad to PCDF
2-MCP	2-MCP	Dibenzodioxin	1-	4,6-
3-MCP	3-MCP	n/a	n/a	1,9- 3,7- 1,7-
4-MCP	4-MCP	n/a	n/a	2,8-
2,3-DCP	2,3-DCP	1,6- 1,9-	1,2,9- 1,2,6-	3,4,6,7-
2,4-DCP	2,4-DCP	2,7- 2,8-	1,3,8,- 1,3,7,-	2,4,6,8-
2,5-DCP	2,5-DCP	2,7- 2,8-	1,4,7-	1,4,6,9-
2,6-DCP	2,6-DCP	1,6- 1,9-	n/a	n/a
3,4-DCP	3,4-DCP	n/a	n/a	1,2,8,9- 2,3,7,8- 1,2,7,8-
3,5-DCP	3,5-DCP	n/a	n/a	1,3,7,9-
2,3,4-TriCP	2,3,4-TriCP	1,2,6,7- 1,2,8,9-	1,2,3,8,9- 1,2,3,7,8-	2,3,4,6,7,8-
2,3,5- TriCP	2,3,5-TriCP	1,3,6,8- 1,3,7,9-	1,2,4,7,9- 1,2,4,6,8-	1,3,4,6,7,9-
2,3,6- TriCP	2,3,6-TriCP	1,4,6,9-, 1,2,6,7-, 1,2,8,9-, 1,2,6,9-,	n/a	n/a
2,4,5- TriCP	2,4,5-TriCP	2,3,7,8-	1,2,4,7,8-	1,2,4,6,8,9-
2,4,6- TriCP	2,4,6-TriCP	1,3,6,8- and 1,3,7,9-	n/a	n/a
3,4,5- TriCP	3,4,5-TriCP	n/a	n/a	1,2,3,7,8,9-
2,3,4,5- TCP	2,3,4,5-TCP	1,2,3,6,7,8- 1,2,3,7,8,9-	1,2,3,4,6,7,8-	1,2,3,4,6,7,8,9-
2,3,4,6-TCP	2,3,4,6-TCP	1,2,4,6,7,9- 1,2,4,6,8,9- 1,2,3,6,8,9- 1,2,3,6,7,9- 1,2,3,6,7,8- 1,2,3,7,8,9-	n/a	n/a
2,3,5,6-TCP	2,3,5,6-TCP	1,2,4,6,7,9- 1,2,4,6,8,9-	n/a	n/a

PCP	PCP	1,2,3,4,6,7,8,9-	n/a	n/a
2-MCP	3-MCP	n/a	2- 1-	3,6- 1,6-
2-MCP	4-MCP	n/a	2-	2,6-
2-MCP	2,3-DCP	1-	1,2- 1,9- 1,6-	3,4,6-
2-MCP	2,4-DCP	2-	1,3- 1,8- 1,7-	2,4,6-
2-MCP	2,5-DCP	2-	1,4- 1,7- 1,8-	1,4,6-
2-MCP	2,6-DCP	1-	1,6- 1,9-	n/a
2-MCP	3,4-DCP	n/a	2,3- 1,2-	2,3,6- 1,2,6-
2-MCP	3,5-DCP	n/a	1,3-	1,3,6-
2-MCP	2,3,4-TriCP	1,2-	1,2,3- 1,2,9- 1,2,6-	2,3,4,6-
2-MCP	2,3,5-TriCP	1,3-	1,2,4- 1,3,9- 1,3,6-	1,3,4,6-
2-MCP	2,3,6-TriCP	1,4- 1,2-	1,4,6- 1,2,6- 1,2,9-	n/a
2-MCP	2,4,5-TriCP	2,3-	1,2,4- 1,7,8-	1,2,4,6-
2-MCP	2,4,6-TriCP	1,3-	1,3,6- 1,3,9-	n/a
2-MCP	3,4,5-TriCP	n/a	1,2,3-	1,2,3,6-
2-MCP	2,3,4,5-TCP	1,2,3-	1,2,3,4- 1,2,3,9- 1,2,3,6-	1,2,3,4,6-
2-MCP	2,3,4,6-TCP	1,2,4- 1,2,3-	1,2,4,9- 1,2,4,6- 1,2,3,6- 1,2,3,9-	n/a
2-MCP	2,3,5,6-TCP	1,2,4-	1,2,4,6- 1,2,4,9-	n/a
2-MCP	PCP	1,2,3,4-	1,2,3,4,6-	n/a
3-MCP	4-MCP	n/a	n/a	2,7- 1,8-
3-MCP	2,3-DCP	n/a	1,6- 1,9-	3,4,7- 1,6,7-

			1,8- 1,7-	
3-MCP	2,4-DCP	n/a	1,7- 1,8- 2,8- 2,7-	2,4,7- 1,6,8-
3-MCP	2,5-DCP	n/a	1,8- 1,7- 2,7- 2,8-	1,4,9- 1,4,7-
3-MCP	2,6-DCP	n/a	1,9- 1,6- 1,7- 1,8-	n/a
3-MCP	3,4-DCP	n/a	n/a	2,3,7- 1,2,9- 1,2,7- 1,7,8-
3-MCP	3,5-DCP	n/a	n/a	1,3,7- 1,3,9-
3-MCP	2,3,4-TriCP	n/a	1,2,8- 1,2,7- 1,2,6- 1,2,9-	2,3,4,7- 1,6,7,8-
3-MCP	2,3,5-TriCP	n/a	1,3,8- 1,3,7- 1,3,6- 1,3,9-	1,3,4,7- 1,3,4,9-
3-MCP	2,3,6-TriCP	n/a	1,4,7- 1,2,7- 1,4,6- 1,2,9- 1,2,6-	n/a
3-MCP	2,4,5-TriCP	n/a	2,3,7- 1,7,8-	1,2,4,7- 1,2,4,9-
3-MCP	2,4,6-TriCP	n/a	1,3,7- 1,3,8- 1,3,9- 1,3,6-	n/a
3-MCP	3,4,5-TriCP	n/a	n/a	1,2,3,7- 1,2,3,9-
3-MCP	2,3,4,5-TCP	n/a	1,2,3,8- 1,2,3,7- 1,2,3,6- 1,2,3,9-	1,2,3,4,7- 1,2,3,4,9-
3-MCP	2,3,4,6-TCP	n/a	1,2,4,8-	n/a

			1,2,4,7- 1,2,3,7- 1,2,3,8- 1,2,4,6- 1,2,4,9- 1,2,3,9- 1,2,3,6-	
3-MCP	2,3,5,6-TCP	n/a	1,2,4,7- 1,2,4,8- 1,2,4,9- 1,2,4,6-	n/a
3-MCP	PCP	n/a	1,2,3,4,7- 1,2,3,4,6-	n/a
4-MCP	2,3-DCP	n/a	1,7- 1,8-	2,6,7-
4-MCP	2,4-DCP	n/a	2,7- 2,8-	2,4,8-
4-MCP	2,5-DCP	n/a	2,8- 2,7-	1,4,8-
4-MCP	2,6-DCP	n/a	1,8- 1,7-	n/a
4-MCP	3,4-DCP	n/a	n/a	2,3,8- 1,2,8-
4-MCP	3,5-DCP	n/a	n/a	1,3,8-
4-MCP	2,3,4-TriCP	n/a	1,2,7- 1,2,8-	2,3,4,8-
4-MCP	2,3,5-TriCP	n/a	1,3,7- 1,3,8-	1,3,4,8-
4-MCP	2,3,6-TriCP	n/a	1,4,7- 1,2,8- 1,2,7-	n/a
4-MCP	2,4,5-TriCP	n/a	2,3,7-	1,2,4,8-
4-MCP	2,4,6-TriCP	n/a	1,3,8- 1,3,7-	n/a
4-MCP	3,4,5-TriCP	n/a	n/a	1,2,3,8-
4-MCP	2,3,4,5-TCP	n/a	1,2,3,7- 1,2,3,8-	1,2,3,4,8-
4-MCP	2,3,4,6-TCP	n/a	1,2,4,7- 1,2,4,8- 1,2,3,8- 1,2,3,7-	n/a
4-MCP	2,3,5,6-TCP	n/a	1,2,4,8- 1,2,4,7-	n/a
4-MCP	PCP	n/a	1,2,3,4,7-	n/a
2,3-DCP	2,4-DCP	1,7- 1,8-	1,3,9- 1,3,6-	2,4,6,7-

			1,2,8- 1,2,7-	
2,3-DCP	2,5-DCP	1,8- 1,7-	1,4,6- 1,2,7- 1,2,8-	1,4,6,7-
2,3-DCP	2,6-DCP	1,9- 1,6-	1,2,6- 1,2,9-	n/a
2,3-DCP	3,4-DCP	n/a	1,7,8- 1,2,6- 1,2,9-	2,3,6,7- 1,2,6,7-
2,3-DCP	3,5-DCP	n/a	1,3,6- 1,3,9-	1,3,6,7-
2,3-DCP	2,3,4-TriCP	1,2,6- 1,2,9-	1,2,3,9- 1,2,3,6- 1,2,8,9- 1,2,6,7-	2,3,4,6,7-
2,3-DCP	2,3,5-TriCP	1,3,6- 1,3,9-	1,2,4,9- 1,2,4,6- 1,2,7,9- 1,2,6,8-	1,3,4,6,7-
2,3-DCP	2,3,6-TriCP	1,4,6- 1,2,9- 1,2,6-	1,2,6,9- 1,2,6,7- 1,2,8,9-	n/a
2,3-DCP	2,4,5-TriCP	1,3,6- 1,3,9-	1,2,4,6- 1,2,4,9- 1,2,7,8-	1,2,4,6,7-
2,3-DCP	2,4,6-TriCP	1,3,9- 1,3,6-	1,2,6,8- 1,2,7,9-	n/a
2,3-DCP	3,4,5-TriCP	n/a	1,2,3,6- 1,2,3,9-	1,2,3,6,7-
2,3-DCP	2,3,4,5-TCP	1,2,3,6- 1,2,3,9-	1,2,3,4,6- 1,2,3,8,9- 1,2,3,6,7-	1,2,3,4,6,7-
2,3-DCP	2,3,4,6-TCP	1,2,4,6- 1,2,4,9- 1,2,3,9- 1,2,3,6-	1,2,4,8,9- 1,2,4,6,7- 1,2,3,6,7- 1,2,3,8,9-	n/a
2,3-DCP	2,3,5,6-TCP	1,2,4,9- 1,2,4,6-	1,2,4,6,7- 1,2,4,8,9-	n/a
2,3-DCP	PCP	1,2,3,4,6-	1,2,3,4,6,7-	n/a
2,4-DCP	2,5-DCP	2,8- 2,7-	1,4,7- 1,3,7- 1,3,8-	1,4,6,8-
2,4-DCP	2,6-DCP	1,8- 1,7-	1,3,6- 1,3,9-	n/a
2,4-DCP	3,4-DCP	n/a	2,3,7-	2,3,6,8-

			1,2,7- 1,2,8-	1,2,6,8-
2,4-DCP	3,5-DCP	n/a	1,3,7- 1,3,8-	1,3,6,8-
2,4-DCP	2,3,4-TriCP	1,2,7- 1,2,8-	1,2,3,8- 1,2,3,7- 1,2,7,9- 1,2,6,7-	2,3,4,6,8-
2,4-DCP	2,3,5-TriCP	1,3,7- 1,3,8-	1,2,4,8- 1,2,4,7- 1,3,7,9- 1,3,6,8-	1,3,4,6,8-
2,4-DCP	2,3,6-TriCP	1,4,7- 1,2,8- 1,2,7-	1,3,6,9- 1,3,6,9- 1,2,6,8- 1,2,7,9-	n/a
2,4-DCP	2,4,5-TriCP	2,3,7-	1,2,4,7- 1,2,4,8- 1,3,7,8-	1,2,4,6,8-
2,4-DCP	2,4,6-TriCP	1,3,9- 1,3,6-	1,3,6,8- 1,3,7,9-	n/a
2,4-DCP	3,4,5-TriCP	n/a	1,2,3,7- 1,2,3,8-	1,2,3,6,8-
2,4-DCP	2,3,4,5-TCP	1,2,3,7- 1,2,3,8-	1,2,3,4,7- 1,2,3,7,9- 1,2,3,6,8-	1,2,3,4,6,8-
2,4-DCP	2,3,4,6-TCP	1,2,4,7- 1,2,4,8- 1,2,3,8- 1,2,3,7-	1,2,4,7,9- 1,2,4,6,8- 1,2,3,6,8- 1,2,3,7,9-	n/a
2,4-DCP	2,3,5,6-TCP	1,2,4,8- 1,2,4,7-	1,2,4,6,8- 1,2,4,7,9-	n/a
2,4-DCP	PCP	1,2,3,4,7-	1,2,3,4,6,8-	n/a
2,5-DCP	2,6-DCP	1,7- 1,8-	1,4,6-	n/a
2,5-DCP	3,4-DCP	n/a	2,3,7- 1,2,8- 1,2,7-	1,4,7,8- 1,2,6,9-
2,5-DCP	3,5-DCP	n/a	1,3,8-	1,3,6,9-
2,5-DCP	2,3,4-TriCP	1,2,8- 1,2,7-	1,2,3,7- 1,2,3,8- 1,2,6,9-	1,4,6,7,8-
2,5-DCP	2,3,5-TriCP	1,3,8- 1,3,7-	1,2,4,7- 1,2,4,8- 1,3,6,9-	1,3,4,6,9-
2,5-DCP	2,3,6-TriCP	1,4,7-	1,4,6,9-	n/a

		1,2,7- 1,2,8-	1,2,6,9-	
2,5-DCP	2,4,5-TriCP	2,3,7-	1,2,4,8- 1,2,4,7- 1,4,7,8-	1,2,4,6,9-
2,5-DCP	2,4,6-TriCP	1,3,7- 1,3,8-	1,3,6,9-	n/a
2,5-DCP	3,4,5-TriCP	n/a	1,2,3,8- 1,2,3,7-	1,2,3,6,9-
2,5-DCP	2,3,4,5-TCP	1,2,3,8- 1,2,3,7-	1,2,3,4,7- 1,2,3,6,9-	1,2,3,4,6,9-
2,5-DCP	2,3,4,6-TCP	1,2,4,8- 1,2,4,7- 1,2,3,7- 1,2,3,8-	1,2,4,6,9- 1,2,3,6,9-	n/a
2,5-DCP	2,3,5,6-TCP	1,2,4,7- 1,2,4,8-	1,2,4,6,9-	n/a
2,5-DCP	PCP	1,2,3,4,7-	1,2,3,4,6,9-	n/a
2,6-DCP	3,4-DCP	n/a	1,7,8- 1,2,9- 1,2,6-	n/a
2,6-DCP	3,5-DCP	n/a	1,3,9- 1,3,6-	n/a
2,6-DCP	2,3,4-TriCP	1,2,9- 1,2,6-	1,2,3,6- 1,2,3,9-	n/a
2,6-DCP	2,3,5-TriCP	1,3,9- 1,3,6-	1,2,4,6- 1,2,4,9-	n/a
2,6-DCP	2,3,6-TriCP	1,4,6- 1,2,6- 1,2,9-	n/a	n/a
2,6-DCP	2,4,5-TriCP	1,7,8-	1,2,4,9- 1,2,4,6-	n/a
2,6-DCP	2,4,6-TriCP	1,3,6- 1,3,9-	n/a	n/a
2,6-DCP	3,4,5-TriCP	n/a	1,2,3,9- 1,2,3,6-	n/a
2,6-DCP	2,3,4,5-TCP	1,2,3,9- 1,2,3,6-	1,2,3,4,6-	n/a
2,6-DCP	2,3,4,6-TCP	1,2,4,9- 1,2,4,6- 1,2,3,6- 1,2,3,9-	n/a	n/a
2,6-DCP	2,3,5,6-TCP	1,2,4,6- 1,2,4,9-	n/a	n/a
2,6-DCP	PCP	1,2,3,4,6-	n/a	n/a
3,4-DCP	3,5-DCP	n/a	n/a	1,2,7,9-

				1,3,7,8-
3,4-DCP	2,3,4-TriCP	n/a	1,2,7,8- 1,2,6,7- 1,2,8,9-	1,2,6,7,8- 2,3,4,7,8-
3,4-DCP	2,3,5-TriCP	n/a	1,3,7,8- 1,2,6,8- 1,2,7,9-	1,2,6,7,9- 1,3,4,7,8-
3,4-DCP	2,3,6-TriCP	n/a	1,4,7,8- 1,2,7,8- 1,2,6,9- 1,2,8,9- 1,2,6,7-	n/a
3,4-DCP	2,4,5-TriCP	n/a	2,3,7,8- 1,2,7,8-	1,2,4,8,9- 1,2,4,7,8-
3,4-DCP	2,4,6-TriCP	n/a	1,3,7,8- 1,2,7,9- 1,2,6,8-	n/a
3,4-DCP	3,4,5-TriCP	n/a	n/a	1,2,3,8,9- 1,2,3,7,8-
3,4-DCP	2,3,4,5-TCP	n/a	1,2,3,7,8- 1,2,3,6,7- 1,2,3,8,9-	1,2,3,4,8,9- 1,2,3,4,7,8-
3,4-DCP	2,3,4,6-TCP	n/a	1,2,4,7,8- 1,2,3,7,8- 1,2,4,6,7- 1,2,4,8,9- 1,2,3,8,9- 1,2,3,6,7-	n/a
3,4-DCP	2,3,5,6-TCP	n/a	1,2,4,7,8- 1,2,4,8,9- 1,2,4,6,7-	n/a
3,4-DCP	PCP	n/a	1,2,3,4,7,8- 1,2,3,4,6,7-	n/a
3,5-DCP	2,3,4-TriCP	n/a	1,2,6,8- 1,2,7,9-	1,3,6,7,8-
3,5-DCP	2,3,5-TriCP	n/a	1,3,6,8- 1,3,7,9-	1,3,4,7,9-
3,5-DCP	2,3,6-TriCP	n/a	1,3,6,9- 1,2,7,9- 1,2,6,8-	n/a
3,5-DCP	2,4,5-TriCP	n/a	1,3,7,8-	1,2,4,7,9-
3,5-DCP	2,4,6-TriCP	n/a	1,3,7,9- 1,3,6,8-	n/a
3,5-DCP	3,4,5-TriCP	n/a	n/a	1,2,3,7,9-
3,5-DCP	2,3,4,5-TCP	n/a	1,2,3,6,8- 1,2,3,7,9-	1,2,3,4,7,9-

3,5-DCP	2,3,4,6-TCP	n/a	1,2,4,6,8- 1,2,4,7,9- 1,2,3,7,9- 1,2,3,6,8-	n/a
3,5-DCP	2,3,5,6-TCP	n/a	1,2,4,7,9- 1,2,4,6,8-	n/a
3,5-DCP	PCP	n/a	1,2,3,4,6,8-	n/a
2,3,4-TriCP	2,3,5-TriCP	1,2,6,8- 1,2,7,9-	1,2,4,8,9- 1,2,4,6,7- 1,2,3,7,9- 1,2,3,6,8-	1,3,4,6,7,8-
2,3,4-TriCP	2,3,6-TriCP	1,2,6,9- 1,2,8,9- 1,2,6,7-	1,2,3,6,9- 1,2,3,6,7- 1,2,3,8,9-	n/a
2,3,4-TriCP	2,4,5-TriCP	1,2,7,8-	1,2,4,6,7- 1,2,4,8,9- 1,2,3,7,8-	1,2,4,6,7,8-
2,3,4-TriCP	2,4,6-TriCP	1,2,7,9- 1,2,6,8-	1,2,3,6,8- 1,2,3,7,9-	n/a
2,3,4-TriCP	3,4,5-TriCP	n/a	1,2,3,6,7- 1,2,3,8,9-	1,2,3,6,7,8-
2,3,4-TriCP	2,3,4,5-TCP	1,2,3,6,7- 1,2,3,8,9-	1,2,3,4,6,7- 1,2,3,7,8,9- 1,2,3,6,7,8-	1,2,3,4,6,7,8-
2,3,4-TriCP	2,3,4,6-TCP	1,2,4,6,7- 1,2,4,8,9- 1,2,3,8,9- 1,2,3,6,7-	1,2,3,6,8,9- 1,2,3,6,7,9- 1,2,3,6,7,8- 1,2,3,7,8,9-	n/a
2,3,4-TriCP	2,3,5,6-TCP	1,2,4,8,9- 1,2,4,6,7-	1,2,3,6,7,9- 1,2,3,6,8,9-	n/a
2,3,4-TriCP	PCP	1,2,3,4,6,7-	1,2,3,4,6,7,8-	n/a
2,3,5-TriCP	2,3,6-TriCP	1,3,6,9- 1,2,7,9- 1,2,6,8-	1,2,4,6,9- 1,2,4,6,7- 1,2,4,8,9-	n/a
2,3,5-TriCP	2,4,5-TriCP	1,3,7,8-	1,2,4,6,8- 1,2,4,7,9- 1,2,4,7,8-	1,2,4,6,7,9-
2,3,5-TriCP	2,4,6-TriCP	1,3,7,9- 1,3,6,8-	1,2,4,6,7- 1,2,4,7,9-	n/a
2,3,5-TriCP	3,4,5-TriCP	n/a	1,2,3,6,8- 1,2,3,7,9-	1,2,3,6,7,9
2,3,5-TriCP	2,3,4,5-TCP	1,2,3,6,8- 1,2,3,7,9-	1,2,3,4,6,8- 1,2,3,6,8,9- 1,2,3,6,7,9-	1,2,3,4,6,7,9-
2,3,5-TriCP	2,3,4,6-TCP	1,2,4,6,8- 1,2,4,7,9-	1,2,4,6,8,9- 1,2,4,6,7,9-	n/a

		1,2,3,7,9- 1,2,3,6,8-	1,2,3,6,7,9 1,2,3,6,8,9-	
2,3,5-TriCP	2,3,5,6-TCP	1,2,4,7,9- 1,2,4,6,8-	1,2,4,6,7,9- 1,2,4,6,8,9-	n/a
2,3,5-TriCP	PCP	1,2,3,4,6,8-	1,2,3,4,6,7,9-	n/a
2,3,6-TriCP	2,4,5-TriCP	1,4,7,8- 1,2,7,8-	1,2,4,6,9- 1,2,4,8,9- 1,2,4,6,7-	n/a
2,3,6-TriCP	2,4,6-TriCP	1,3,6,9- 1,2,6,8- 1,2,7,9-	n/a	n/a
2,3,6-TriCP	3,4,5-TriCP	n/a	1,2,3,6,9- 1,2,3,8,9- 1,2,3,6,7-	n/a
2,3,6-TriCP	2,3,4,5-TCP	1,2,3,6,9- 1,2,3,8,9- 1,2,3,6,7-	1,2,3,4,6,9- 1,2,3,4,6,7-	n/a
2,3,6-TriCP	2,3,4,6-TCP	1,2,4,6,9- 1,2,3,6,9- 1,2,4,8,9- 1,2,4,6,7- 1,2,3,6,7- 1,2,3,8,9-	n/a	n/a
2,3,6-TriCP	2,3,5,6-TCP	1,2,4,6,9- 1,2,4,6,7- 1,2,4,8,9-	n/a	n/a
2,3,6-TriCP	PCP	1,2,3,4,6,7- 1,2,3,4,6,9-	n/a	n/a
2,4,5-TriCP	2,4,6-TriCP	1,3,7,8-	1,2,4,7,9- 1,2,4,6,8-	n/a
2,4,5-TriCP	3,4,5-TriCP	n/a	1,2,3,7,8-	1,2,3,6,8,9-
2,4,5-TriCP	2,3,4,5-TCP	1,2,3,7,8-	1,2,3,4,7,8- 1,2,3,6,7,9- 1,2,3,6,8,9-	1,2,3,4,6,8,9-
2,4,5-TriCP	2,3,4,6-TCP	1,2,4,7,8- 1,2,3,7,8-	1,2,4,6,7,9- 1,2,4,6,8,9- 1,2,3,6,8,9- 1,2,3,6,7,9-	n/a
2,4,5-TriCP	2,3,5,6-TCP	1,2,4,7,8-	1,2,4,6,8,9- 1,2,4,6,7,9-	n/a
2,4,5-TriCP	PCP	1,2,3,4,7,8-	1,2,3,4,6,7,9-	n/a
2,4,6-TriCP	3,4,5-TriCP	n/a	1,2,3,7,9- 1,2,3,6,8-	n/a
2,4,6-TriCP	2,3,4,5-TCP	1,2,3,7,9- 1,2,3,6,8-	1,2,3,4,6,8-	n/a
2,4,6-TriCP	2,3,4,6-TCP	1,2,4,7,9-	n/a	n/a

		1,2,4,6,8- 1,2,3,6,8- 1,2,3,7,9-		
2,4,6-TriCP	2,3,5,6-TCP	1,2,4,6,8- 1,2,4,7,9-	n/a	n/a
2,4,6-TriCP	PCP	1,2,3,4,6,8-	n/a	n/a
3,4,5-TriCP	2,3,4,5-TCP	n/a	1,2,3,6,7,8- 1,2,3,7,8,9-	1,2,3,4,7,8,9-
3,4,5-TriCP	2,3,4,6-TCP	n/a	1,2,3,6,7,9- 1,2,3,6,8,9- 1,2,3,7,8,9- 1,2,3,6,7,8-	n/a
3,4,5-TriCP	2,3,5,6-TCP	n/a	1,2,3,6,8,9- 1,2,3,6,7,9-	n/a
3,4,5-TriCP	PCP	n/a	1,2,3,4,6,7,8-	n/a
2,3,4,5-TCP	2,3,4,6-TCP	1,2,3,6,7,9- 1,2,3,6,8,9- 1,2,3,7,8,9- 1,2,3,6,7,8-	1,2,3,4,6,7,9- 1,2,3,4,6,7,8-	n/a
2,3,4,5-TCP	2,3,5,6-TCP	1,2,3,6,8,9- 1,2,3,6,7,9-	1,2,3,4,6,7,9-	n/a
2,3,4,5-TCP	PCP	1,2,3,4,6,7,8-	1,2,3,4,6,7,8,9-	n/a
2,3,4,6-TCP	2,3,5,6-TCP	1,2,4,6,8,9- 1,2,4,6,7,9- 1,2,3,6,7,9- 1,2,3,6,8,9-	n/a	n/a
2,3,4,6-TCP	PCP	1,2,3,4,6,7,9- 1,2,3,4,6,7,8-	n/a	n/a
2,3,5,6-TCP	PCP	1,2,3,4,6,7,9-	n/a	n/a

VITA

Steven L. Alderman was born October 30, 1975, in Greenville, Mississippi. He earned a Bachelor of Science degree in chemistry from Mississippi State University in August of 1998. Immediately after, he began his graduate studies at Louisiana State University, in Baton Rouge, Louisiana, where he pursued a doctoral degree in physical chemistry under the direction of Dr. Barry Dellinger. The degree was granted in May of 2005.